POLITECNICO DI MILANO

Industrial Engineering
Energy Engineering Department
Master of Science in Energy Engineering
for an Environmentally Sustainable World (EEESW)

Equations of State for Mixtures: an Optimization-Based Approach

Relatore: Prof. Marco Verani
Corelatore: Ing. Silvia Lasala

Master Thesis of: Ing. Alan Marmo Nehemy
Matricola: 710516

Academic Year 2012

Abstract

To bring the costs of carbon capture and storage plants (CCS) down to more competitive prices, there have been developments to optimize the plant's processes. As a consequence, the fluid's thermodynamic properties need to be predicted with higher accuracy. This study analyzes one possible route for improving the accuracy of the prediction of thermodynamic properties: the mathematical optimization method used for the fitting of the experimental data. Using recent experimental data obtained by Mantovani et al. [1] for CO_2 –based mixtures (CO_2-N_2, CO_2-Ar, CO_2-O_2), both the Levenberg-Marquardt and Trust-Region methods were compared for the nonlinear fitting of the Peng-Robinson (PR) cubic equation of state. By applying the van der Waals mixing rules, the binary interaction parameters (BIP) were optimized using a Matlab code and the built-in function *nonlincurvefit* with these two different algorithms. As a result, there appears to be no influence of the optimization method in the accuracy of the predicted properties using the optimized BIP. Nonetheless, the use of the PR equation of state to predict the volumetric properties of the CO_2-based mixtures cited above was carried out successfully and provided results with deviations in the range 1.2% to 2.8%.

Index

Index of Figures

Index of Tables

Introduction

The necessity of reducing the cost of Carbon dioxide Capture and Storage (CCS) technologies has been requiring the optimization of all the involved processes. In CCS plants, the removal of the CO_2 can be made by its liquefaction, since the condensation temperature of the carbon dioxide is different from the other gases in the stream (N_2, O_2, Ar). However, a small percentage of these gases mixes with the CO_2 and, for that reason, the estimation of thermodynamic properties of CO_2 mixtures with high accuracy has become a subject of interest [2].

The evaluation of the properties of fluids is often a demanding task in real-life projects. Both pure fluids and mixtures behave differently than what is predicted by the traditional Equations of State (EoS), especially when the interactions between the molecules are strong or when the fluids are subjected to near-critical conditions [3]. This justifies the need for developing estimates that can accurately predict the thermodynamic and volumetric properties of the fluids in those circumstances.

The presented study aims to explain the basics surrounding the development of Equations of State and to bring into further detail two of the most used classes of models: cubic and multi-parameter equations of state. This work is divided into six chapters:

Chapter 1 is a review of equations of state (EoS), both analytical and non-analytical. It gives an introduction to the equations of state, describes the importance of the estimation of properties and how they can be generally accomplished. It covers the van der Waals EoS, the Peng-Robinson EoS and the Redlich-Kwong-Soave-Penelux EoS, for the analytical ones, and briefly describes some multi-parameter EoS. At the end, it also provides a comparison between analytical and non-analytical EoS for CO_2 mixtures,

Chapter 2 introduces the mathematical part of the work, the least square problems. It starts from the linear least squares as a primary step for the understanding of the non-linear least square problems, for which two algorithms are described: Gauss-Newton and Levenberg-Marquardt methods,

Chapter 3 describes how the optimization will be applied to the mixtures using the Peng-Robinson EoS,

Chapter 4 presents the results obtained from the simulations using Matlab,

Chapter 5 gives the interpretations of the results presented previously, explaining their significance and providing information regarding possible further developments.

Chapter 1: Review of Equations of State

1.1. Estimation of Properties

In real-life situations, it is often the case that the value of a property is needed but there exist no experimental values for those exact conditions (composition, pressure, temperature) [3]. When these situations arise, it becomes crucial to have a proper way to estimate or predict those values. There are primarily three ways of proceeding: theoretical, empirical or semi-empirical basis.

From a theoretical base, for an ideal gas:

$$Pv = R^*T \qquad \text{(Eq. 1.)}$$

where $v\left[\frac{m^3}{kg}\right]$ is the specific volume, $R^*\left[\frac{kJ}{kg.K}\right]$ the specific gas constant, $P[Pa]$ the pressure and $T[K]$ the temperature.

When applied to real gases, the ideal gas equation (Eq.1.) may present large deviations. For that reason, it is common practice to introduce experimental data to improve the accuracy of the predicted results. The resulting equations are empirical and semi-empirical relationships.

An improvement of the ideal gas relationship is the van der Waals Equation of State [4]. Starting from (Eq.1.), and assuming the following ideas [3]:

1- the total volume occupied by the gas, that coincides with the volume of the recipient for an ideal gas, is reduced by the volume occupied by the molecules themselves, expressed by the *co-volume (b),*
2- the pressure exerted by gas molecules on the recipient wall is reduced because of the attraction between the molecules due to their mass, expressed by the *energy parameter (a)*, and increases with square of density,

the following equation is obtained:

$$\left(P - \frac{a}{v^2}\right)(v - b) = R^*T. \qquad \text{(Eq. 2.)}$$

The parameters *a* and *b* are based upon the theoretical principles stated above. However, in practice, their values are known to depend on actual thermodynamic conditions and composition [3]. In this study, only the dependence on the mixture is considered, and that dependence is introduced by the mixing rules.

1.2. Corresponding States Principle (CSP)

According to van der Waals, in a paper published in 1873 [4], the corresponding states principle indicates that all fluids (pure substances or mixtures), when compared at the same non-dimensional reduced temperature ($T_r = T/T_{cr}$) and non-dimensional reduced pressure ($P_r = P/P_{cr}$), present a behavior that deviate from the ideal gas by approximately the same degree. In a general form, the corresponding states principle can be first expressed as a 2-parameter function [3]:

$$P_r = P_r(v_r, T_r) \qquad \text{(Eq. 3.)}$$

where v_r and T_r are the reduced specific volume and reduced temperature, respectively.

In reality, the principle works only for one group of substances at a time, whose molecular constitution is relatively similar. However, to account for the situations when that is not the case, a third parameter is introduced into Eq.3, the compressibility factor (Z), defined as [3]:

$$Z \triangleq \frac{Pv}{R^*T}. \qquad \text{(Eq. 4.)}$$

The compressibility factor may also be expressed in a non-dimensional form. Given the critical compressibility factor:

$$Z_{cr} = \frac{P_{cr}v_{cr}}{R^*T_{cr}} \qquad \text{(Eq. 5.)}$$

and the reduced one,

$$Z_r = \frac{Z}{Z_{cr}} = \frac{P_r v_r}{T_r} \qquad \text{(Eq. 6.)}$$

the compressibility factor Z can be expressed as:

$$Z = Z_{cr}\frac{P_r v_r}{T_r}. \qquad \text{(Eq. 7.)}$$

According to Bejan, pure substances can be described with a 2-parameter CSP and a compressibility factor. [5] That way, it is possible to eliminate v_r from the previous equation to obtain the following 3-parameter relationship:

$$Z = Z(T_r, P_r, Z_{cr}) \quad \text{(Eq. 8.)}$$

where Z_{cr} may act as the parameter related to the molecular constitution.

As a consequence of expressing the compressibility factor in a non-dimensional form, many substances can be represented in the same generalized graphic. The following graphic was obtained experimentally by Nelson and Obert (1954) for several substances from experimental PVT data. It may be used for most substances, but it should not be used for strongly polar fluids, helium, hydrogen, or neon unless special, modified critical constants are used. [3]

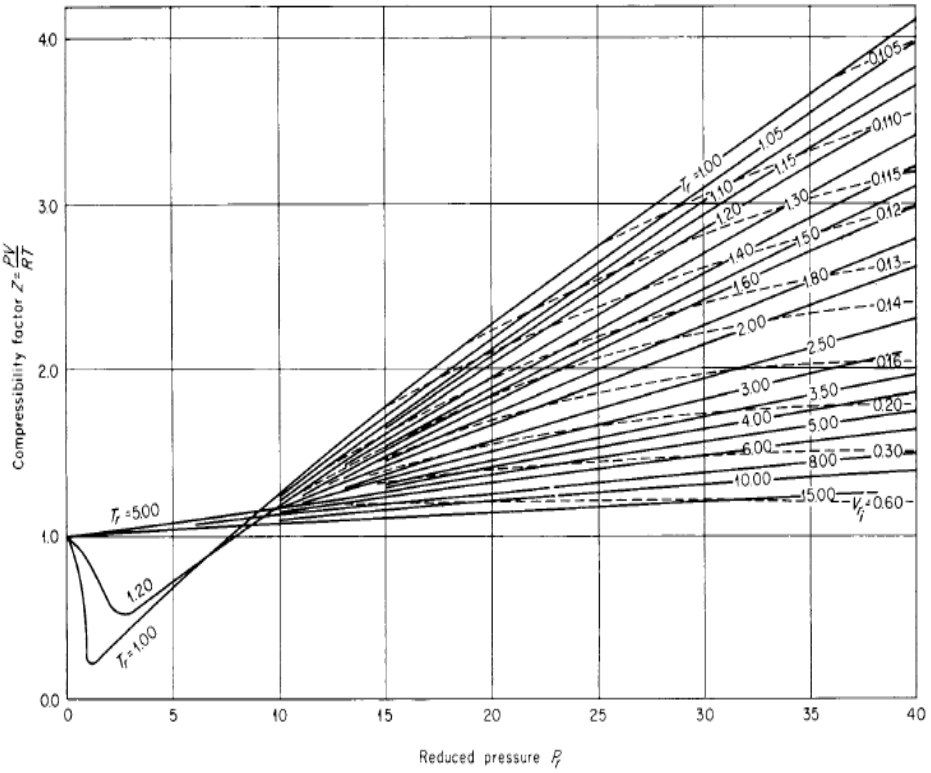

Figure 1: Generalized compressibility factor for all P_r, $V_r=V/(RT_c/P_c)$ (Nelson and Obert 1954)

1.3. Acentric Factor

An alternative for the third parameter was proposed by Pitzer et al. [6]. With the introduction of the *Pitzer acentric factor ω,* defined as:

$$\omega = -\log_{10} P_r - 1 \; for \; T_r = 0{,}7 \quad \text{(Eq. 9.)}$$

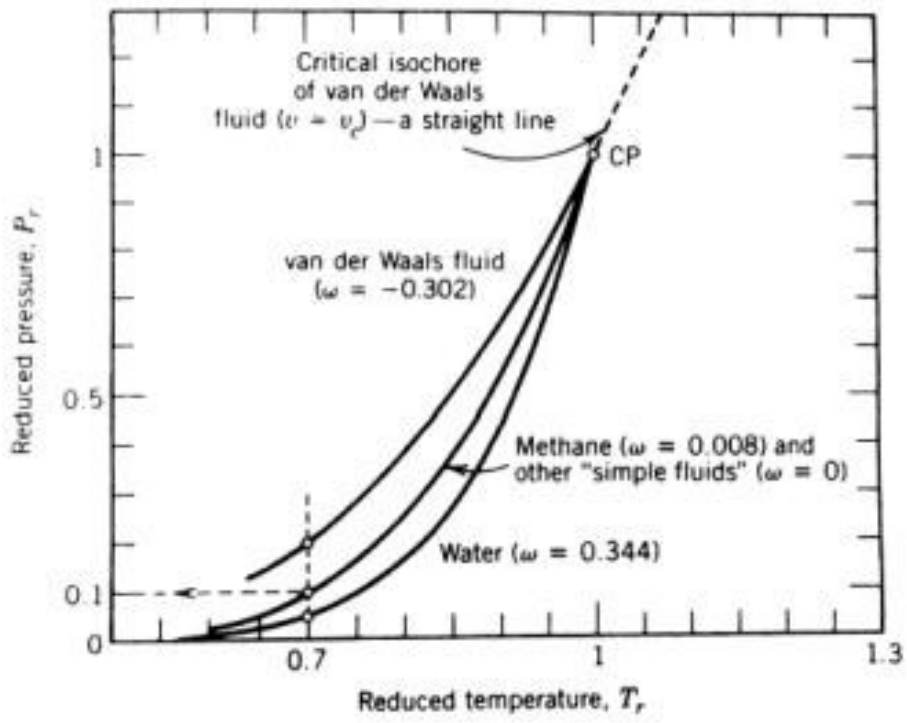

Figure 2: Pr x Tr Diagram [5]

That expression assumes the value ω=0 for the "simple fluids", that were defined by Pitzer as the permanent gases with heavy molecules, such as Ar, Xe and Ne [5]. The position of these substances in the $P_r(T_r)$ – each curve presented in (Figure 2) represents one substance - was taken as the reference from which the acentric factor is calculated. The practical meaning of the *Pitzer acentric factor* is that each pure substance has a different value of ω that increases with the fluid polarization. That way, highly polarized fluids, such as H_2O and NH_3, have high *Pitzer acentric factors* ($\omega_{H_2O} = 0.344$; $\omega_{NH_3} = 0.250$).

Therefore, the 3-parameter CSP can be rewritten as:

$$Z = Z(T_r, P_r, \omega). \qquad \text{(Eq. 10.)}$$

1.4. Cubic Equations of State

Cubic Equations of State (EoS) are a general class of equations where the specific volume has powers no higher than three. They are classified as analytical equations because they have a closed-form solution. That is important when the computational effort needs to be minimized, because iterative solutions tend to be much more time consuming. Regarding its use, the cubic EoS are accurate for predicting a fluid's characteristics when not in near-critical conditions - for pure simple substances and non-polar mixtures. That occurs

because some of the assumptions used for their development are not valid anymore in near-critical conditions or for strong polar substances.

In the following sections, a description of the cubic equations of state is presented, along with a description of the main improvements proposed to increase the accuracy of predictions for either the critical or other specified conditions. Furthermore, the cubic EoS have parameters that are specific for each substance and need to be defined *a priori*. The most used methods for obtaining those parameters will also be described.

1.4.1. Van der Waals Equation of State

The first EoS was published by J. D. van de Waals in 1873 [4] and more than a hundred others have been published since. By rewriting (Eq. 2) in the form $P = P(v, T)$ we obtain:

$$P = \frac{R^* T}{v - b} - \frac{a}{v^2}. \qquad \text{(Eq. 11.)}$$

Overall, this equation gives a good qualitative description of fluid properties, but it overestimates the critical compressibility factor (Z_{cr}). Consequently, it poorly predicts the density in the critical region.

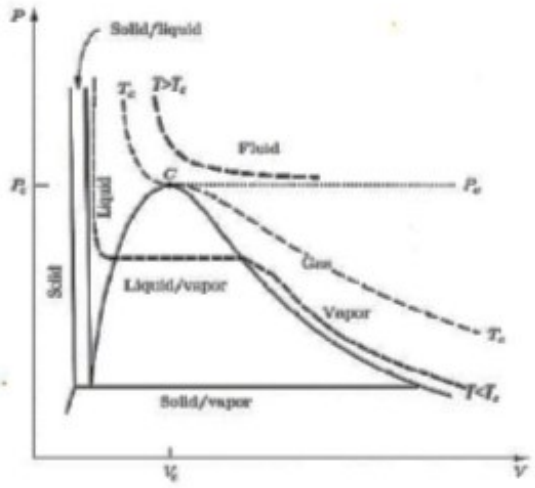

Figure 3: P-V Diagram

To calculate Z_{cr}, we first impose the critical-point conditions for the critical isothermal line. It can be seen from (Figure 3) that, for the critical conditions, the critical isotherm has a double inflexion point (point C), therefore:

$$\left(\frac{\partial P}{\partial v}\right)_{cr} = 0 \qquad \text{(Eq. 12.)}$$

$$\left(\frac{\partial^2 P}{\partial v^2}\right)_{cr} = 0\,. \qquad \text{(Eq. 13.)}$$

By solving the system of equations obtained from applying (Eq. 12.) and (Eq. 13.) to (Eq. 11.), the following expressions for the constants *a* and *b* are obtained:

$$a = 0{,}4218\frac{R^2 T_{cr}^2}{P_{cr}} \qquad \text{(Eq. 14.)}$$

$$b = 0{,}125\frac{RT_{cr}}{P_{cr}}\,. \qquad \text{(Eq. 15.)}$$

Now, by rewriting the van der Waals expression as $Z = Z(v,T)$ we can calculate the value of Z_{cr}, for which we obtain $Z_{cr} = \frac{3}{8} = 0{,}375$. In practice, it has been verified experimentally that the critical compressibility factor of pure fluids is in the range $Z_{cr}^{H_2O} = 0.23$ to $Z_{cr}^{H_2} = 0.3$, [3] which justifies the need for improvements.

1.4.2. General Form of Cubic Equations of State

Cubic EoS are very often used for the estimation of properties because they present a good compromise between accuracy and computational demand [3]. Nonetheless, different expressions may be more suitable for different situations (fluids, mixtures, thermodynamic conditions). According to Poling et al [3], a general form for all cubic EoS was proposed by Abbot, 1979, and can be represented in terms of P, as:

$$P = \frac{RT}{V-b} - \frac{\theta(V-\eta)}{(V-b)(V^2+\delta V+\varepsilon)}\,. \qquad \text{(Eq. 16.)}$$

Depending on the model $b, \varepsilon, \delta, \theta \; and \; \eta$ may be constants, including 0, or functions of the temperature and composition. The difference among the different models is what value those parameters have and how they are made to vary.

Furthermore, the first term $\left(\frac{RT}{V-b}\right)$ is called the *repulsive* term, and the second one $\left(\frac{\theta(V-\eta)}{(V-b)(V^2+\delta V+\varepsilon)}\right)$, the *attractive* term.

1.4.3. Improvements to the van der Waals EoS

The van der Waals equation of state does not describe the working fluids normally used in today's industrial processes with the required accuracy. Nonetheless, cubic EoS are very attractive because they have a closed-form solution and they can represent both liquid and vapor phases of many fluids [3]. Therefore, to obtain higher accuracies, especially in the near-critical region, modifications to the original van der Waals EoS have been proposed.

1.4.3.1. Volume Translation

A *volume translation* is a technique to improve the EoS predictability where the specific volume is computed from an original EoS and shifted so that the translated volume matches some experimental value or values from an estimation method (CSP, Group Contribution Methods). The underlying assumption is that the translation is small and does not materially change the gas or vapor phase densities [3]. It is common to express the shift by substituting $(v - b)$ for (v) in (Eq.16.).

1.4.3.2. The alpha function

Another improvement to the van der Waals EoS is the introduction of the so called alpha function. According to A. Bejan [5], it was first introduced by G. Soave [7] as a modification of the Redlich-Kwong (RK) equation of state, which has the following characteristics:

1- the attractive term presents the dependence on the *co-volume*,
2- the energy parameter varies with temperature as $\theta = aT^{-0.5}$

The RK-EoS can be written as:

$$P = \frac{RT}{v - b} - \frac{aT^{-0.5}}{v(v + b)} \quad \text{(Eq. 17.)}$$

According to Poling et al [3], this equation has been subjected to extensive testing and can be used not only for pure fluids, but also for mixtures whose critical points are not situated too far from one another.

The *alpha function* $(\alpha(T))$ was introduced by G. Soave [7] to include the ability of accurately predict the vapor tension at a reduced temperature $T_r = 0.7$:

$$\alpha(T, m) = aT^{-0.5}\left\{1 + m\left[1 - \left(\frac{T}{T_{cr}}\right)^{0.5}\right]\right\}^2 \quad \text{(Eq. 18.)}$$

and it matches the expression of $aT^{-0.5}$ for the critical point.

There have been many other expressions proposed for the *alpha* function. They generally present at least one of the following characteristics [3]:

1- polynomial functions of the reduced temperature,
2- exponential functions of the reduced temperature, or
3- a combination of both.

Moreover, the *alpha function* expressions must satisfy the following fundamental conditions [3]:

1- they must be finite and positive at each temperature,
2- they must have a value equal to one at the critical point,
3- they must tend to zero when the temperature tends to infinity,
4- they must be continuous with defined finite first and second order derivatives.

As previously presented, the *Pitzer acentric factor* ω takes into consideration the fact that not all substances can be approximated as having a spherical shaped molecule. Soave correlated the alpha function parameter *m* against the Pitzer acentric factor as:

$$m = 0.48 + 1.574\omega - 0.176\omega^2 \ . \qquad \text{(Eq. 19.)}$$

That way, we obtain the Redlich-Kwong-Soave (RKS) equation of state:

$$P = \frac{RT}{v-b} - \frac{\alpha(T)}{v(v+b)} \ . \qquad \text{(Eq. 20.)}$$

By imposing the critical point conditions (Eq. 12. and Eq. 13.) and calculating the parameters *a* and *b* (Eq. 14 and Eq. 15.), the critical compressibility factor of $Z_{cr} = 0.33$ is obtained. That value, even though it presents a clear improvement from the van de Waals EoS, is still higher than the experimental values obtained for pure substances. Nonetheless, the RKS EoS is considered adequate for hydrocarbons and other nonpolar compounds [8].

1.5. Other Equations of State

As a result of the improvements presented above, many other EoS have been developed. In the following sections, two cubic EoS will be examined. They are two of the most commonly used equations that resulted from the improvements made to the van der Waals equation of state.

1.5.1. Peng-Robinson Equation of State

In 1976 Peng and Robinson [09] modified the attractive term denominator in the Eq. 17 and proposed the following expression:

$$P = \frac{RT}{v-b} - \frac{\alpha(T,\omega)}{v^2 + 2bv - b^2} \quad \text{(Eq. 21.)}$$

where, by applying the critical-point conditions,

$$a = 0.45724 \frac{R^2 T_{cr}^2}{P_{cr}} \quad \text{(Eq. 22.)}$$

$$b = 0.0778 \frac{RT_{cr}}{P_{cr}} \ . \quad \text{(Eq. 23.)}$$

The *alpha function* assumes the same expression as in Eq. 18, but the function *m* has different coefficients:

$$m = 0.37364 + 1.5422\omega - 0.26922\omega^2 \ . \quad \text{(Eq. 24.)}$$

With those values, the critical compressibility factor can be calculated,

$$\frac{P_{cr}}{RT_{cr}} = \frac{Z_{cr}}{v} = \frac{1}{v-b} - \frac{\alpha(T,\omega)/RT_{cr}}{v^2 + 2bv - b^2} \quad \text{(Eq. 25.)}$$

and its value is $Z_{cr} = 0.3$, closer to the interval previously mentioned ($0.23 : 0.3$), showing an improvement at the critical region compared to the RKS model.

1.5.2. Redlich-Kwong-Soave-Peneloux Equation of State

This model introduces a volume translation to improve the molar liquid volume calculation $\left(v\left[\frac{m^3}{mol}\right]\right)$. The EoS expression is:

$$P = \frac{RT}{v+c-b} - \frac{\alpha(T,\omega)}{(v+c)(v+c+b)} \ . \quad \text{(Eq. 26.)}$$

The *co-volume* and *energy parameter* can be calculated with the same expressions provided for the RKS model. The parameter *c* is calculated with the following expression:

$$c = 0.47068(0.29441 - Z_{RA}) \frac{RT_{cr}}{P_{cr}} \quad \text{(Eq. 27.)}$$

where Z_{RA} is the Rackett compressibility factor.

1.6. Obtaining analytical cubic EoS parameters

To use either the generalized equations of state (such as RKS) or the corresponding states principle, one needs information on the critical point and

other properties of the fluids of interest. An issue that arises is what to do when such data is not available.

1.6.1. Goup Contribution Methods – obtaining thermodynamic properties

The most common way to make properties estimates in the absence of experimental data is to use a group contribution methods [9]. The basis of the method is that a molecule is thought of as a collection of functional groups, each of which makes an additive contribution to the properties of the molecule. Then, as a result of summing up the contributions of each of the functional groups, the properties of the molecule are obtained.

A group contribution method is based on the principle that some aspects of the structures of chemical components are always the same in many different molecules. The smallest common constituents are the atoms and the bonds.

A group contribution method is used to predict properties of pure components and mixtures by using group or atom properties. This dramatically reduces the number of needed data.

There are mainly two categories for contribution methods:

I. Additive group contribution method
   a. it is the simplest form of a group contribution method;
   b. it is accomplished by the determination of a property summing up the group's contribution
   c. it assumes that there is no interaction between groups and molecules
   d. it is used in the Joback's method for some properties

II. Additive group contributions and correlations
   a. it uses the pure additive group contributions to correlate the wanted property with an easily accessible property
   b. it usually gives better results than purely additive equations due to the introduction of a molecule's known property
   c. commonly used additional properties are the molecular weight, the number of atoms, chain length, ring sizes and counts

III. Group interactions
   a. It is used for the prediction of mixture properties when the other methods are not sufficiently accurate
   b. It is determined from group interaction parameters.

1.6.1.1. Lydersen method

The Lydersen method was one of the first group methods proposed for the calculation of the critical pressure, critical temperature and critical specific volume. The Lydersen method is based on the Guldberg rule, which establishes that a rough estimate of the normal boiling temperature T_b is roughly two-thirds

of the critical temperature T_{cr}. The Lyndersen method uses the same basic idea but it calculates more accurate values:

$$T_{cr} = \frac{T_b}{0.567 + \sum G_i - (\sum G_i)^2} \quad \text{(Eq. 28.)}$$

This method is the ancestor of many new models like Joback, Klincewicz, Ambrose, Gani-Constantinou and others.

1.6.1.2. Joback method

The Joback method assumes that there are no interactions between the groups and therefore only uses additive contributions and no contributions for interactions between groups. It is known due to the fact that:

1- It uses a single group list for all properties, what makes it possible to obtain all supported properties from a single analysis of the molecular structure;
2- It uses a very simple and easy-to-assign group scheme.

The group contributions can be found in a table, like the one presented below [10]:

Table 1: Group Contributions

Group	T_c	P_c	V_c	T_b	T_m
-CH3	0.0141	-0.0012	65	23.58	-5.10
-CH2-	0.0189	0.0000	56	22.88	11.27
>CH-	0.0164	0.0020	41	21.74	12.64
>C<	0.0067	0.0043	27	18.25	46.43
=CH2	0.0113	-0.0028	56	18.18	-4.32
=CH-	0.0129	-0.0006	46	24.96	8.73

The properties can be calculated with the following equations:

$$T_{cr}(K) = \frac{T_b(K)}{0.584 + 0.965 \sum_i v_i \Delta T_{cr,i} - \left(\sum_i v_i \Delta T_{cr,i}\right)^2} \quad \text{(Eq. 29.)}$$

$$P_{cr}(bar) = \frac{1}{\left(0.113 + 0.0032n - \sum_i v_i \Delta P_{cr,i}\right)^2} \quad \text{(Eq. 30.)}$$

$$v_{cr}\left(\frac{cm^3}{mol}\right) = 17.5 + \sum_i v_i \Delta v_{cr,i} \quad \text{(Eq. 31.)}$$

$$T_b(K) = 198 + \sum_i v_i \Delta T_{b,i} \quad \text{(Eq. 32.)}$$

$$T_f(K) = 122 + \sum_i v_i \Delta T_{f,i} \quad \text{(Eq. 33.)}$$

where the subscripts *b, cr* and *f* indicate the boiling, critical and freezing points, respectively. The Δ's are the contributions of each group to each property, found on the presented table.

1.6.2. CSP – obtaining model parameters

Critical constants are very commonly used for cubic EoS. Although not strictly necessary, it is convenient to force the EoS to fit the critical condition because three relationships exist to obtain the parameter values in that case:

The third equation is obtained by rewriting the cubic EoS $P = P(v,T)$ in the form $= Z(v,T)$, applying the definition of the compressibility factor for the critical region. The general expression of the cubic EoS becomes:

$$Z_{cr} = \frac{1}{1 - {}^{b}/_{v_{cr}}} - \frac{({}^{\theta}/_{RT})({}^{b}/_{v_{cr}})}{(1 + {}^{\delta}/_{b})({}^{b}/_{v_{cr}}) + ({}^{\varepsilon}/_{b^2})({}^{b}/_{v_{cr}})^2} \quad \text{(Eq. 34.)}$$

Since that equation is cubic in ${}^{b}/_{v_{cr}}$, the closed-form solution may be obtained, that is [3]:

$$\frac{bP_{cr}}{RT_{cr}} = Z_{cr} + \Omega - 1 \qquad \frac{\delta P_{cr}}{RT_{cr}} = \Omega - 2Z_{cr} \qquad \varepsilon\left(\frac{P_{cr}}{RT_{cr}}\right)^2 = Z_{cr}^2 - \Omega Z_{cr} - \Omega^2(\Omega - 1) \quad \text{(Eq. 35.)}$$

$$\Omega = \frac{aP_{cr}}{R^2 T_{cr}^2} \quad \text{(Eq. 36.)}$$

By enforcing that the cubic equations meet the true critical conditions, there will be increased error because the cubic Equations of State were defined for regions far enough from the critical point. Therefore, the expression above should only be used if the critical region is not of importance. Otherwise, it might occur that a value of Z_{cr} different from the true critical compressibility must be used to reduce the error in other regions of more importance. So, by

reducing the accuracy at the critical point, it is possible to decrease the error at other conditions. Furthermore, depending on the model used for the cubic EoS, not all three equations are needed (Eq. 12, Eq. 13 and Eq. 34). If the model is a 2-parameter EoS, only two equations are needed and, usually, the first two are used due to their simplicity.

It is also important to notice that the (Eq. 34.) does not apply to the case where there is a volume translation. In that case, the relationships expressed by (Eq. 12, Eq. 13 and Eq. 34) need to be modified.

1.6.3. Regression of data

In cases where CSP or group contributions are not used, the parameter values (*a, b, etc*) must be obtained by fitting data. However, even when CSP is used, it may also be desirable to use a combination of CSP and fitting. The fitting may be accomplished by the regression of data over the entire range of the liquid or by matching a particular state, such as at $T_r = 0.7$, to obtain ω. According to Poling et al. [3], there have been many studies on the matching of saturation volumes to obtain EoS parameters, on the discussion regarding the best choice of data for fitting parameters and other strategies. As a useful result, it has been shown by Soave et al. (1994) [3] that most CSP formulations require only T_{cr}/P_{cr}, that can be estimated from simple data sets.

1.7. Extension of cubic EoS for mixtures

To be able to use a cubic EoS for a mixture of fluids, its parameters must be calculated in an appropriate way. Cubic EoS have been successfully used for predicting fluid phase equilibrium of nonpolar mixtures [3]. The tools used for calculating the EoS parameters for a mixture are called mixing rules. The simplest one is the van der Waals mixing rules, presented in this section.

1.7.1. Van der Waals Mixing Rules

One possibility for extending the EoS for fluid mixtures is to increase the number of parameters in the virial EoS with an expansion of $\left(b/v\right)$ [3]. The virial EoS is not part of the presented study, but it should be noted that the van der Waals mixing rules only match the composition dependence basis imposed by the second virial coefficient, that is:

$$B_{mix} = \sum_{i=1}^{n}\sum_{j=1}^{m} x_i x_j B_{ij} = \sum_{i=1}^{n}\sum_{j=1}^{m} x_i x_j \left(b - \frac{a}{RT}\right)_{ij} \quad \text{(Eq. 37.)}$$

where *b* is the co-volume and *a*, the energy parameter. The *energy parameter* is calculated from the energy parameter of each species and their mol fraction.

When the values of b_{ij} are not very different between themselves, the *co-volume* is calculated as follows:

$$b = \sum_{i=1}^{n}\sum_{j=1}^{m} x_i x_j b_{ij} \quad \text{(Eq. 38.)}$$

$$b_{ij} = \left(\frac{b_{ii} + b_{jj}}{2}\right)^{0.5}\left(1 - I_{ij}\right) \quad where\ I_{ii} > 0 \quad \text{(Eq. 39.)}$$

And *a is*

$$a = \sum_{i=1}^{n}\sum_{j=1}^{m} x_i x_j a_{ij} \quad \text{(Eq. 40.)}$$

$$a_{ij} = \sqrt{a_i a_j}\left(1 - k_{ij}\right) \quad \text{(Eq. 41.)}$$

where k_{ij} are called binary interaction parameters.

1.8. Nonanalytical Equations of State

When one needs high accuracy in the properties description, cubic or quartic analytical equations of state cannot be generally used. "Though the search for better models began well before computers, the ability to rapidly calculate results or do parameter regression with complicated expressions has introduced increasing levels of complexity in the Equations of State" [3]. Two of the most used multi-parameter EoS are presented in this section.

1.8.1. Benedict-Webb-Rubin Equation of State

The first non-analytical equation of state was proposed by Benedict-Webb-Rubin (BWR) in 1940. They combined polynomials in temperature with power series and exponentials of density into an 8-parameter form [3]:

$$P = \rho RT + \left(B_0 RT - A_0 - \frac{C_0}{T^2}\right)\rho^2 + (bRT - a)\rho^3 + \alpha a\rho^6 + \frac{c\rho^3}{T^2}(1 + \gamma\rho^2)e^{(-\gamma\rho^2)} \quad \text{(Eq. 42.)}$$

where $A_0, B_0, C_0, a, b, c, \alpha\ and\ \gamma$ are the eight adjustable parameters. As an improvement from the cubic EoS, the BWR equation can treat supercritical components and is able to work in the critical area with good accuracy [3].

1.8.2. Benedict-Webb-Rubin-Starling Equation of State

Han and Starling (1973) introduced modifications to the BWR equation of state and the resulting equation is an 11-parameter EoS that can be used for

hydrocarbon systems that include the common light gases, such as H_2S, CO_2 and N2 [8] :

$$P = \rho RT + \left(B_0 RT - A_0 - \frac{C_0}{T^2} + \frac{D_0}{T^3} - \frac{E_0}{T^4}\right)\rho^2 + \left(bRT - a - \frac{d}{T}\right)\rho^3 + \alpha\left(a + \frac{d}{T}\right)\rho^6 + \frac{c\rho^3}{T^2}(1 + \gamma\rho^2)e^{(-\gamma\rho^2)} \quad \text{(Eq. 43.)}$$

where the additional parameters are $D_0, E_0 \; and \; d$.

To obtain the eleven parameters, one option is to resort to relationships with the critical properties and the acentric factor [2] :

Table 2: 11-Parameter EoS Relationships

Expressions	
$\boldsymbol{\rho_{cr} B_0 = A_1 + B_1 \omega}$	$\frac{\rho_{cr} a}{RT_{cr}} = A_6 + B_6 \omega$
$\boldsymbol{\frac{\rho_{cr} A_0}{RT_{cr}} = A_2 + B_2 \omega}$	$\rho_{cr}{}^3 \alpha = A_7 + B_7 \omega$
$\boldsymbol{\frac{\rho_{cr} C_0}{RT_{cr}{}^3} = A_3 + B_3 \omega}$	$\frac{\rho_{cr} c}{RT_{cr}{}^3} = A_8 + B_8 \omega$
$\boldsymbol{\rho_{cr}{}^2 \gamma = A_4 + B_4 \omega}$	$\frac{\rho_{cr} D_0}{RT_{cr}{}^4} = A_9 + B_9 \omega$
$\boldsymbol{\rho_{cr}{}^2 b = A_5 + B_5 \omega}$	$\frac{\rho_{cr} d}{RT_{cr}{}^2} = A_{10} + B_{10} \omega$
$\boldsymbol{\frac{\rho_{cr} E_0}{RT_{cr}{}^5} = A_{11} + B_{11} \omega e^{(-3.8\omega)}}$	

Table 3: 11-parameter EoS Relationships 2

Parameter Subscript (j)	A_j	B_j
1	0.44369	0.115449
2	1.28438	-0.92073
3	0.356306	1.70871
4	0.544979	-0.2709
5	0.528629	0.349261
6	0.484011	0.75413
7	0.705233	-0.04445
8	0.504087	1.32245

9	0.030745	0.179433
10	0.073283	0.463492
11	0.00645	-0.02214

1.8.3. BWRS Mixing Rules

Another option to determine the parameters is to resort to experimental data or estimates. In case of a mixture, the mixing rules used for determining the parameters of the BWRS EoS are based on the van der Waals mixing rules presented previously [8] :

$$A_0 = \sum_i \sum_j x_i x_j A_{oi}^{0.5} A_{oj}^{0.5} \left(1 - k_{ij}\right) \quad \text{(Eq. 44.)}$$

$$B_0 = \sum_i x_i B_{0i} \quad \text{(Eq. 45.)}$$

$$C_0 = \sum_i \sum_j x_i x_j C_{oi}^{0.5} C_{oj}^{0.5} \left(1 - k_{ij}\right)^3 \quad \text{(Eq. 46.)}$$

$$D_0 = \sum_i \sum_j x_i x_j D_{oi}^{0.5} D_{oj}^{0.5} \left(1 - k_{ij}\right)^4 \quad \text{(Eq. 47.)}$$

$$E_0 = \sum_i \sum_j x_i x_j E_{oi}^{0.5} E_{oj}^{0.5} \left(1 - k_{ij}\right)^5 \quad \text{(Eq. 48.)}$$

$$\gamma = \left[\sum_i x_i \gamma_i^{0.5}\right]^2 \quad \text{(Eq. 49.)}$$

$$a = \left[\sum_i x_i a_i^{\frac{1}{3}}\right]^3 \quad \text{(Eq. 50.)}$$

$$b = \left[\sum_i x_i b_i^{\frac{1}{3}}\right]^3 \quad \text{(Eq. 51.)}$$

$$c = \left[\sum_i x_i c_i^{\frac{1}{3}}\right]^3 \quad \text{(Eq. 52.)}$$

$$d = \left[\sum_i x_i d_i^{\frac{1}{3}}\right]^3 \quad \text{(Eq. 53.)}$$

$$\alpha = \left[\sum_i x_i \alpha_i^{\frac{1}{3}}\right]^3 \quad \text{(Eq. 54.)}$$

$$k_{ij} = k_{ji} \ . \quad \text{(Eq. 55.)}$$

The parameters $A_{0i}, B_{0i}, C_{0i}, D_{0i}, E_{0i}, a_i, b_i, c_i, d_i, \alpha_i \ and \ \gamma_i$ are pure component constants that can either be found on literature or estimated. The k_{ij} are the binary interaction parameters and the matrix *k* is symmetric.

1.9. Comparison between Analytical and Non-Analytical Equations of State for CO_2 mixtures

It is important to have a general understanding of the advantages and drawbacks of using analytical or non-analytical equations of state for a certain application. Especially when one needs to decide which model to use for a certain application for which the standard model has not been defined, a general comparison might provide a better initial guess from which to start the development of a specific EoS. Nowadays, with the increased need of improving carbon CCS processes and the need to estimate accurately the thermodynamic properties of CO_2 mixtures (usually containing N_2, O_2 and Ar), the non-existence of highly accurate EoS models is noticeable.

Generally, multi-parameter equations of state provide a more accurate prediction of most thermodynamic properties. However, the evaluation of multi-parameter EoS requires an increased computational effor. For CO_2, the Span and Wagner 12-parameter EoS is considered to be the reference EoS. According to Span et al. [11], this equation represents most of the data within $\Delta\rho/\rho \leq 0.01\%$ for pressures below 20MPa, which is usually well beyond (10-100 times) the accuracy of the cubic EoS.

In practice, for mixtures of more than two components, what is usually done is to obtain experimental data of the binary constituents and to fit the binary interaction parameters (BIP) of the mixing rule such that the deviations from the experimental and calculated data are minimized. On that basis, Mario Mantovani [12] analyzed the binary mixtures CO_2 - N_2, CO_2 – O_2, CO_2 – Ar with the cubic EoS models. The BIP were obtained from the data in the Vapor-Liquid equilibrium (VLE) condition using the software AspenTech for the fitting. His results are presented on the following table for the methods covered in his text [12](PR, RKSP – van der Waals mixing rules):

Table 4: Mantovani et al results - study 1

	CO_2 - N_2		**CO_2 – O_2**		**CO_2 – Ar**	
EoS	k_{ij}	Total deviation	k_{ij}	Total deviation	k_{ij}	Total deviation
PR	-0,030	6,2%	0,116	9,2%	0,097	8,1%
RKSP	-0,030	6,2%	0,114	8,5%	0,103	7,8%

In his studies [12] [1], Mantovani found that both temperature and mixing rules influence significantly the accuracy of the models. In particular, the BIP were found to be strongly dependent on the temperature and, on the other hand, the increased complexity of the alpha function was found to be ineffective in the accuracy increase.

Michela Mazzoccoli [2] compared different EoS for both pure CO_2 and mixtures using experimental data from literature and the Aspen Plus V7.3 software. In her study, the non-analytical EoS were included and demonstrated the expected increase in accuracy. However, depending on the region where the mixture's behavior was predicted (bubble point, dew point, single phase vapor) the model that presented the lowest deviations changed. Therefore, there doesn't seem to exist a direct general way to decide which model to use for CO_2 mixtures.

For the CO_2 - N_2 mixture, the deviations (for the density prediction) encountered by Mazzoccoli are shown in table 5 [2]:

Table 5: Mazzoccoli et al results

	CO_2 - N_2
EoS	Total deviation - Single phase
PR	3,8%
RKS	3,8%
BWRS	2%

Although the results shown above are low, large deviations were observed for other regions, ranging from **1% to 90%.** Also, for the study performed by Mazzoccoli, limited data was available for the CO_2 – O_2 and CO_2 – Ar mixtures [2].

In another study [1], Mantovani et al obtained new experimental data for CO_2 binary mixtures (CO_2 – N_2, CO_2 – O_2 and CO_2 – Ar) and fitted the data with EoS models. The results are shown in table 6:

Table 6: Mantovani et al results - study 2

	CO_2 - N_2		CO_2 – O_2		CO_2 – Ar	
EoS	k_{ij}	Total deviation	k_{ij}	Total deviation	k_{ij}	Total deviation
PR	-0,097	2,1%	0,151	2,37%	-0,031	2,56%
RKSP	-0,512	3,05%	0,169	3,92%	0,408	4,07%
BWRS	-0,037	1,71%	0,057	1,97%	-0,041	1,75%

Where a general improvement in the precision of the BIP estimation has been achieved.

Overall, to determine the best suited EoS for a given CO_2 mixture and conditions, the choice is not yet clearly visible. So far, two main aspects of the property calculation have been discussed: the EoS model and the mixing rules.

However, another possibility for improvement is the mathematical optimization used for the fitting of a given EoS results to the experimental data obtained.

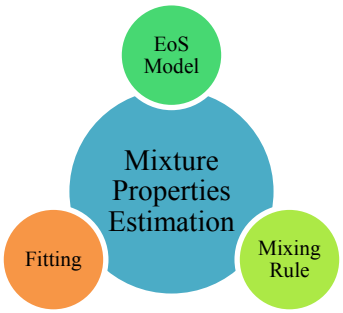

Figure 4: Mixture Properties Estimation Diagram

For that matter, the optimization method that will be used for the fitting is the non-linear least squares. However, before proceeding, the review of least square problems are presented in the following sections:

Chapter 2: The Least Square Problem

2.1. Presentation

In optimization problems, the function to be minimized is called *objective function*. The least square problems are a widely used class of optimization problems where the objective function has the following structure:

$$f(k) = \frac{1}{2}\sum_{i=1}^{n} r_i^2(k) \ . \qquad \text{(Eq. 56.)}$$

These kind of problems are usually the ones where the results of a model need to be compared to experimental ones [13]. In those cases, the difference between each measured and modeled data is called a *residual* (usually noted as r_i). If one wants to fit the data in such a way that both under and over estimates are punished equally, it makes mathematical sense to minimize the sum of squares instead of minimizing the simple sum, since the squares ensure that the value to be minimized is always positive. That way, the minimization problem can be written as:

$$\min_k \frac{1}{2}\sum_{i=1}^{n} r_i^2(k). \qquad \text{(Eq. 57.)}$$

In another notation, the residuals may also be expressed as a vector. Writting $\overline{r(k)} = (r_1(k) \quad ... \quad r_n(k))^T$, where $r_i(k)$ are the residuals at each point, the sum of squares can be written in a more compact way by using the ℓ_2 norm:

$$\frac{1}{2}\sum_{i=1}^{n} r_i^2(k) = \frac{1}{2}\left\|\overline{r(k)}\right\|_2^2. \qquad \text{(Eq. 58.)}$$

In the problem at study we are estimating the density value, and the optimization of the BIP is such that a certain model fits the experimental data for the CO_2 mixtures. Therefore, the residual is defined as:

$$\overline{r(k)} = \overline{\rho_{calc}\left(k, P_{exp}\right)} - \overline{\rho_{exp}} \qquad \text{(Eq. 59.)}$$

where k is the binary interaction parameter (BIP), $\overline{\rho_{calc}\left(k, P_{exp}\right)}$ is the set of calculated densities (using a model, i.e. Peng Robinson, BWR) and $\overline{\rho_{exp}}$ is the set of experimental densities.

In a general form, the BIP is a 2x2 matrix (the combinations between the two species of the binary interaction):

$$k = \begin{bmatrix} k_{11} & k_{12} \\ k_{21} & k_{22} \end{bmatrix}. \quad \text{(Eq. 60.)}$$

However, since we are using the Van der Waals mixing model, $k_{12}=k_{21}$. Furthermore, the interaction of each species with itself is null, therefore $k_{11}=k_{22}=0$. That way, the BIP can be represented only as real number k.

$$k = \begin{bmatrix} 0 & k \\ k & 0 \end{bmatrix}. \quad \text{(Eq. 61.)}$$

2.2. Introducing the Statistical Uncertainty of the Measurements

In experiments, a crucial part of the work is the determination of the statistical properties of the measure data. Suppose a measured density ρ and the residual, as defined above, between that value and a certain calculated one (using a model). If we suppose that the residuals r_i's are independent of each other, i.e. one measurement doesn't influence the others, that they are equally distributed with a certain standard deviation σ and that they can be described by probability density function $f(r)$, the likelihood of a particular set of calculated values $\rho_{calc}^{(1)}, \rho_{calc}^{(2)} \dots \rho_{calc}^{(n)}$, given that the actual parameter vector is $\overline{\rho_{exp}}$, is given by the function [13]:

$$p\left(\overline{\rho_{calc}(k, P_{exp})}, \overline{\rho_{exp}}, \sigma_r\right) = \prod_{i=1}^{m} f(r_i) \ . \quad \text{(Eq. 62.)}$$

If we assume that the probability density function follows normal distribution, the expression $f(r_i)$ can be written as:

$$f(r_i) = \frac{1}{\sigma_r \sqrt{2\pi}} e^{-\frac{r_i^2}{2\sigma_r^2}} \quad \text{(Eq. 63.)}$$

that is, the values of the residuals are normally distributed. Integrating the above function, it is possible to calculate the probability of a certain measurement to be inside a range of values, usually expressed in terms of the standard deviation σ_r:

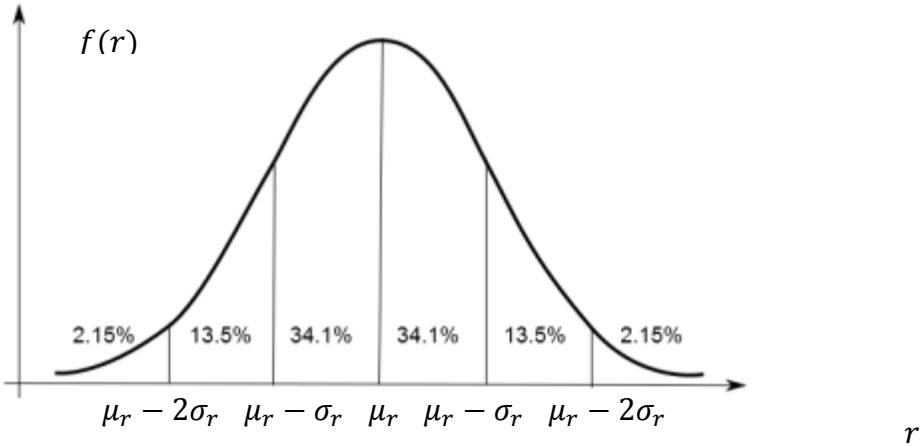

Figure 5: Bell Curve

Where μ_r is the mean of the residuals and the $\sigma_r$is the standard deviation of the residuals.

That way, the likelihood function may be written as the following expression, by substituting the normal distribution equation into the likelihood one [13]:

$$p\left(\overline{\rho_{calc}(k, P_{exp})}, \overline{\rho_{exp}}, \sigma_r\right) = (2\pi\sigma_r^2)^{-m/2} exp\left(-\frac{1}{2\sigma_r^2}\sum_{i=1}^{m} r_i^2\right). \quad \text{(Eq. 64.)}$$

From the above expression, it becomes clear that the maximum likelihood that a certain calculated density $\overline{\rho_{calc}(k, P_{exp})}$ represents well the set of experimental data $\overline{\rho_{exp}}$ is obtained when the sum of the squares of the residuals $\sum_{i=1}^{m} r_i^2$ is minimized. Therefore, in our least square problem, by minimizing the sum of squares of the residuals, we are maximizing the likelihood.

2.3. Linear Least Square Problem

The fitting of experimental data using the Peng-Robinson EoS and the Van der Waals mixing rules is accomplished by the solution of the minimization problem stated above (least square of the residuals). In this case, since the function $\rho_{calc}(k, P_{exp})$ is linear in *k* (the BIP), the residual is also linear in *k* [13]. That way, we are dealing with the solution of the following problem

$$\min_k f(k) = \frac{1}{2}\left\|\overline{r(k)}\right\|_2^2 \quad \text{(Eq. 65.)}$$

where the residual is linear in *k*.

The first step in the minimization problem is to determine the stationary points. To find a minimum of the objective function (local or global minimum), a first-order necessary condition is [13]:

If k^* is a local minimizer and f is continuously differentiable in an open neighborhood of k^*,

$$\nabla\overline{f(k^*)} = 0 \ . \qquad \text{(Eq. 66.)}$$

Writing that explicitly, for any *k*,

$$\nabla\overline{f(\mathrm{k})} = \sum_{i=1}^{n} r_i(\mathrm{k})\nabla r(k)_i \qquad \text{(Eq. 67.)}$$

since the Jacobian is defined as

$$\overline{\overline{J(k)}} = \begin{bmatrix} \nabla r_1 \\ \vdots \\ \nabla r_n \end{bmatrix} \qquad \text{(Eq. 68.)}$$

we can write,

$$\nabla\overline{f(\mathrm{k})} = \overline{\overline{J(k)}}^T\overrightarrow{r(k)} \qquad \text{(Eq. 69.)}$$

and, also

$$\overline{\overline{\nabla^2\mathrm{f(k)}}} = \overline{\overline{J(k)}}^T\overline{\overline{J(k)}} + \sum_{i=1}^{n} r(k)_i\nabla^2 r_i(k) = \overline{\overline{J(k)}}^T\overline{\overline{J(k)}} \ . \qquad \text{(Eq. 70.)}$$

The residual has a linear dependence on *k*, therefore, its second derivative is zero. According to Nocedal & Wright [13], it is possible to define a matrix $\bar{\bar{J}}$, independent of *k*, such that:

$$\overline{r(k)} = \bar{\bar{J}}\bar{k} - \overline{\rho_{exp}} \qquad \text{(Eq. 71.)}$$

and, therefore, the gradient and Hessian of the objective function become

$$\nabla\overline{\mathrm{f(k)}} = \bar{\bar{J}}^T\left(\bar{\bar{J}}\bar{k} - \overline{\rho_{exp}}\right) \ and \ \nabla^2\overline{\mathrm{f(k)}} = \bar{\bar{J}}^T\bar{\bar{J}} \qquad \text{(Eq. 72.)}$$

It is clear from (Eq. 65.) that *f*(k) is convex. As a consequence, the following theorem holds [13]:

$$if\ k^* \in \mathbb{R}\ is\ a\ local\ minimizer, i.e.$$

$$\nabla\overline{\mathrm{f(k^*)}} = 0, then\ \mathrm{k}^*\ is\ a\ global\ minimizer.$$

That is a powerful result in case of a linear objective function, and it permits us to write the following system of equations:

$$\bar{\bar{J}}^T \bar{\bar{J}}\, \bar{k}^* = \bar{\bar{J}}\overline{\rho_{exp}} \qquad \text{(Eq. 73.)}$$

that are known as the *normal equations* [13], and the solution is the minimizer of the linear objective function, that differs mainly on how this equation is solved (Cholesky factorization, QR factorization and so on).

2.4. Non-linear least square problem

When the residual function is non-linear, the fitting problem described above needs a more detailed solution, mainly because the structure of the Hessian $\nabla^2\overline{\mathrm{f(k)}} = \overline{\overline{J(k)}}^T\overline{\overline{J(k)}} + \sum_{i=1}^{n} r(k)_i \nabla^2 r_i(k)$ is more complex. That way, we can no longer say that the objective function is always convex and, therefore, the stationary points will be local minima (or maxima), depending on the result of the Hessian calculation.

From the expression of the Hessian

$$\nabla^2\overline{\mathrm{f(k)}} = \overline{J(k)}^T\overline{J(k)} + \sum_{i=1}^{n} r(k)_i \nabla^2 r_i(k) \qquad \text{(Eq. 74.)}$$

we now need to evaluate the Hessian of the residuals ($\nabla^2 r_i(k)$) and that may require considerable additional computational effort. In the following two sections, a description of two methods commonly used to circumvent that issue will be presented.

2.4.1. Gauss-Newton Method

This method is used with a line search algorithm, where a descendent search direction $p_j \; s.t. f(k_i + p_j) < f(k_i)$ is chosen. The most important search direction is the *Newton direction*, derived from the second-order Taylor expansion

$$f\left(k_i + p_j\right) \approx \bar{f}_J + \bar{p}^T \nabla \bar{f}_J + \frac{1}{2}\bar{p}^T \nabla^2 \bar{f}_J \qquad \text{(Eq. 75.)}$$

where the search direction is the solution obtained by minimizing the above function. By setting the first derivative to zero

$$p_j^{GN} = -\left(\overline{\overline{\nabla^2 f_J}}\right)^{-1}\overline{\nabla f_J}\,. \qquad \text{(Eq. 76.)}$$

That way, the interest in simplifying the Hessian calculation becomes clear. The Gauss-Newton method is the simplest method for minimizing the

non-linear least square problem and it is based in the principle that the Hessian calculation can be approximated as:

$$\overline{\overline{\nabla^2 \mathrm{f(k)}}} \approx \overline{\overline{J(k)}}^T \overline{\overline{J(k)}}\,. \qquad \text{(Eq. 77.)}$$

This simplification holds well [13], since there are many situations in which the term $\overline{\overline{J(k)}}^T \overline{\overline{J(k)}}$ dominates the second one ($\sum_{i=1}^{n} r(k)_i \nabla^2 r_i(k)$), at least close to the solution, and the convergence rate of Gauss–Newton is similar to that of Newton's method. That will occur when the norm of each second-order term (that is, $\|r(k)_i \nabla^2 r_i(k)\|$) is significantly smaller than the eigenvalues of $\overline{\overline{J(k)}}^T \overline{\overline{J(k)}}$. This behavior is usually seen when either the residuals $r(k)_i$ are small or when they are nearly affine (so that the $\|\nabla^2 r_i(k)\|$ are small). Therefore, if the least square solution presents relatively large residuals or the initial guess is too far from the solution, the approximation may no longer be adequate.

2.4.2. Levenberg-Marquardt Method

This method is used with the trust region algorithm. Reminding that we are interested in solving the least square problem posed by (Eq. 67.):

$$\min_k \overline{f(k)} = \frac{1}{2} \left\| \overline{r(k)} \right\|_2^2 \qquad \text{(Eq. 78.)}$$

we need to define, at each iteration *i*, a region with radius Δ_i, where the function f will be evaluated using a Taylor-series approximation:

$$\overline{f(k_\iota + p)} = \overline{f(k_\iota)} + \overline{\nabla f(k_\iota)}^T \bar{p} + \frac{1}{2} \bar{p}^T \overline{\overline{\nabla^2 f(k_\iota + t\bar{p})}} \bar{p} \qquad \text{(Eq. 79.)}$$

where the real scalar $t \in (0,1)$.

The Levenberg–Marquardt method can be obtained by using the same Hessian approximation as in the Gauss-Newton method, but replacing the line search with a trust-region strategy. One motivation to use a trust region strategy is avoid one of the deficiencies of Gauss–Newton method - when the Jacobian is rank-deficient, or nearly so. Since the same Hessian approximations are used both for Gauss-Newton and Levenberg-Marquardt, the local convergence properties of the two methods are similar [13] .

Recalling the approximation for the Hessian (Eq. 77.), (Eq. 79.) can be written as [13]:

$$\overline{m_\iota(p)} = \frac{1}{2} \left\| \overline{r(k_\iota)} \right\|_2^2 + \bar{p}^T \overline{\mathrm{J}_\iota(k)}^T \overline{r(k_\iota)} + \frac{1}{2} \bar{p}^T \overline{\overline{\mathrm{J}_\iota(k)}}^T \overline{\overline{J_\iota(k)}} \bar{p} \qquad \text{(Eq. 80.)}$$

where $m_i(p)$is the *model function* of the objective function *f* at each iteration i , that is supposed to be a good approximation of the function in a region of radius p, sufficiently small.

At each iteration the following sub problem needs to be solved:

$$\min_p \left\| \bar{\bar{J}}_i \bar{p} + \overline{r(k_i)} \right\| \; subject\ to\ \|\bar{p}\| \leq \Delta_i \qquad \text{(Eq. 81.)}$$

and the solution of the minimization algorithm can be classified in the following way:

1- If a solution of the Gauss-Newton step lies inside the trust region, i.e. $p_j^{GN} < \Delta_j$, then it will also be a solution to (Eq. 80),
2- Otherwise, there is a $\lambda > 0$ such that the solution $p_j^{LM} = \left\| \Delta_j \right\|$ and $\left(\bar{\bar{J}}_J^T \bar{\bar{J}}_J + \lambda I \right) p = -\bar{\bar{J}}^T r_j$.

To find a λ that satisfies the conditions above, a root finding algorithm based on the Cholesky or QR factorization may be used.

Chapter 3: Optimization Applied to the Peng-Robinson EoS

For the purpose of optimizing the binary interaction parameter (BIP), the least square problem was solved using built-in Matlab optimization code. The idea is to study the difference between optimization algorithms and to analyze BIP dependence on the temperature.

One crucial characteristic of the PR EoS is that an explicit expression of the form $\rho(P,T)$ is not easily found.

$$\rho(P,T) = P^{-1}(\rho,T) \qquad \text{(Eq. 82.)}$$

where $P(\rho,T)$ is the Peng-Robinson EoS as written in (Eq. 21).

Another way to proceed with the optimization algorithm explained in the previous sections is to calculate the density for each point (P,T) instead of finding a general expression. If we write the EoS explicitly as a cubic in v, as follows:

$$Pv^3 + (Pb_{mix} - RT)v^2 + \left(\alpha_{mix} - 2b_{mix}RT - 3{b_{mix}}^2P\right)v + \left(\alpha_{mix}b_{mix} - {b_{mix}}^2RT + P{b_{mix}}^3\right) = 0. \qquad \text{(Eq. 83.)}$$

A numerical solution in v, given P, T and the other parameters, can be easily found. We verify that this equation has only one real solution by verifying that it has no inflexion points, i.e. it is strictly ascendant. For that, first derivative should be always positive and, therefore, its determinant is always negative – since the derivative is a second-order equation.

Overall, the procedure to find a solution is the following:

1- write the EoS as $av^3 + bv^2 + cv + d = 0$
2- write the first derivative of the cubic as $3av^2 + 2bv + c = 0$
3- calculate $\Delta = (2b)^2 - 4(3a)c$ and calculate its value, if it's negative, continue
4- calculate the parameters $p = \frac{3ac-b^2}{9a^2}$, $q = \frac{bc}{6a^2} - \frac{b^3}{27a^3} - \frac{d}{2a}$
5- calculate the $\Delta = \sqrt{q^2 + p^3}$
6- calculate two more parameters $A = \sqrt[3]{q + \Delta}$, $B = \sqrt[3]{q - \Delta}$
7- The cubic will have two imaginary and one real solution, the real one can be calculated from the following expression $v = \frac{-b}{3a} + A + B$

1.1. Application – binary mixtures CO_2-N_2, CO_2-O_2, CO_2-Ar

The procedure mentioned above was applied to a real case, where the experimental data obtained by Mantovani et al. [1] is used for the density estimation of the referred binary mixtures.

The experimental set of data is given by six tables, where the properties of the binary mixtures CO_2-N_2, CO_2-O_2 and CO_2-Ar are measured for two different compositions each [1]:

Table 7: Mantovani et al experiment - mixtures composition

Mixture molar composition						
	N1	N2	O1	O2	A1	A2
CO2	0,9585	0,9021	0,9393	0,8709	0,9692	0,8306
N2	0,0415	0,0979	–	–	–	–
O2	–	–	0,0607	0,1291	–	–
Ar	–	–	–	–	0,0308	0,1694

Table 8: Mantovani et al experiment - exp. data N1

Mixture N1 experimental data

T = 303.22 K		T = 323.18 K		T = 343.15 K		T = 363.15 K		T = 383.14 K	
p [MPa]	[kg/m3]	p [MPa]	[kg/m3]	p [MPa]	[kg/m3]	p [MPa]	[kg/m3]	p [MPa]	[kg/m3]
1,001	17,91	1,001	16,79	1,003	15,2	1,002	14,03	1,002	13,08
2,000	37,75	2,004	34,95	2,001	32,23	2,002	30,39	2,001	27,55
3,001	60,12	3,000	54,72	3,001	50,12	3,000	46,57	3,000	42,75
4,001	85,65	4,001	76,45	4,002	68,52	4,002	63,73	4,003	58,6
5,001	116,38	5,003	100,8	5,003	89,33	5,001	81,83	5,003	74,95
6,000	155,97	6,001	128,5	6,002	111,99	6,001	101,2	6,000	92,1
7,001	213,29	7,001	160,99	7,000	136,56	7,002	121,6	7,003	109,94
8,001	330,92	8,001	200,41	8,001	163,71	8,005	143,48	8,001	128,59
9,001	544,54	9,001	249,73	9,000	193,75	9,003	166,64	9,002	148,16
10,002	634,72	10,001	312,81	10,001	227,23	10,001	191,38	10,001	168,52
11,001	683,11	11,002	389,63	11,002	264,48	11,002	217,83	11,002	189,95
12,001	715,67	12,001	467,33	12,000	305,25	12,002	245,86	12,002	212,12
13,001	740,35	13,001	532,26	13,000	348,75	13,001	275,07	13,002	234,83
14,002	759,32	14,001	582,79	14,000	393	14,000	305,51	14,002	258,37
15,004	774,69	15,002	619,85	15,001	435,95	15,001	336,55	15,002	282,34
16,001	788,63	16,001	649,44	16,001	475,71	16,002	367,63	16,001	306,66
17,003	801,56	17,001	673,37	17,003	510,93	17,001	397,82	17,001	331,02
18,001	813,51	18,003	693,69	18,001	541,92	18,001	426,94	–	–
19,005	824,42	19,002	711,83	19,002	569,42	19,001	454,58	–	–
20,001	833,58	20,001	728,16	20,004	593,72	20,002	480,85	–	–

Table 9: Mantovani et al experiment - exp. data N2

Mixture N2 experimental data

T = 303.22 K		T = 323.18 K		T = 343.15 K		T = 363.15 K		T = 383.14 K	
p [MPa]	[kg/m3]	p [MPa]	[kg/m3]	p [MPa]	[kg/m3]	p [MPa]	[kg/m3]	p [MPa]	[kg/m3]
1.000	17.42	1.002	16.15	1.001	14.29	1.001	13.43	1.000	12.48
2.000	36.62	2.000	33.57	2.003	30.68	2.001	28.57	2.003	26.68
3.001	58.04	3.003	52.68	3.001	47.56	3.000	44.28	3.001	41.5
4.001	82.12	4.001	73.32	4.001	66.13	4.003	61.87	4.001	56.89
5.000	110.12	5.001	95.85	5.003	85.97	5.003	79.14	5.002	72.61
6.002	144	6.000	121.04	6.003	107.13	6.001	97.56	6.001	88.97
7.000	187.15	7.002	149.69	7.003	129.96	7.001	116.91	7.000	106
8.001	248.76	8.001	182.41	8.001	154.43	8.004	137.17	8.003	123.69
9.000	341.94	9.000	220.69	9.002	181.2	9.002	158.53	9.001	142.03
10.003	453.92	10.001	265.42	10.000	210.13	10.001	181.15	10.000	161.18
11.002	541.32	11.002	316.33	11.001	241.54	11.001	204.87	11.001	180.9
12.003	599.42	12.001	371.76	12.002	275.24	12.000	229.68	12.002	201.21
13.000	640.25	13.000	426.12	13.001	310.56	13.002	255.53	13.000	222.01
14.002	671.43	14.002	475.97	14.001	346.77	14.000	282.04	14.002	243.35
15.002	695.05	15.001	519.15	15.001	382.74	15.001	309	15.001	264.96
16.001	715.04	16.000	554.51	16.000	417.63	16.001	336.03	16.001	286.73
17.005	731.98	17.001	584.29	17.002	450.07	17.003	362.76	17.001	308.77
18.001	747.85	18.000	610.03	18.002	480.07	18.000	388.68	18.001	330.77
19.003	761.75	19.001	632.79	19.001	507.72	19.001	413.59	19.002	352.16
20.001	773.45	20.001	652.97	20.002	532.73	20.001	438.02	20.002	373.05

Table 10: Mantovani et al experiment - exp. data O1

Mixture O1 experimental data

T = 303.22 K		T = 323.18 K		T = 343.15 K		T = 363.15 K		T = 383.14 K	
p [MPa]	[kg/m3]	p [MPa]	[kg/m3]	p [MPa]	[kg/m3]	p [MPa]	[kg/m3]	p [MPa]	[kg/m3]
1.003	17.930	1.000	16.790	1.020	15.270	1.004	13.750	1.009	12.820
2.004	37.390	2.003	34.810	2.006	31.710	2.010	29.690	2.002	27.150
3.000	59.690	3.003	54.280	3.001	48.820	3.011	45.050	3.001	42.340
4.000	84.800	4.002	75.650	4.010	67.220	4.006	62.670	4.001	58.120
5.002	114.540	5.001	99.330	5.002	88.500	5.000	81.480	5.002	74.460
6.003	152.040	6.001	126.150	6.001	110.670	6.000	100.750	6.001	91.550
7.000	203.610	7.003	156.990	7.001	134.860	7.003	120.600	7.000	109.210
8.001	289.700	8.001	193.320	8.003	161.060	8.002	142.170	8.001	127.600
9.002	461.140	9.001	237.430	9.001	189.880	9.004	164.800	9.000	146.880
10.001	588.570	10.001	291.610	10.003	222.010	10.002	188.990	10.000	167.030
11.002	651.970	11.000	356.070	11.000	257.280	11.001	214.480	11.000	187.900
12.004	691.780	12.001	426.040	12.001	295.230	12.000	241.380	12.002	209.570
13.000	721.430	13.000	491.280	13.001	335.990	13.001	269.730	13.002	231.830
14.000	743.520	14.000	543.710	14.002	377.880	14.000	299.130	14.002	254.660
15.002	761.680	15.001	586.850	15.003	418.590	15.003	329.230	15.001	278.160
16.001	777.530	16.001	620.780	16.001	457.590	16.001	359.230	16.000	301.720
17.001	791.430	17.001	648.030	17.001	493.830	17.001	388.810	–	–
18.001	804.780	18.000	671.450	18.002	525.510	18.001	417.420	–	–
19.006	816.570	19.001	691.460	19.002	553.760	19.001	444.670	–	–
20.003	826.460	20.003	709.440	20.002	579.120	20.003	471.170	–	–

Table 11: Mantovani et al experiment - exp. data O2

Mixture O2 experimental data

T = 303.22 K		T = 323.18 K		T = 343.15 K		T = 363.15 K		T = 383.14 K	
p [MPa]	[kg/m3]	p [MPa]	[kg/m3]	p [MPa]	[kg/m3]	p [MPa]	[kg/m3]	p [MPa]	[kg/m3]
1.001	16.960	1.004	15.670	1.000	14.270	1.000	13.330	1.002	11.840
2.001	35.970	2.002	33.230	2.003	30.630	2.002	28.810	2.003	25.910
3.000	56.910	3.004	51.850	3.001	47.700	3.002	44.410	3.003	40.570
4.001	80.030	4.006	71.910	4.001	64.980	4.000	60.550	4.004	55.670
5.002	106.480	5.001	93.510	5.001	84.150	5.002	77.510	5.005	71.220
6.001	137.250	6.001	117.620	6.006	104.830	6.003	95.460	6.001	87.230
7.001	175.070	7.002	144.290	7.003	126.590	7.002	114.200	7.003	103.830
8.002	222.690	8.002	174.220	8.005	149.970	8.003	133.650	8.003	120.960
9.003	286.100	9.002	208.250	9.000	174.890	9.000	154.090	9.000	138.660
10.000	369.360	10.001	246.730	10.001	201.760	10.003	175.660	10.002	157.100
11.003	453.810	11.000	289.900	11.001	230.560	11.000	197.980	11.000	176.050
12.003	524.280	12.001	336.790	12.002	261.070	12.000	221.250	12.001	195.510
13.002	577.680	13.000	385.090	13.002	293.200	13.000	245.220	13.000	215.350
14.004	618.470	14.001	432.340	14.003	326.310	14.000	270.000	14.003	235.590
15.001	651.770	15.001	475.610	15.001	359.740	15.002	295.200	15.001	256.190
16.003	678.160	16.002	514.040	16.003	392.710	16.001	320.510	16.002	276.930
17.003	700.310	17.001	547.480	17.001	424.320	17.001	345.470	17.001	297.680
18.005	719.800	18.001	577.290	18.001	453.960	18.000	369.970	18.000	318.730
19.001	737.040	19.003	602.710	19.001	481.530	19.001	394.150	19.001	339.370
20.001	751.820	20.001	625.500	20.001	507.090	20.003	417.750	20.001	359.410

Table 12: Mantovani et al experiment - exp. data A1

Mixture A1 experimental data

T = 303,22 K		T = 323,18 K		T = 343,15 K		T = 363,15 K		T = 383,14 K	
p [MPa]	[kg/m3]	p [MPa]	[kg/m3]	p [MPa]	[kg/m3]	p [MPa]	[kg/m3]	p [MPa]	[kg/m3]
1.003	18.140	1.001	16.990	1.001	15.840	1.005	14.760	1.010	14.310
2.001	38.320	2.002	35.390	2.003	32.950	2.005	30.570	2.001	28.840
3.001	61.250	3.003	55.470	3.000	50.830	3.002	47.080	3.003	44.320
4.000	87.640	4.001	77.710	4.001	69.030	4.002	64.570	4.001	60.280
5.001	119.810	5.000	102.510	5.003	90.500	5.003	83.150	5.003	76.900
6.002	161.730	6.000	131.350	6.000	113.830	6.002	103.020	6.001	94.350
7.000	228.260	7.000	165.370	7.004	139.400	7.001	124.090	7.003	112.510
8.001	455.320	8.001	207.320	8.002	167.770	8.003	146.770	8.003	131.600
9.002	643.490	9.000	260.660	9.000	199.540	9.001	170.920	9.000	151.500
10.005	699.660	10.000	332.110	10.001	235.380	10.003	196.850	10.003	172.550
11.001	738.090	11.000	417.560	11.001	275.770	11.003	224.690	11.001	194.390
12.002	763.710	12.002	502.330	12.001	320.760	12.001	254.320	12.000	217.230
13.001	783.200	13.003	567.420	13.003	368.580	13.002	285.790	13.001	240.850
14.001	799.340	14.002	616.140	14.006	416.200	14.002	318.500	14.000	265.190
15.003	813.250	15.003	651.850	15.003	462.140	15.003	351.990	15.001	290.230
16.001	825.600	16.003	679.860	16.004	504.430	16.001	384.620	16.000	315.410
17.001	837.220	17.002	702.820	17.001	541.210	17.002	417.310	17.001	340.760
18.004	847.990	18.003	722.640	18.001	573.060	18.001	448.330	18.002	366.360
19.006	858.590	19.003	739.790	19.001	600.370	19.001	477.320	19.001	391.230
20.007	866.610	20.002	755.350	20.003	624.250	20.004	505.010	20.003	415.120

Table 13: Mantovani et al experiment - exp. data A2

Mixture A2 experimental data

T = 303.22 K		T = 323.18 K		T = 343.15 K		T = 363.15 K		T = 383.14 K	
p [MPa]	[kg/m3]	p [MPa]	[kg/m3]	p [MPa]	[kg/m3]	p [MPa]	[kg/m3]	p [MPa]	[kg/m3]
1.002	17.700	1.036	16.390	1.019	15.290	1.004	13.840	1.004	12.620
2.003	37.390	2.003	34.270	2.000	31.410	2.001	29.570	2.000	26.980
3.000	58.810	3.005	53.070	3.001	47.860	3.001	45.560	3.001	41.970
4.003	82.660	4.002	73.420	4.000	66.410	4.001	62.170	4.001	57.440
5.002	109.640	5.001	95.220	5.001	85.940	5.002	79.510	5.001	73.270
6.002	141.430	6.007	119.390	6.001	106.640	6.001	97.510	6.000	89.500
7.002	179.990	7.000	145.740	7.003	128.430	7.000	116.440	7.001	106.400
8.003	229.060	8.001	175.110	8.005	151.850	8.001	136.150	8.001	123.740
9.001	294.030	9.000	208.100	9.004	176.670	9.000	156.770	9.003	141.710
10.000	377.700	10.001	244.800	10.001	203.170	10.003	178.320	10.000	160.360
11.000	465.250	11.001	285.240	11.001	231.270	11.001	200.650	11.000	179.400
12.002	538.570	12.002	328.930	12.004	261.010	12.001	223.900	12.001	199.010
13.002	594.050	13.002	373.810	13.002	291.940	13.001	247.960	13.000	218.970
14.001	635.790	14.000	418.720	14.004	323.970	14.002	272.480	14.002	239.300
15.003	668.490	15.005	461.680	15.003	356.440	15.001	297.600	15.001	259.930
16.001	695.110	16.001	500.310	16.003	388.270	–	–	16.002	280.740
17.001	717.840	17.003	535.060	17.003	419.020	–	–	17.003	301.710
18.000	737.350	18.002	565.870	18.001	448.220	–	–	18.001	322.560
19.001	755.040	19.007	593.010	19.006	476.050	–	–	19.004	343.410
20.004	769.490	20.005	617.440	–	–	–	–	20.003	363.600

For the optimization, the algorithm used was the nonlinear curve fitting - a built-in Matlab function that can be found in the Optimization toolbox. It uses the nonlinear least square for the fitting of a function to a set of data (xdata, ydata) as follows:

bip_opt = lsqcurvefit(rho_PR ,bip,P_exp,rho_exp)

Where rho_PR is the density calculated from the Peng-Robinson relationship, P_exp and rho_exp are the experimental data to be fitted. The tricky part is to define the rho_PR expression with its explicit dependence on the *bip*, because for that, the function needs to include the mixing rules, based on parameters loaded with external files. The algorithm implemented for that was:

1- create a function rho_PR = paramPR(P_exp, T_exp, a, R_spec, b_mix, bip, x) that receives the experimental values (P_exp, T_exp, molar fraction 'x'), the parameters (energy parameter, co-volume) calculated for each species and the bip to calculate the density, also verifying that the equation has only one real root (as explained in the previous point),
2- call that function using an anonymous function, defining that P_exp and bip as the variables rho_PR = @(bip, P_col) paramPR (P_exp, T_exp, data, R_spec, bip, x),
3- define an initial guess for the bip
4- call the optimization function bip_opt = lsqcurvefit (rho_PR ,bip,P_exp,rho_exp) for each isotherm,
5- Calculate the deviation AAD%,

Furthermore, since the bip is known to be strongly dependent on the temperature, an additional step was developed:

1- optimize the bip for each isotherm,
2- regress the data using the function bip(T) = a+b*T+c/T;
3- calculate the rho_PR again but, this time, use the bip(T) for each isotherm,
4- calculate the deviation.

Chapter 4: Results

First, a comprehensive presentation and analysis of the results for the BIP fitting will be presented. Following that, the robustness analysis of the optimization method, by changing its tolerance, initial value and algorithms, along with the study of the implications of the BIP and mixtures variation will also be presented. Conclusions on the effectiveness of the method employed, suggested improvements and/or points to be reviewed to improve the validation of the discrepancies between experimental and calculated data will be presented at the end.

4.1. Optimization of BIP for Each Isotherm

The first approach to the BIP optimization that will be presented considers the BIP as dependent on the temperature. However, its optimization will be done for one isotherm at a time and, therefore, every mixture will have a set of five optimum BIP's.

The results are shown in the following plots (figure 5 to figure 10), where the AAD% is the total deviation of each isotherm, defined as:

$$AAD\% = \frac{100}{N}\sum_{i=1}^{N}\frac{\left|\rho_{PR} - \rho_{exp}\right|}{\rho_{exp}}. \qquad \text{(Eq. 84.)}$$

and the BIP_{opt} are represented as the k_{ij} in the figures. The AAD% and temperature are displayed above each plot.

4.1.1. Plots Mixture N1

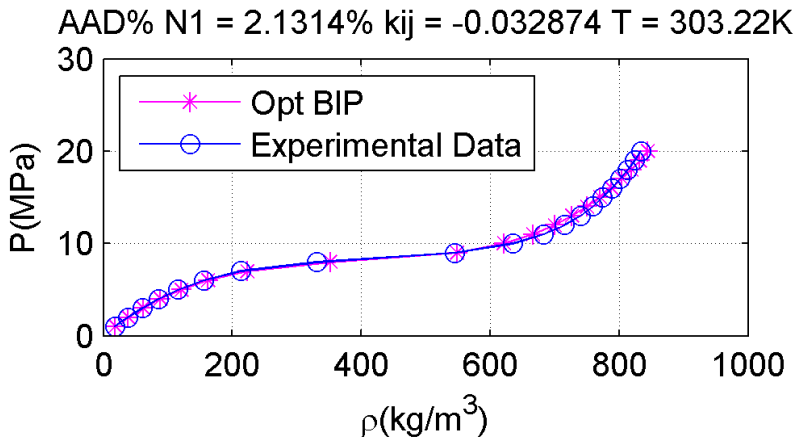

Figure 6: Mixture N1, T=303K

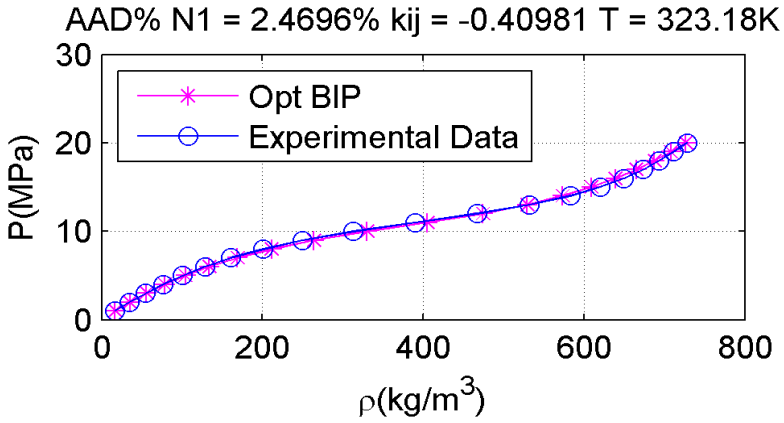

Figure 7: Mixture N1, T=323K

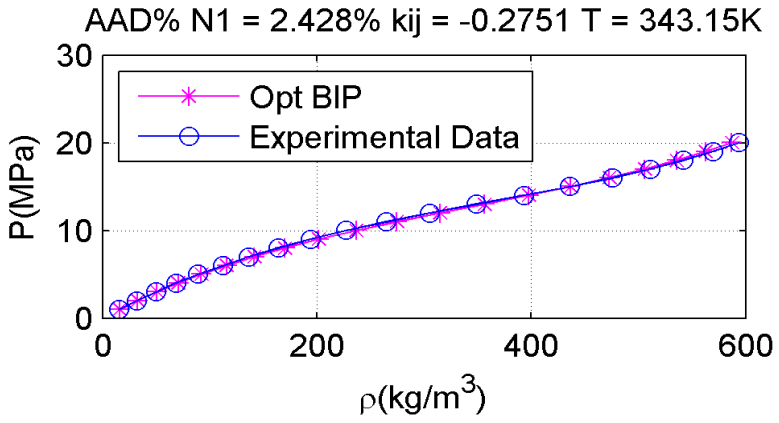

Figure 8: Mixture N1, T=343K

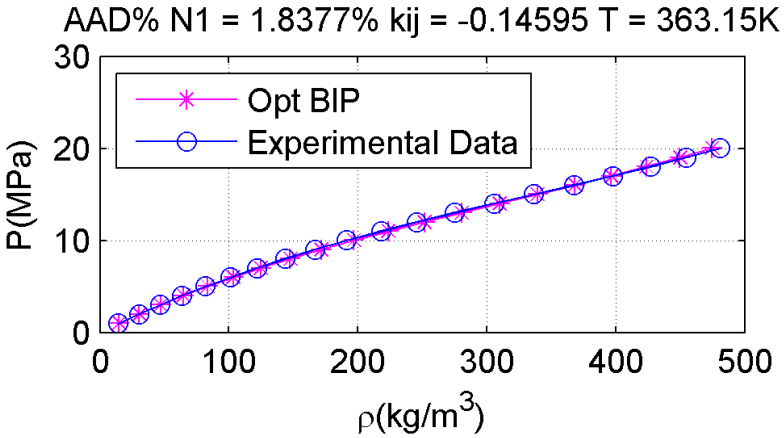

Figure 9: Mixture N1, T=363K

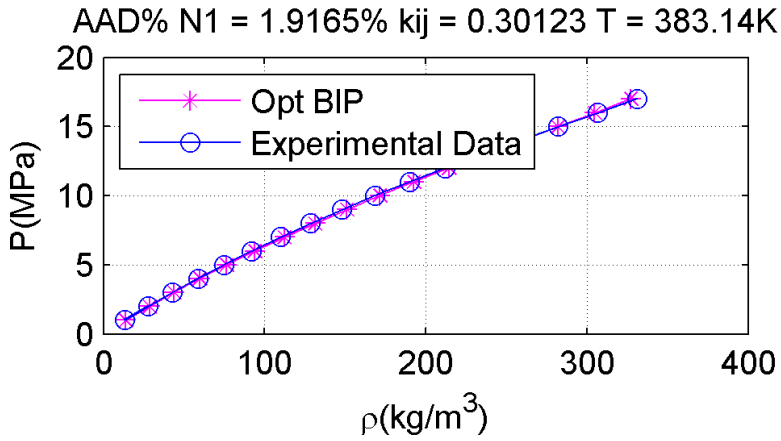

Figure 10: Mixture N1, T=383K

4.1.2. Plots Mixture N2

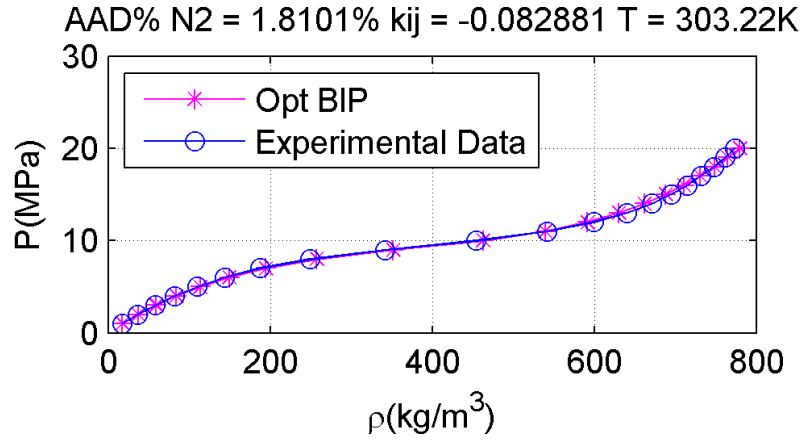

Figure 11: Mixture N2, T=303K

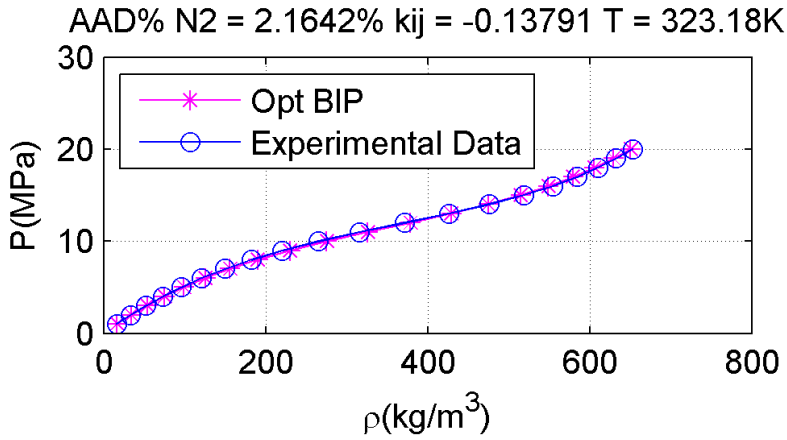

Figure 12: Mixture N2, T=323K

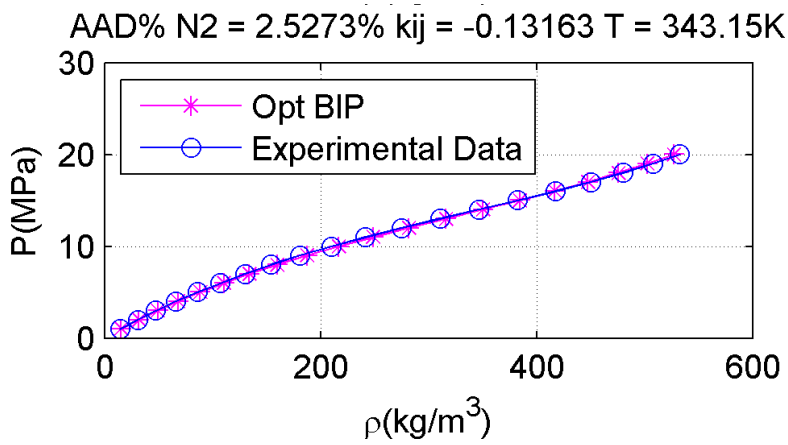

Figure 13: Mixture N2, T=343K

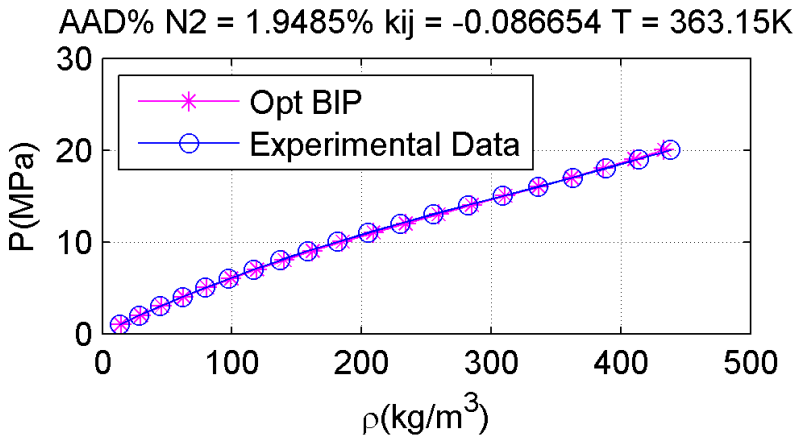

Figure 14: Mixture N2, T=363K

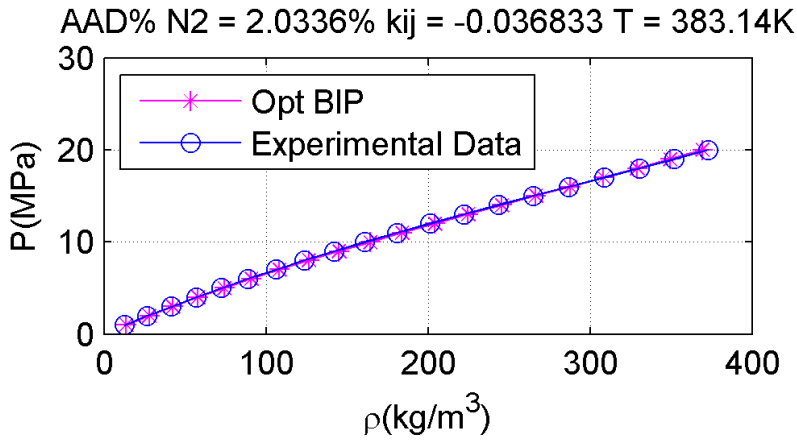

Figure 15: Mixture N2, T=383K

4.1.3. Plots Mixture O1

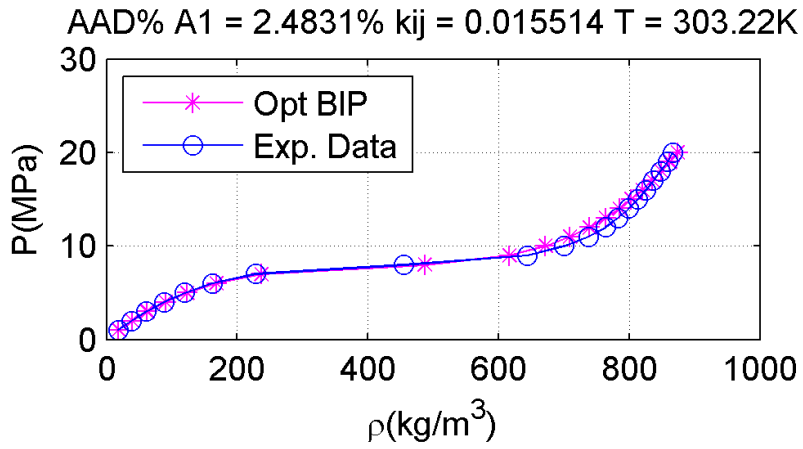

Figure 16 : Mixture A1, T=303K

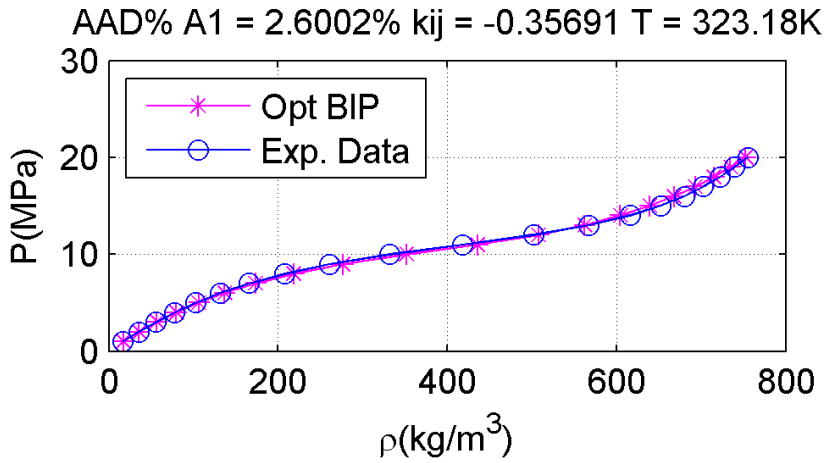

Figure 17: Mixture A1, T=323K

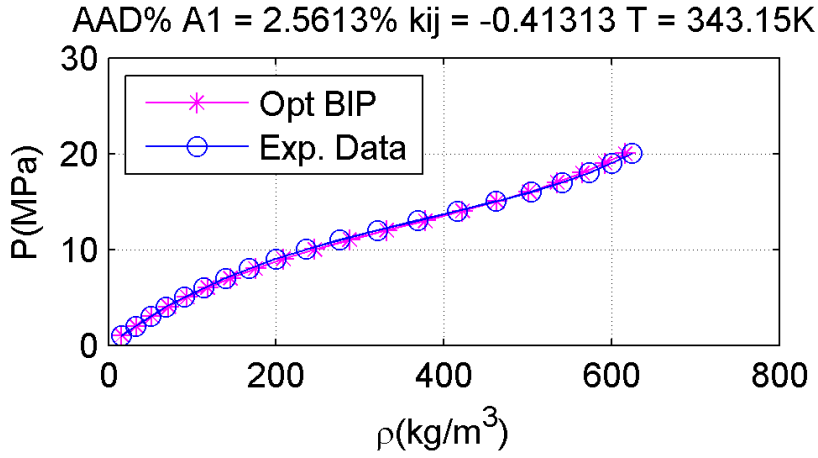

Figure 18: Mixture A1, T=343K

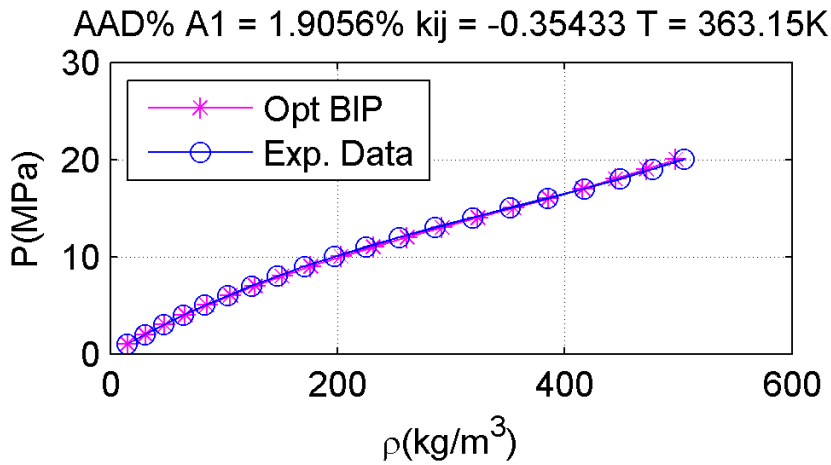

Figure 19: Mixture A1, T=363K

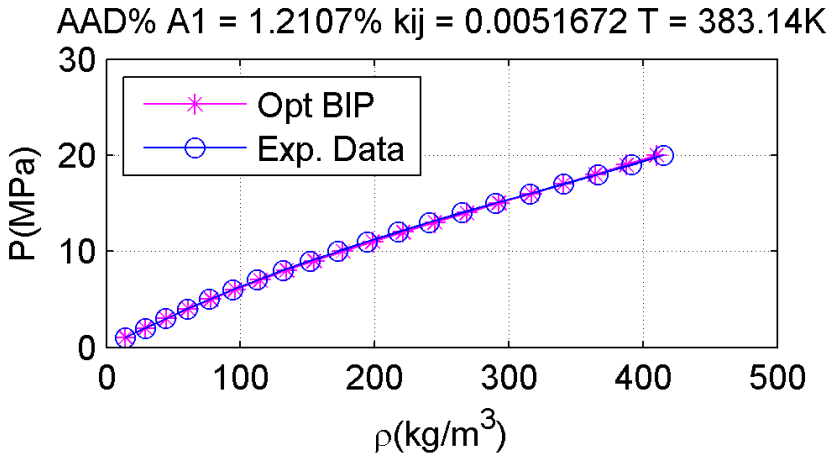

Figure 20: Mixture A1, T=383K

4.1.4. Plots Mixture A2

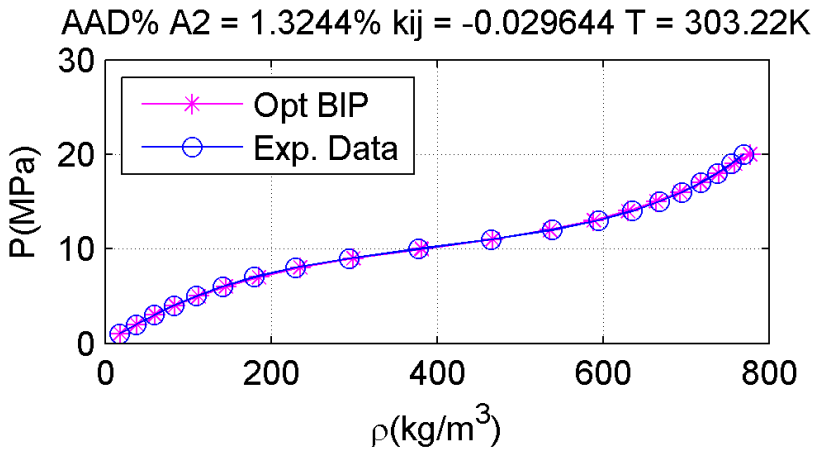

Figure 21: Mixture A2, T=303K

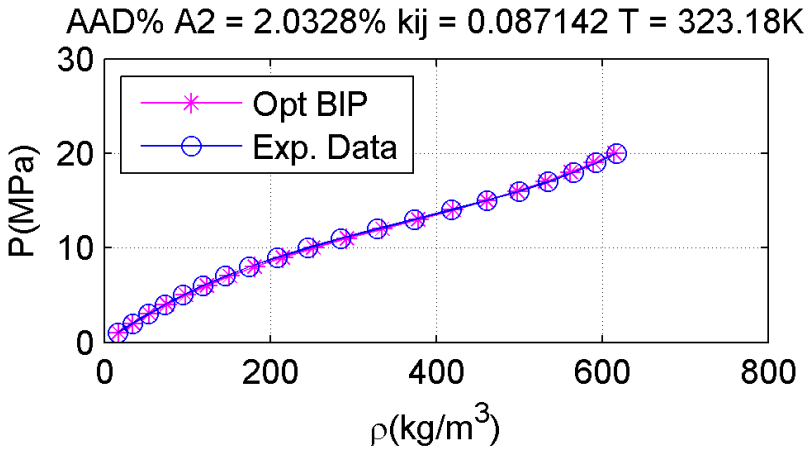

Figure 22: Mixture A2, T=323K

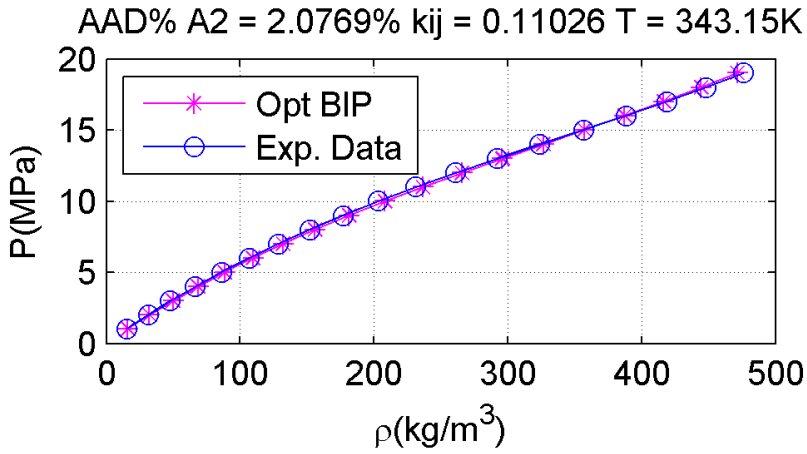

Figure 23: Mixture A2, T=343K

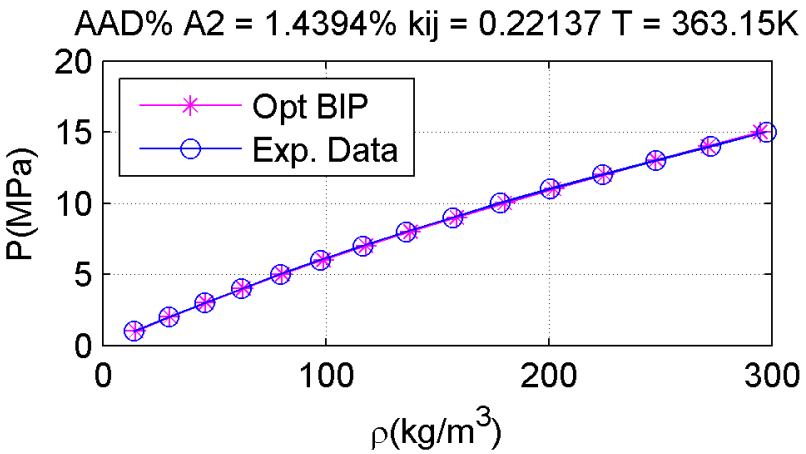

Figure 24: Mixture A2, T=363K

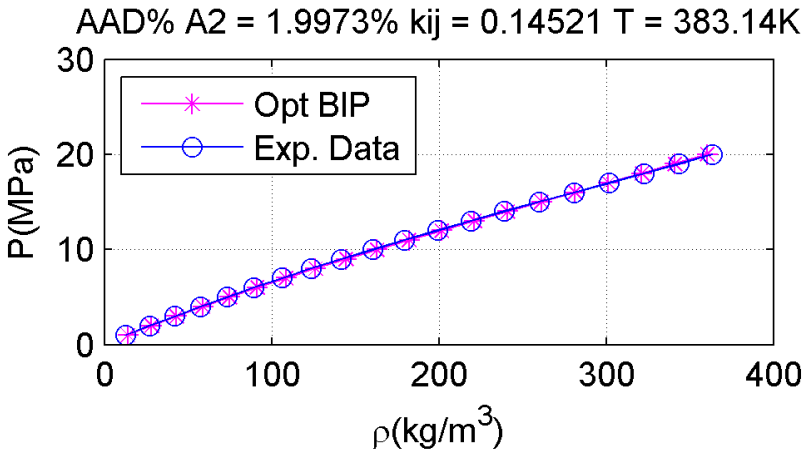

Figure 25: Mixture A2, T=383K

4.1.5. Plots Mixture O1

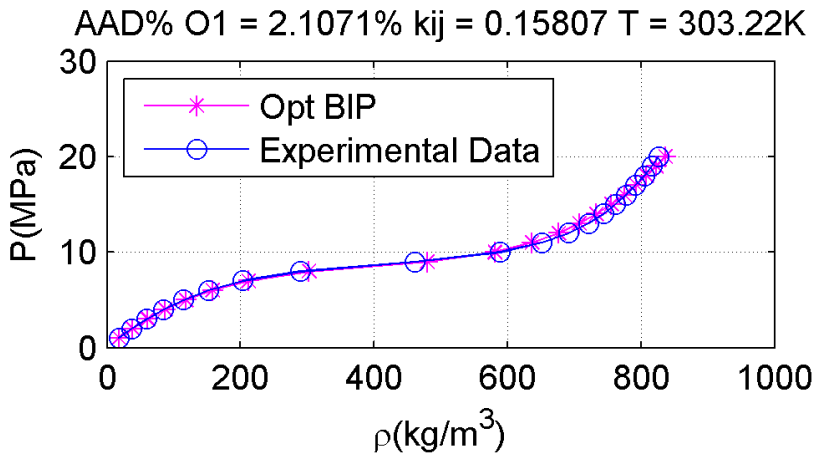

Figure 26: Mixture O1, T=303K

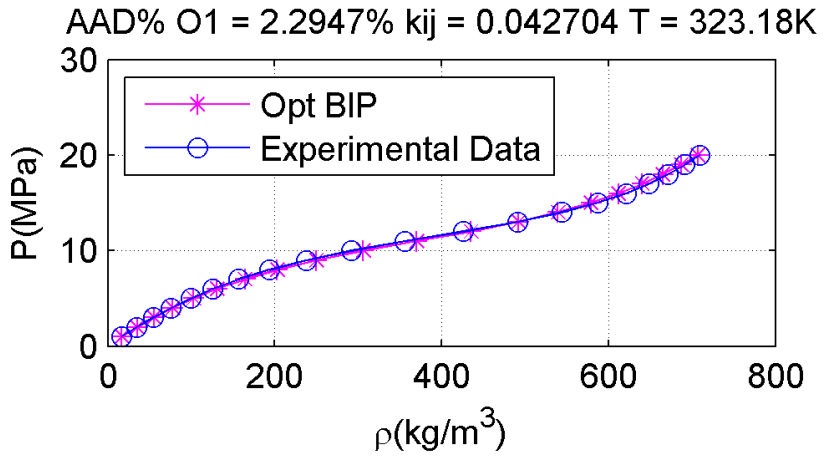

Figure 27: Mixture O1, T=323K

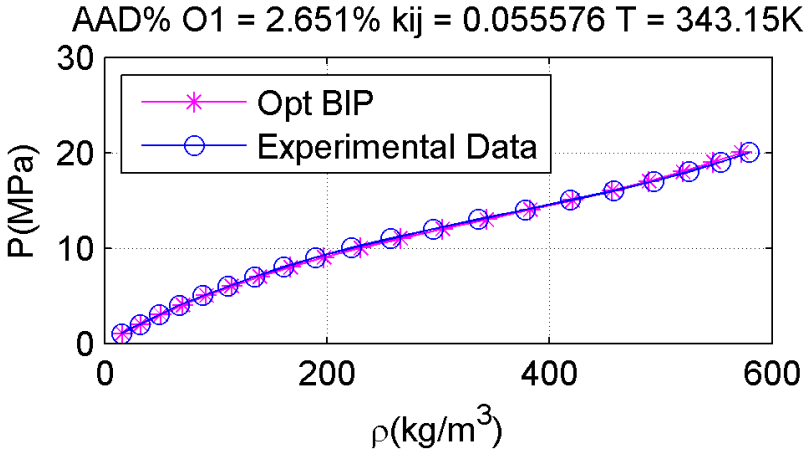

Figure 28: Mixture O1, T=343K

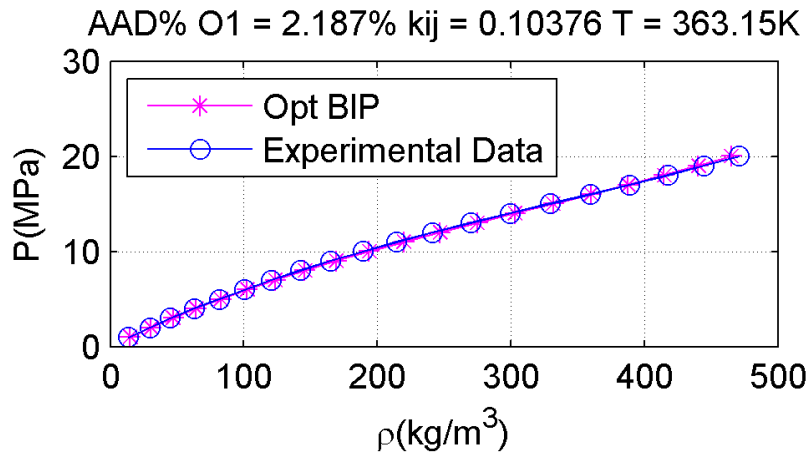

Figure 29: Mixture O1, T=363K

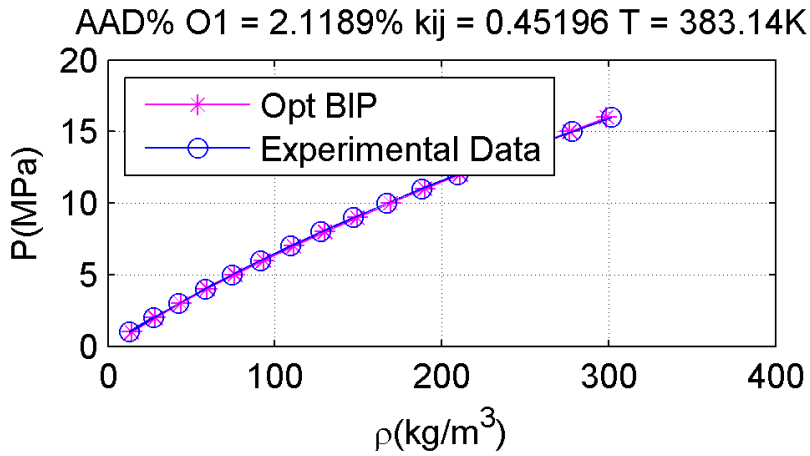

Figure 30: Mixture O1, T=383K

4.1.6. Plots Mixture O1

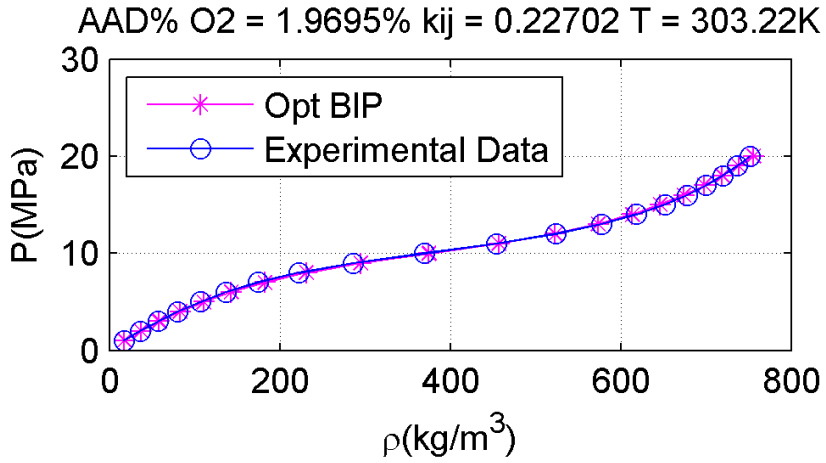

Figure 31: Mixture O2, T=303K

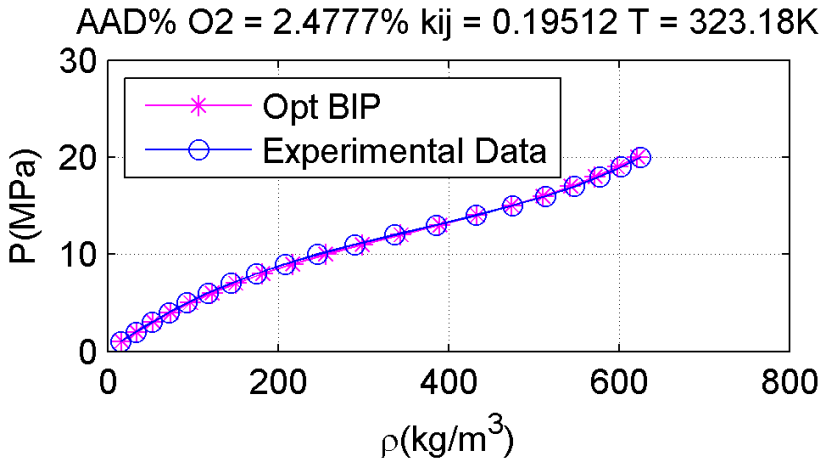

Figure 32: Mixture O2, T=323K

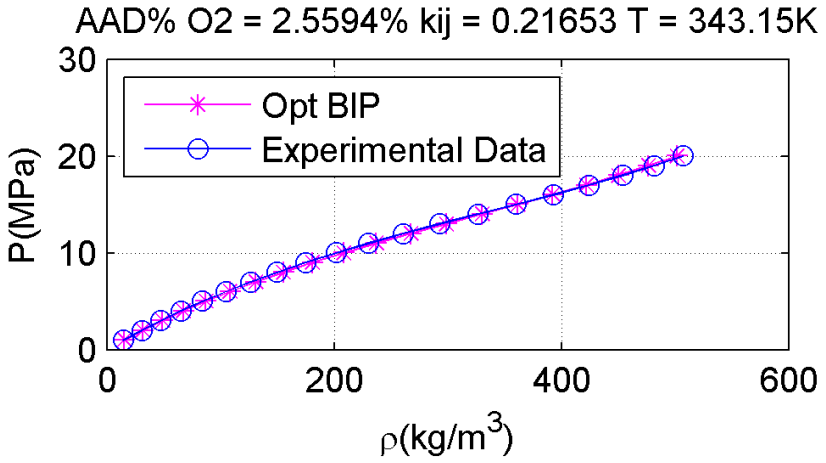

Figure 33: Mixture O2, T=343K

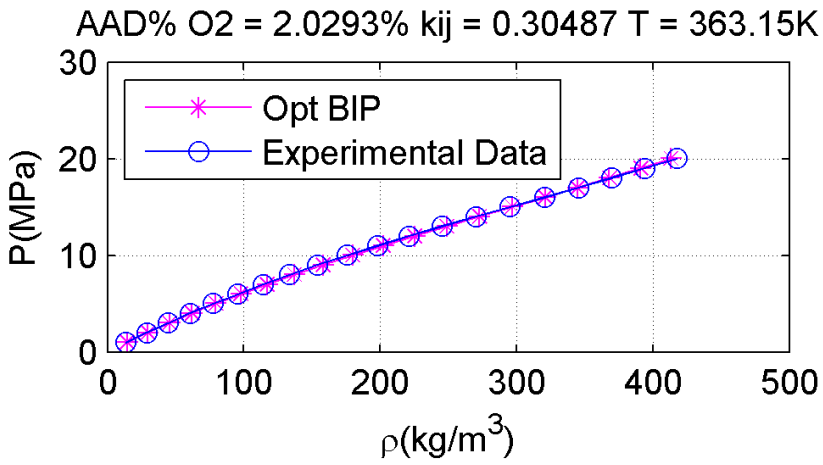

Figure 34: Mixture O2, T=363K

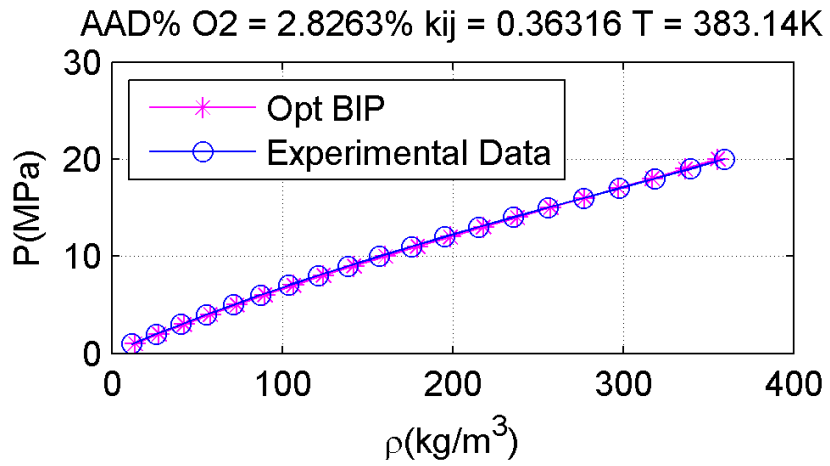

Figure 35: Mixture O2, T=383K

4.1.7. Explanation of the Plots

Overall, from the plots (Fig 6 to 17), it can be seen that a good agreement has been obtained with the Peng-Robinson EoS model for all mixtures. The deviation for each curve remained around 2% (overall, between 1.2107% and 2.8263%). Furthermore, the BIP values showed a strong dependence on the temperature. This fact can be seen in the following plot, where the BIP values for each temperature are plotted for the mixture N1:

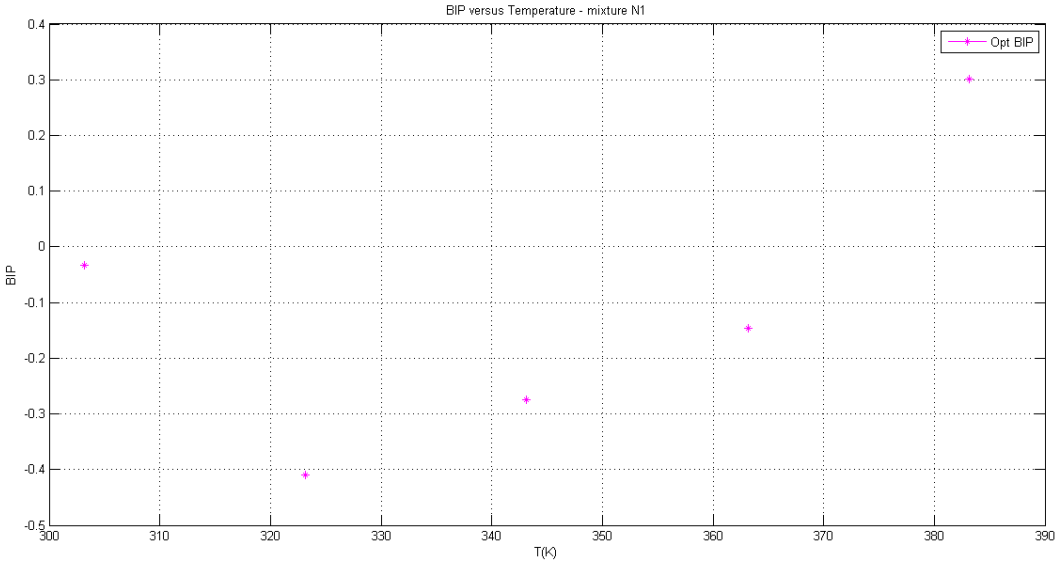

Figure 36: BIPxT Mixture N1

The numerical results of the isotherm plots presented above are summarized in the tables below:

Table 14: Numerical Results - Mixtures N1&N2

N1 Mixture					
T	303,22	323,18	343,15	363,15	383,14
bip	-0,0329	-0,4098	-0,2751	-0,1460	0,3012
AAD%	2,1314	2,4696	2,4280	1,8377	1,9165

N2 Mixture					
T	303,22	323,18	343,15	363,15	383,14
bip	-0,0829	-0,1379	-0,1316	-0,0867	-0,0368
AAD%	1,8101	2,1642	2,5273	1,9485	2,0336

Table 15: Numerical Results - Mixtures O1&O2

O1 Mixture					
T	303,22	323,18	343,15	363,15	383,14
bip	0,1581	0,0427	0,0556	0,1038	0,4520
AAD%	2,1071	2,2947	2,6510	2,1870	2,1189

O2 Mixture					
T	303,22	323,18	343,15	363,15	383,14
bip	0,2270	0,1951	0,2165	0,3049	0,3632
AAD%	1,9695	2,4777	2,5594	2,0293	2,8263

Table 16: Numerical Results - Mixtures A1&A2

A1 Mixture					
T	303,22	323,18	343,15	363,15	383,14
bip	0,0155	-0,3569	-0,4131	-0,3543	0,0052
AAD%	2,4831	2,6002	2,5613	1,9056	1,2107

A2 Mixture					
T	303,22	323,18	343,15	363,15	383,14
bip	-0,0296	0,0871	0,1103	0,2214	0,1452
AAD%	1,3244	2,0328	2,0769	1,4394	1,9973

From the fact that the BIP varies with the temperature, a following step in the optimization is to introduce an explicit expression for the BIP in function of the temperature.

4.2. T-Dependent BIP

With Aspen Properties, the software used by Mantovani [12] to analyse the experimental data, it is possible to introduce the BIP's temperature dependency. In particular, the BIP's formulation is [8]:

$$BIP(T) = a + bT + \frac{c}{T} \quad \text{(Eq. 85.)}$$

where *a, b* and *c* are fitting parameters.

For the fitting of that expression, the Matlab command *fit* was used with a non-linear least square algorithm. For each mixture (N1, N2, A1, A2, O1, and O2) the optimum BIP values (one for each temperature, thus, five for each mixture) were used for the regression. From that, the parameters *a, b* and c (Eq. 85.) were obtained and used for the calculation of the new BIPs (one for each isotherm). Then, the isotherm curves were re-plotted with these new BIPs to analyze their impact in the model.

It is important to be aware that, since the regression introduces errors (the curve is the one that best fits the set of data in the least square sense, not necessarily passing through any of the optimum BIP points), a higher total deviation is expected. Nonetheless, having a direct correlation between BIP and temperature is important, since it provides an expression from which a BIP can be estimated for any temperature inside the range of the experimental data from which it has been regressed.

In the following plots (Fig 13 to 18), the BIP fitting is presented, followed by the newly calculated isotherms using the (Eq. 86.):

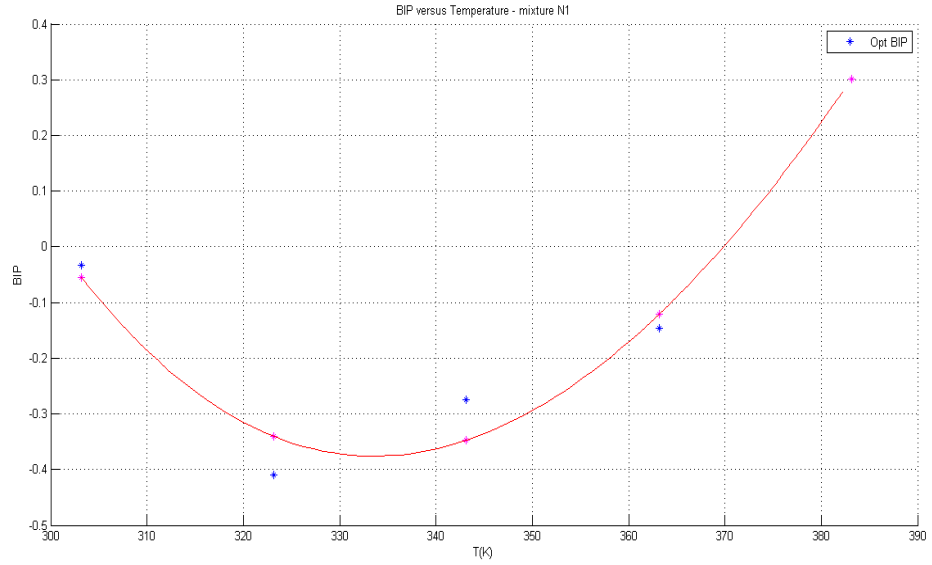

Figure 37: BIPxT Regressed - N1

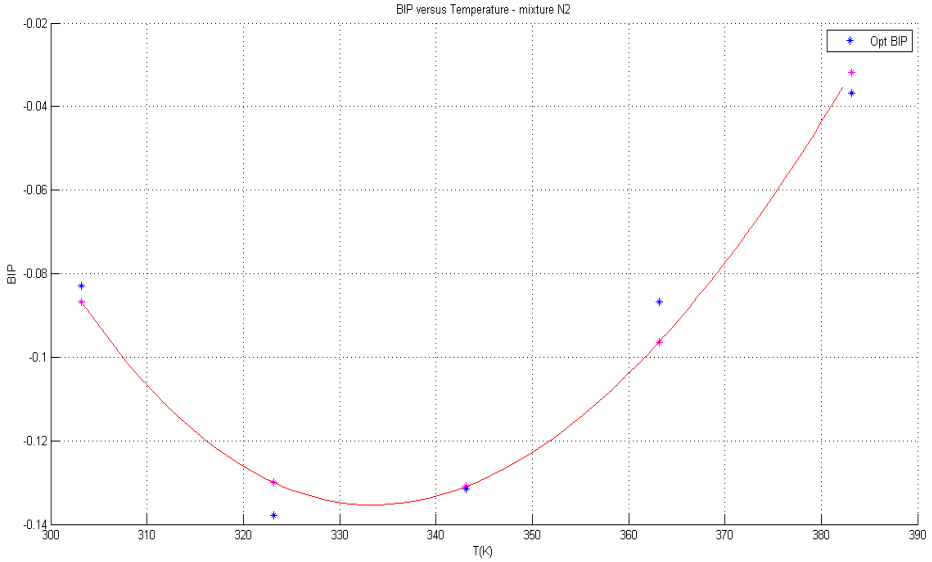

Figure 38: BIPxT Regressed – N2

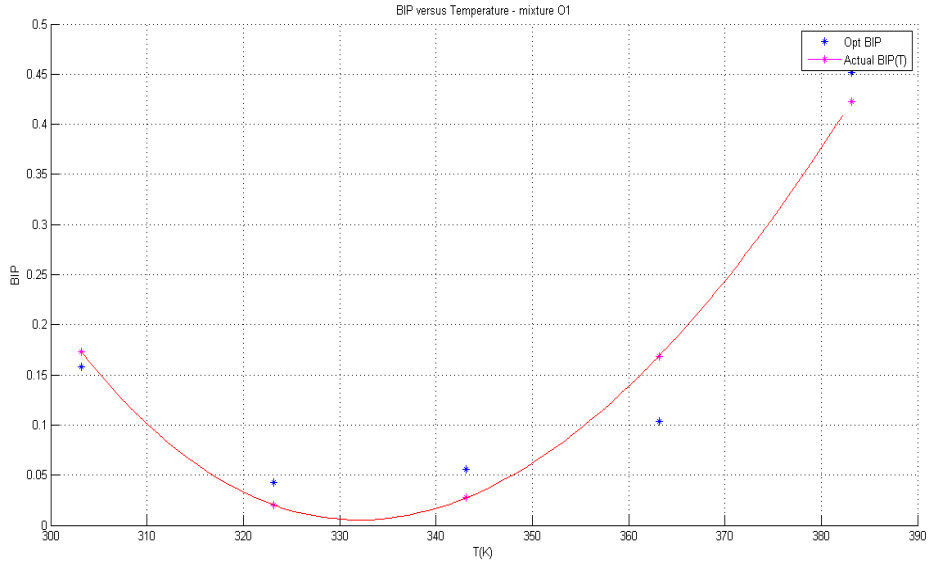

Figure 39: BIPxT Regressed - O1

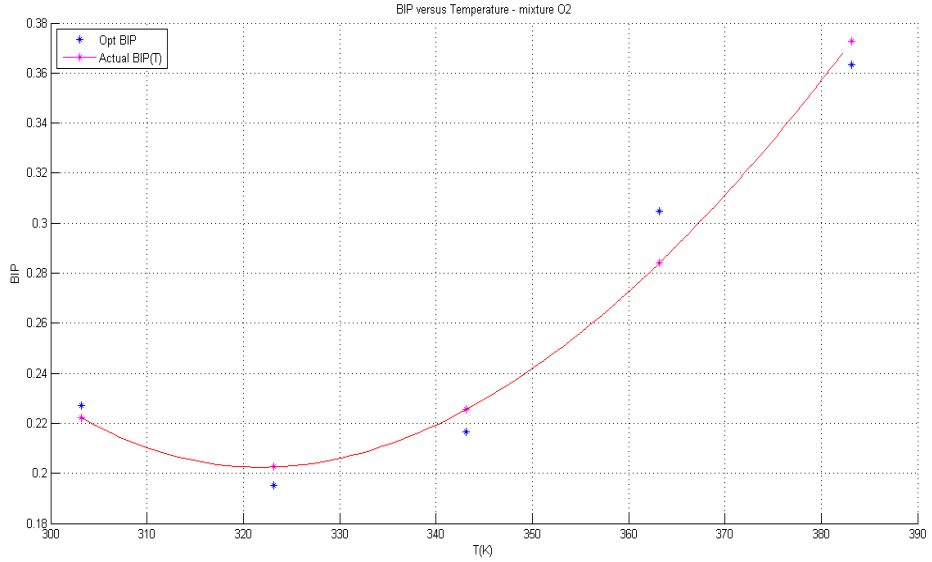

Figure 40: BIPxT Regressed - O2

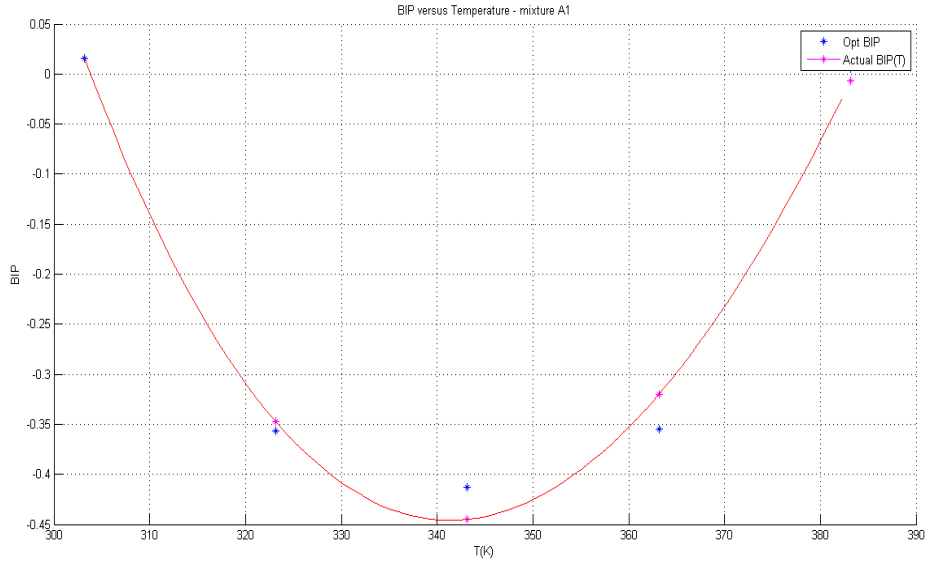

Figure 41: BIPxT Regressed - A1

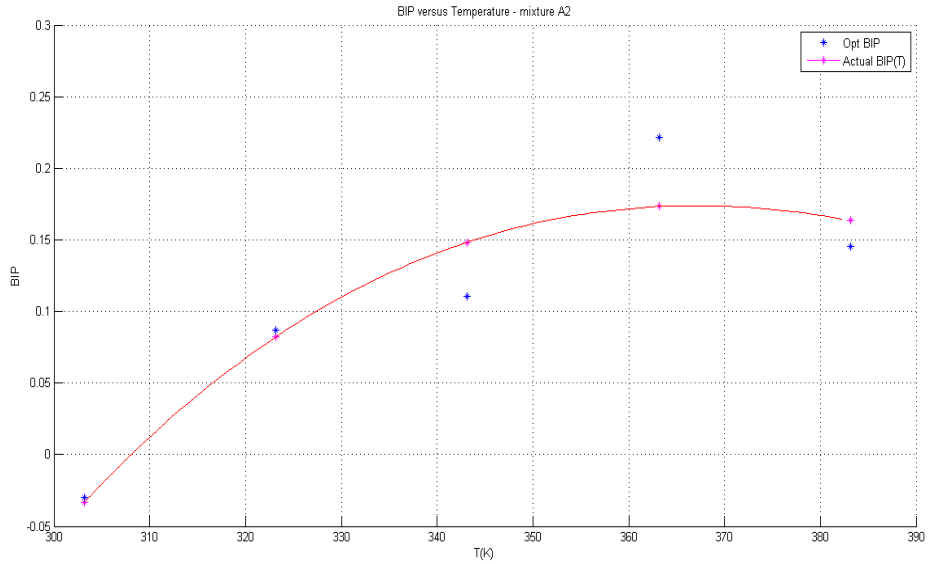

Figure 42: BIPxT Regressed - A2

Where the blue points are the optimum BIP previously calculated, the red curve is the one obtained from the regression using (Eq. 86.) and the magenta points are the actual points used for the calculation. The resulting isotherm curves are presented in the following plots (Fig 19 to 24):

4.2.1. Plots Mixture N1

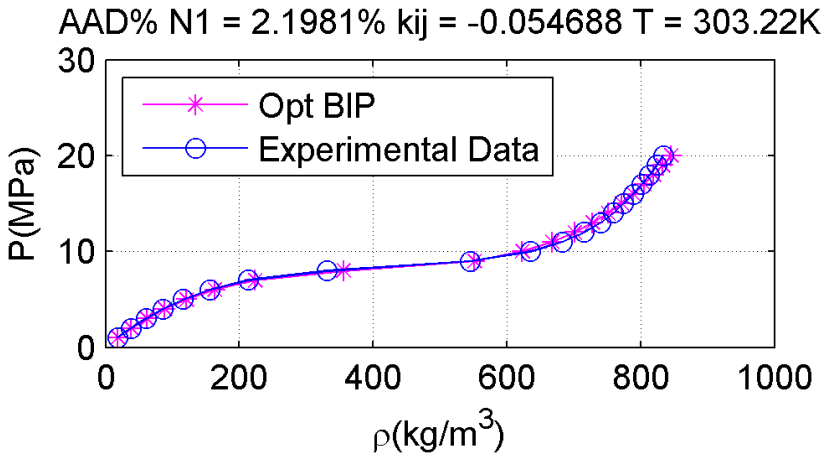

Figure 43: Mixture N1, T=303K, BIP(T)

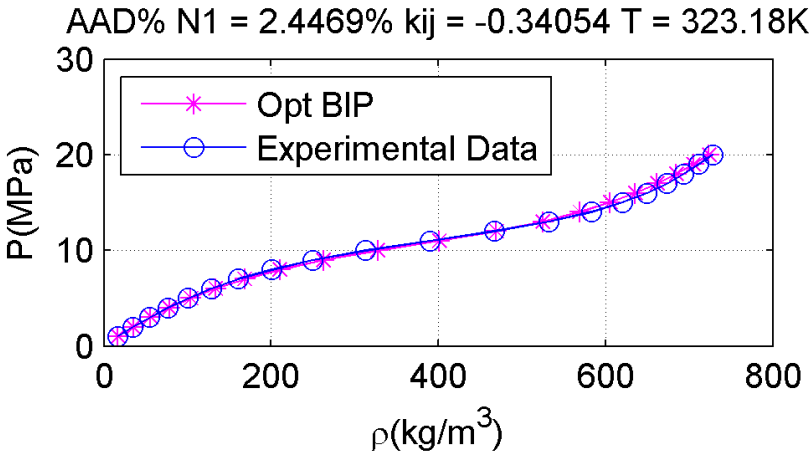

Figure 44: Mixture N1, T=323K, BIP(T)

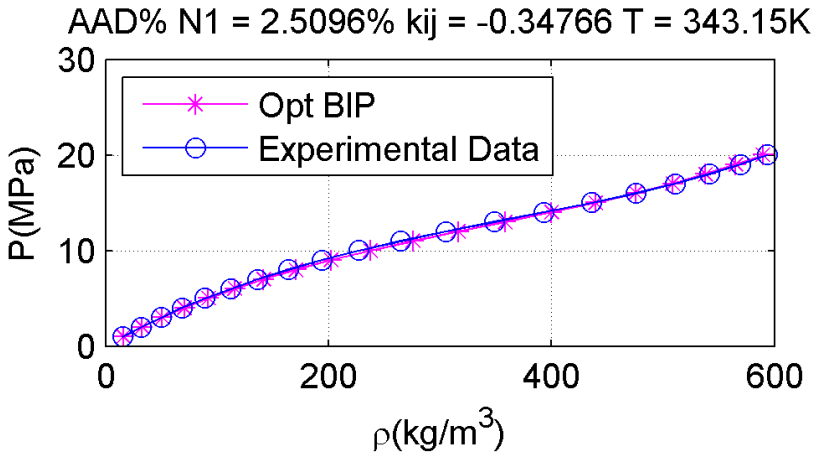

Figure 45: Mixture N1, T=343K, BIP(T)

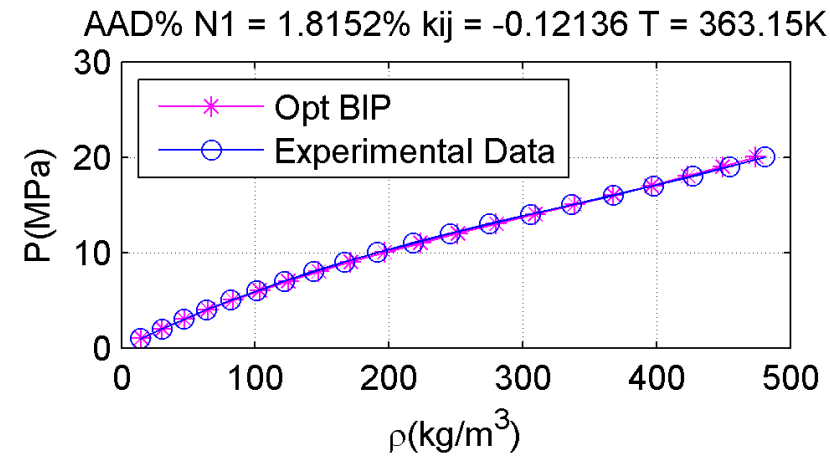

Figure 46: Mixture N1, T=363K, BIP(T)

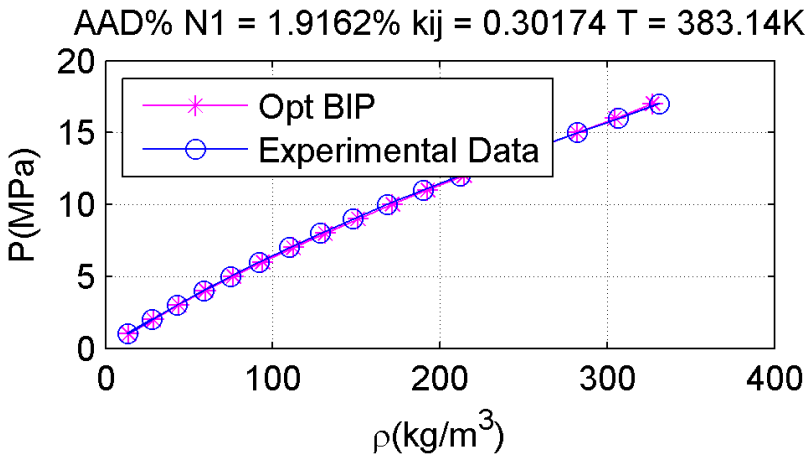

Figure 47: Mixture N1, T=383K, BIP(T)

4.2.2. Plots Mixture N1

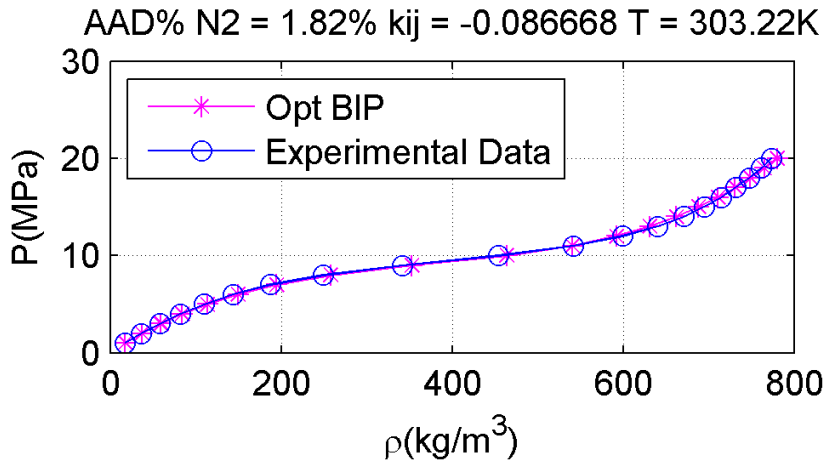

Figure 48: Mixture N2, T=303K, BIP(T)

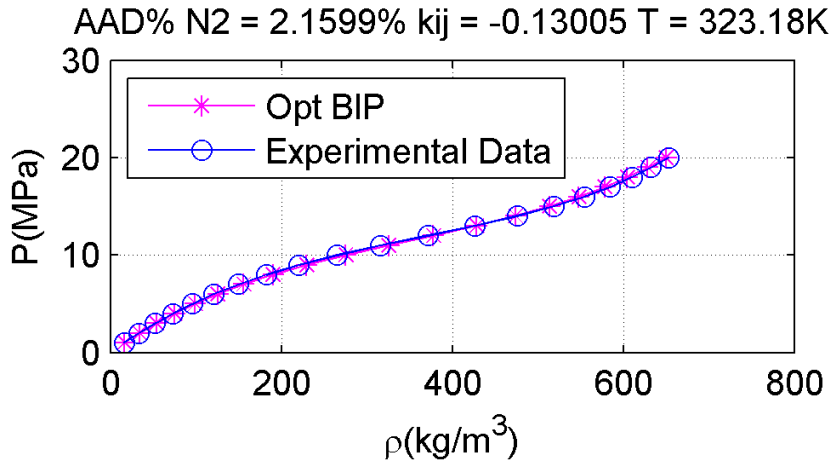

Figure 49: Mixture N2, T=323K, BIP(T)

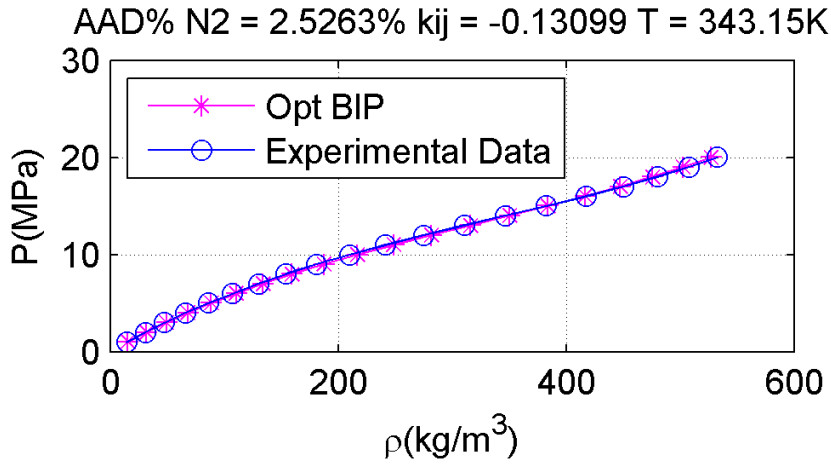

Figure 50: Mixture N2, T=343K, BIP(T)

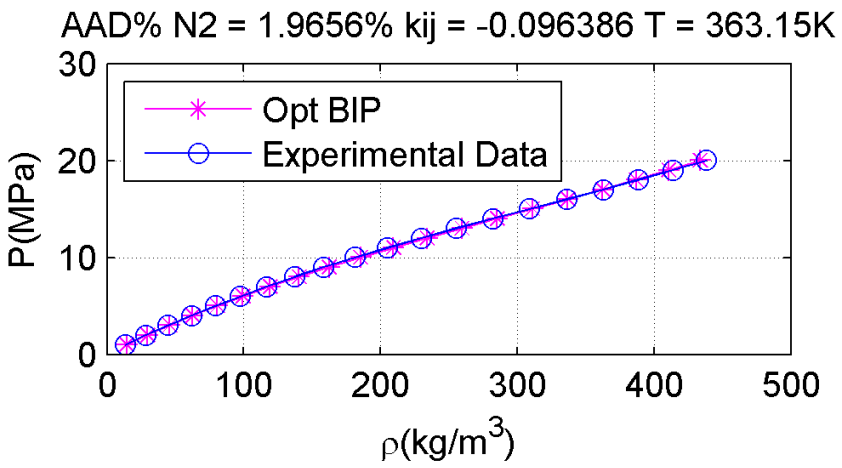

Figure 51: Mixture N2, T=363K, BIP(T)

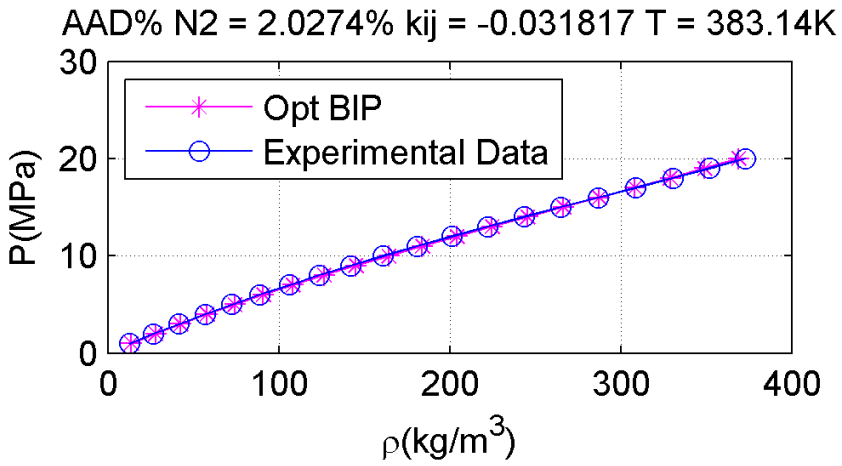

Figure 52: Mixture N2, T=383K, BIP(T)

4.2.3. Plots Mixture O1

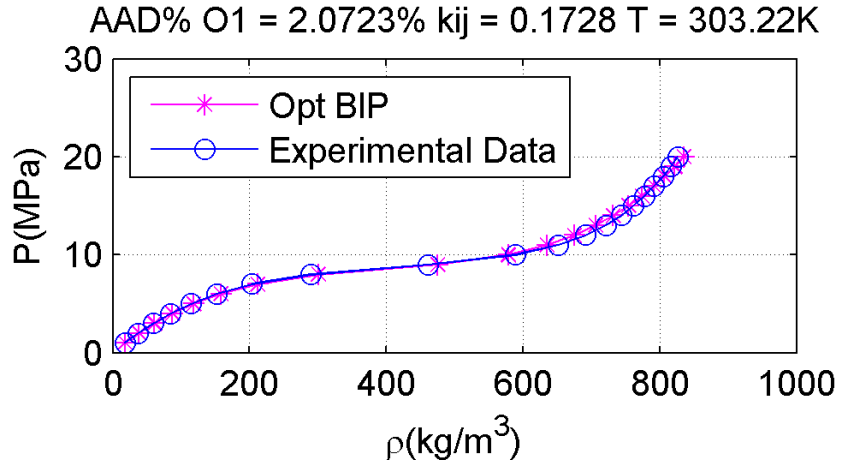

Figure 53: Mixture O1, T=303K, BIP(T)

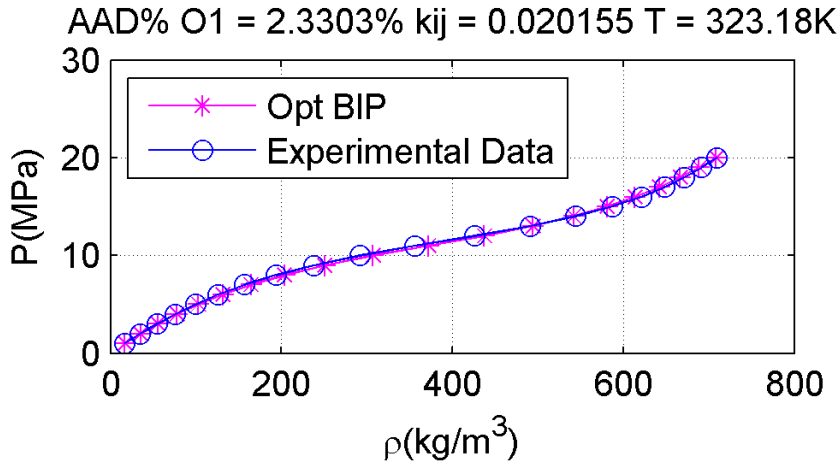

Figure 54: Mixture O1, T=323K, BIP(T)

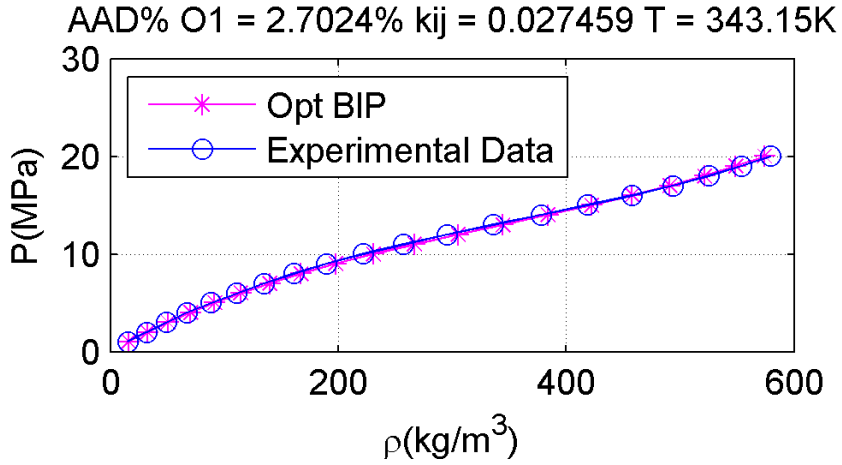

Figure 55: Mixture O1, T=343K, BIP(T)

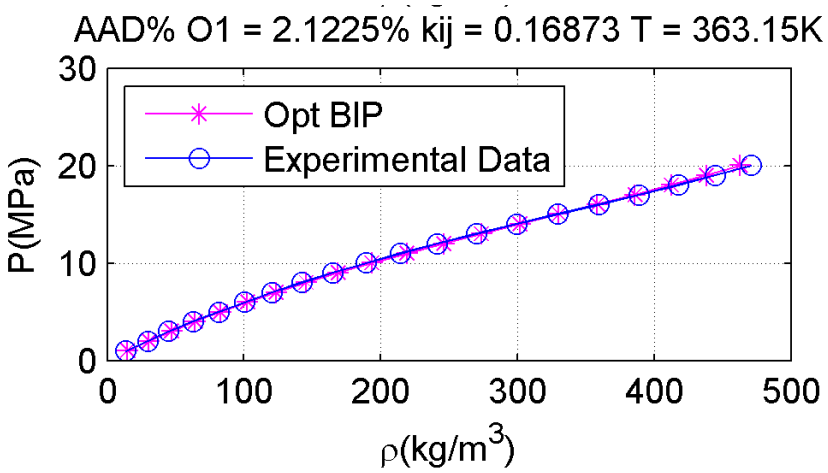

Figure 56: Mixture O1, T=363K, BIP(T)

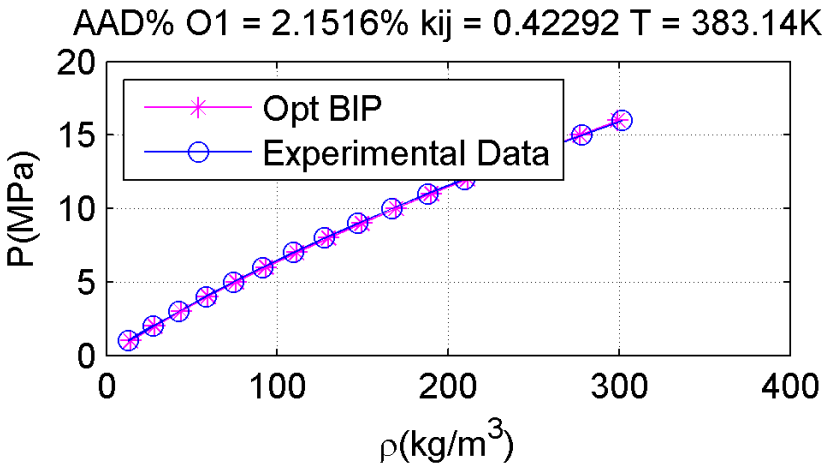

Figure 57: Mixture O1, T=383K, BIP(T)

4.2.4. Plots Mixture O2

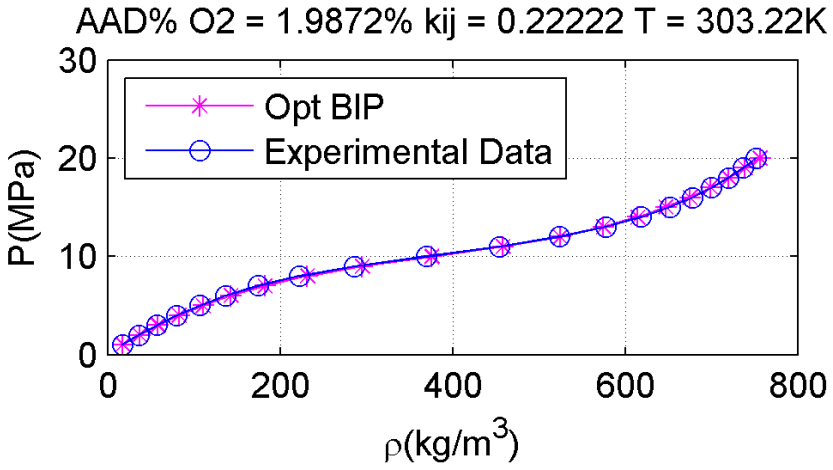

Figure 58: Mixture O2, T=303K, BIP(T)

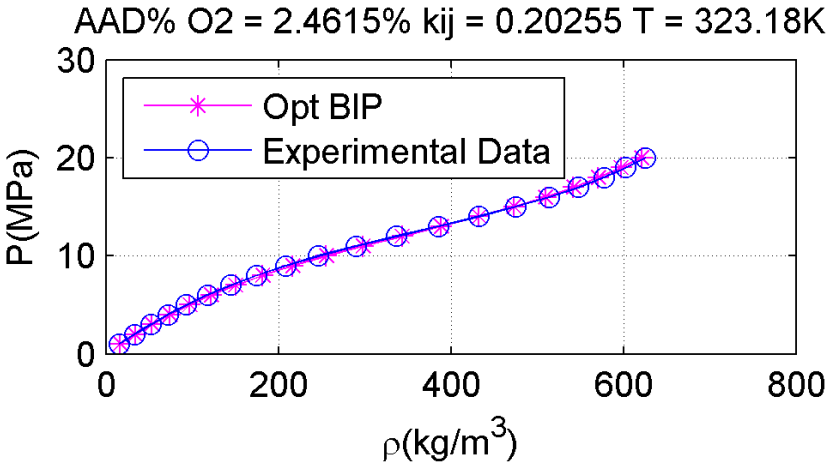

Figure 59: Mixture O2, T=323K, BIP(T)

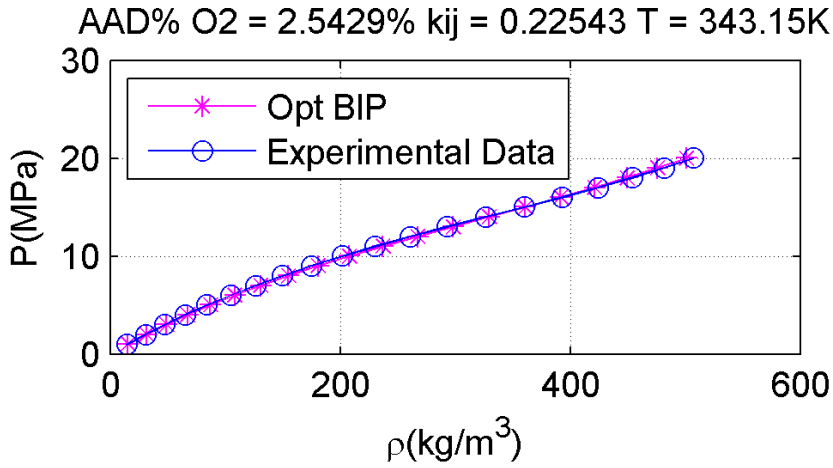

Figure 60: Mixture O2, T=343K, BIP(T)

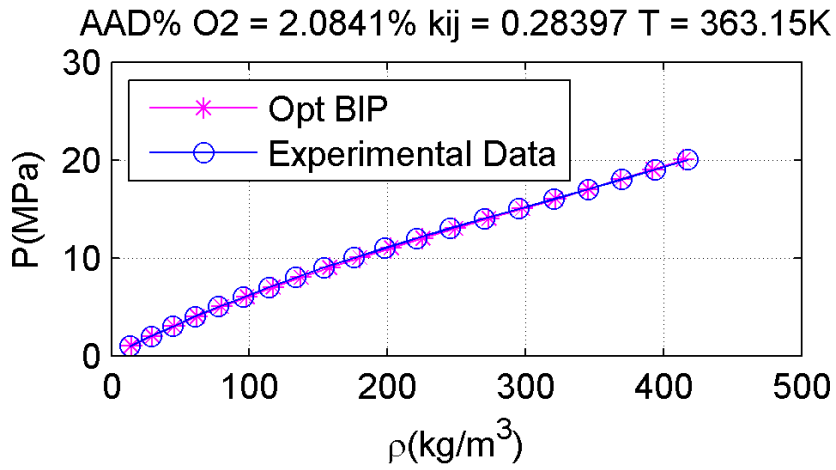

Figure 61: Mixture O2, T=363K, BIP(T)

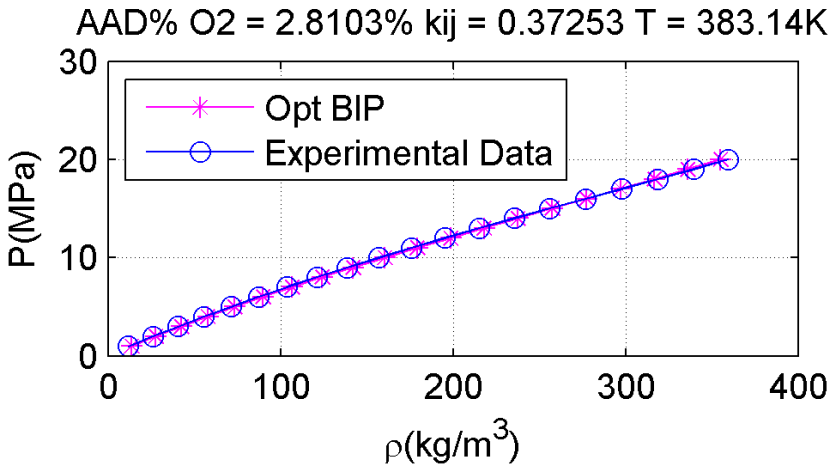

Figure 62: Mixture O2, T=383K, BIP(T)

4.2.5. Plots Mixture A1

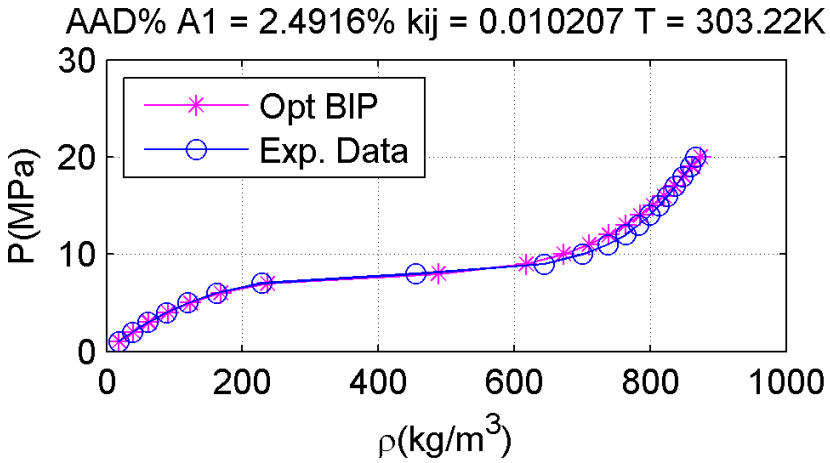

Figure 63: Mixture A1, T=303K, BIP(T)

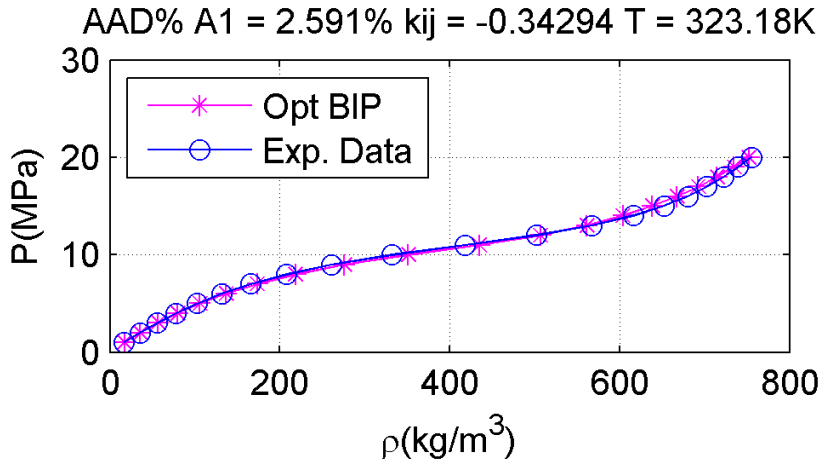

Figure 64: Mixture A1, T=323K, BIP(T)

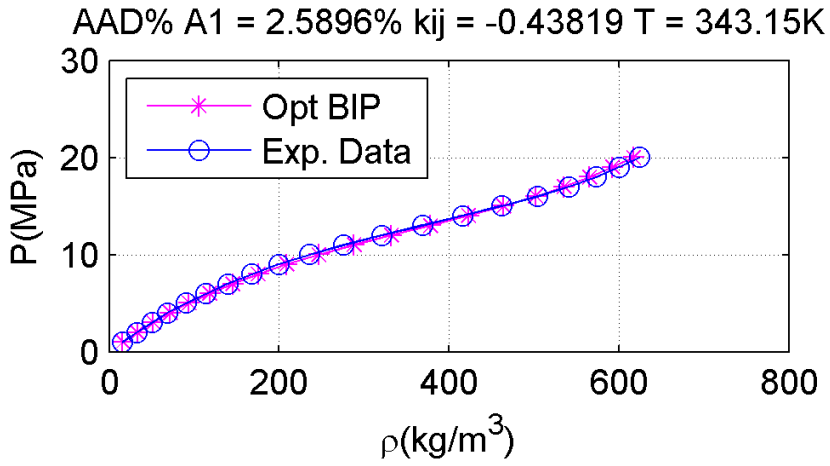

Figure 65: Mixture A1, T=343K, BIP(T)

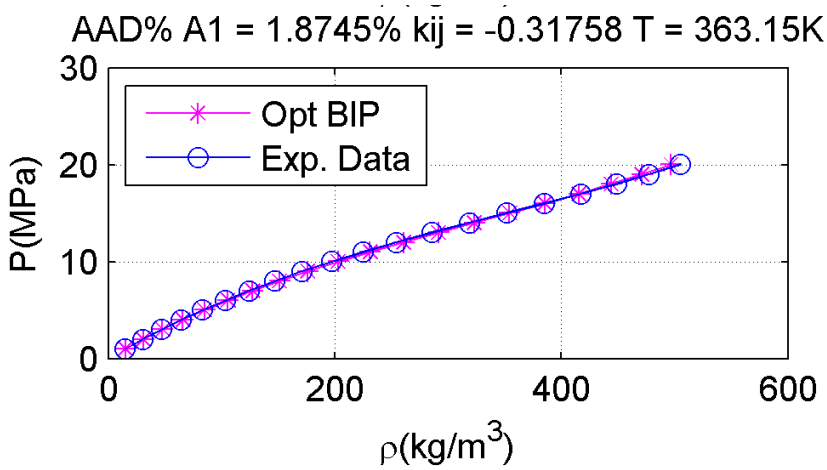

Figure 66: Mixture A1, T=363K, BIP(T)

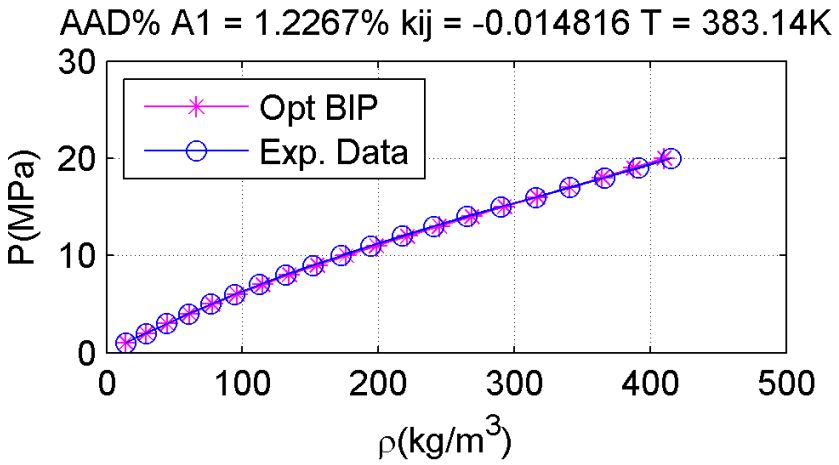

Figure 67: Mixture A1, T=383K, BIP(T)

4.2.6. Plots Mixture A2

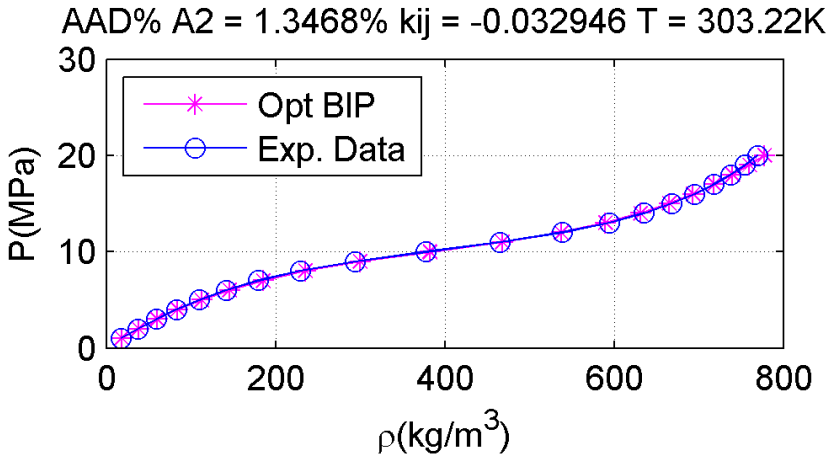

Figure 68: Mixture A2, T=303K, BIP(T)

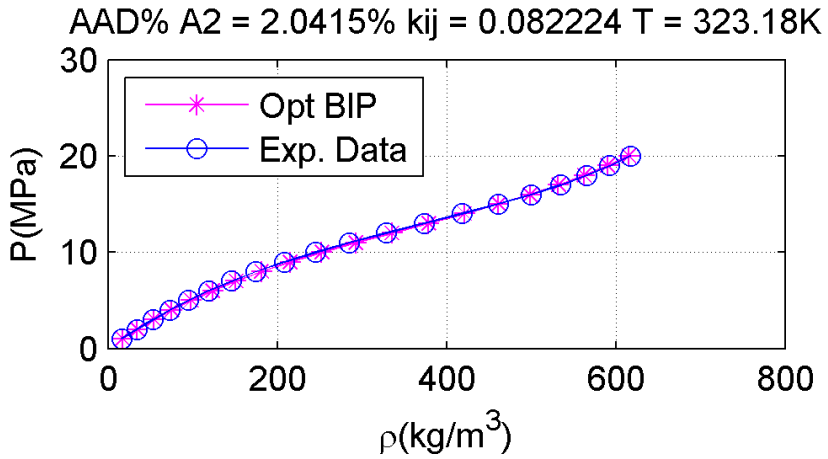

Figure 69: Mixture A2, T=323K, BIP(T)

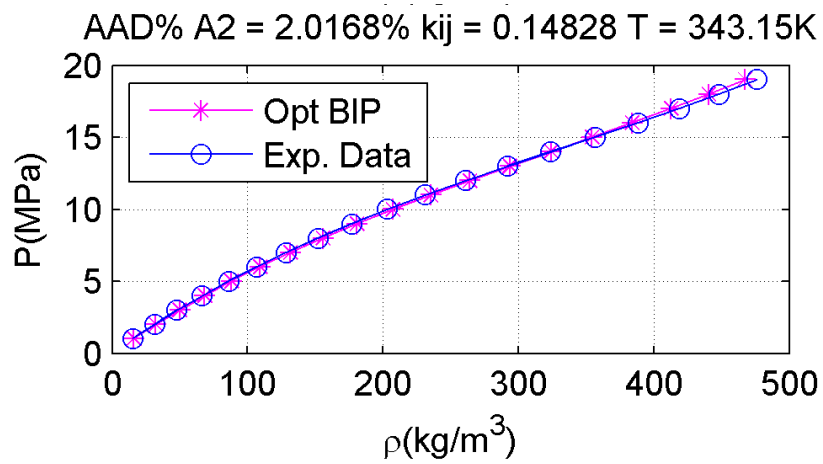

Figure 70: Mixture A2, T=343K, BIP(T)

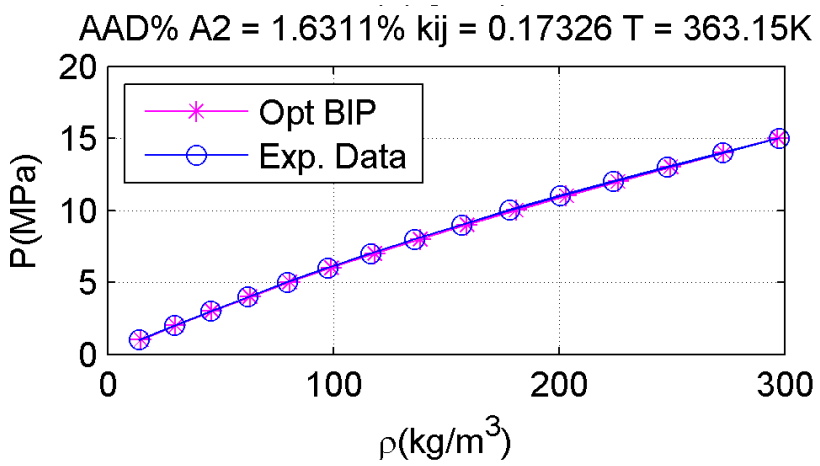

Figure 71: Mixture A2, T=363K, BIP(T)

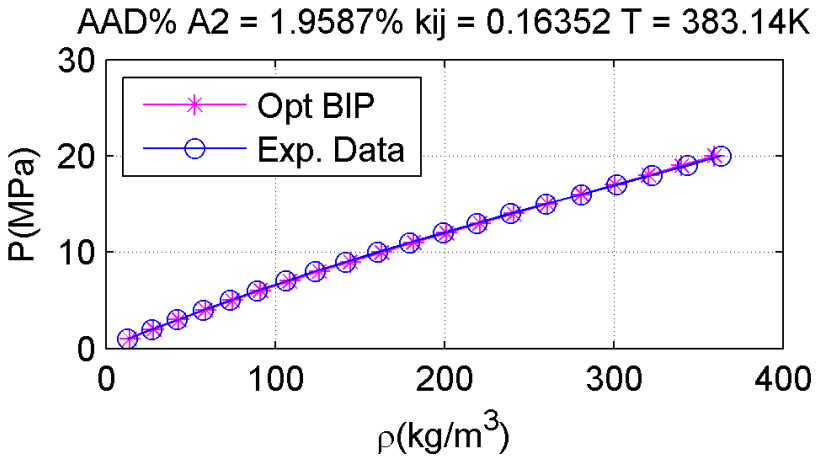

Figure 72: Mixture A2, T=383K, BIP(T)

4.2.7. Explanation of the Plots

Overall, it can be noted that with the introduction of the temperature dependence the deviation varied, but not greatly (figures 25 to 36) – it now varies from 1.2203% to 2.8103% (against 1.2107% to 2.8263% previously calculated).

The numerical results obtained for all mixtures – both with and without the use of the (Eq. 86.) are presented below:

Table 17 : Global Numerical Results - Mixtures N1&N2

N1 Mixture					
T	303,22	323,18	343,15	363,15	383,14
bip	-0,0329	-0,4098	-0,2751	-0,1460	0,3012
AAD%	2,1314	2,4696	2,4280	1,8377	1,9165
bip(T)	-0,0547	-0,3405	-0,3477	-0,1214	0,3017
AAD%	2,1981	2,4469	2,5096	1,8152	1,9162

N2 Mixture					
T	303,22	323,18	343,15	363,15	383,14
bip	-0,0829	-0,1379	-0,1316	-0,0867	-0,0368
AAD%	1,8101	2,1642	2,5273	1,9485	2,0336
bip(T)	-0,0867	-0,1300	-0,1310	-0,0964	-0,0318
AAD%	1,8200	2,1599	2,5263	1,9656	2,0274

Table 18 : Global Numerical Results - Mixtures O1&O2

O1 Mixture					
T	303,22	323,18	343,15	363,15	383,14
bip	0,1581	0,0427	0,0556	0,1038	0,4520
AAD%	2,1071	2,2947	2,6510	2,1870	2,1189
bip(T)	0,1728	0,0202	0,0275	0,1687	0,4229
AAD%	2,0723	2,3303	2,7024	2,1225	2,1516

O2 Mixture					
T	303,22	323,18	343,15	363,15	383,14
bip	0,2270	0,1951	0,2165	0,3049	0,3632
AAD%	1,9695	2,4777	2,5594	2,0293	2,8263
bip(T)	0,2222	0,2026	0,2254	0,2840	0,3725
AAD%	1,9872	2,4615	2,5429	2,0841	2,8103

Table 19: Global Numerical Results - Mixtures A1&A2

A1 Mixture					
T	303,22	323,18	343,15	363,15	383,14
bip	0,0155	-0,3569	-0,4131	-0,3543	0,0052
AAD%	2,4831	2,6002	2,5613	1,9056	1,2107
bip(T)	0,0158	-0,3475	-0,4450	-0,3199	-0,0071
AAD%	2,4826	2,5940	2,5973	1,8765	1,2203

A2 Mixture					
T	303,22	323,18	343,15	363,15	383,14
bip	-0,0296	0,0871	0,1103	0,2214	0,1452
AAD%	1,3244	2,0328	2,0769	1,4394	1,9973
bip(T)	-0,0329	0,0822	0,1483	0,1733	0,1635
AAD%	1,3468	2,0415	2,0168	1,6311	1,9587

The coefficients *a, b* and *c* of the (Eq. 86.) are:

- for the CO_2-N_2 mixture

$$mixture\ N1 \rightarrow a = -70.89, b = 0.1057, c = 11760$$

$$mixture\ N2 \rightarrow a = -10.87, b = 0.0161, c = 1791$$

- for the CO_2-O_2 mixture

$$mixture\ O1 \rightarrow a = -40.65, b = 0.06122, c = 6749$$

$$mixture\ O2 \rightarrow a = -10.95, b = 0.01733, c = 1795$$

- for the CO_2-Ar mixture

$$mixture\ A1 \rightarrow a = -66.18, b = 0.09628, c = 11220$$

$$mixture\ A2 \rightarrow a = 11.47, b = -0.01539, c = -2074\,.$$

4.3. Robustness Analysis – Tolerance, Algorithm and Starting Point

For the results presented so far, the non-linear curve fitting was obtained with the following parameters:

$$Tolerance = 10^{-6}$$

$$Algorithm = Levemberg - Marquardt$$

$$BIP^{(0)} = -0.5$$

Now, to understand the robustness of the results obtained so far, those parameters are varied and the change in the deviation is analyzed.

4.3.1. Tolerance

To analyze the impact of the tolerance in the optimization, the tolerance was varied between four values: 10^{-3}, 10^{-6}, 10^{-9} and 10^{-12} for the N1 mixture. The resulting optimum BIP and AAD% were compared using the relative difference of the average values of the BIP and AAD% for each tolerance, having the value 10^{-6} (the default used in the non-linear curve fitting Matlab algorithm) as a reference. The results are shown in the following table:

Table 20: Sensitivity Analysis - Tolerance

N1 Mixture						
T(K)	303,22	323,18	343,15	363,15	383,14	Relative Difference of Avg
Tol = 1e-3						
bip	-0,032547	-0,409723	-0,275097	-0,145965	0,301135	-0,0562%
AAD%	2,130532	2,469583	2,428011	1,837681	1,916503	-0,0082%
Tol = 1e-6						
bip	-0,032873	-0,409818	-0,275097	-0,145953	0,301229	reference
AAD%	2,131443	2,469618	2,428011	1,837671	1,916450	reference
Tol = 1e-9						
bip	-0,032878	-0,409815	-0,275102	-0,145953	0,301229	0,0010%
AAD%	2,131456	2,469617	2,428017	1,837671	1,916449	0,0002%
Tol = 1e-12						
bip	-0,032877	-0,409815	-0,275102	-0,145953	0,301229	0,0009%
AAD%	2,131455	2,469617	2,428017	1,837671	1,916449	0,0001%

Where the relative difference of average is calculated as:

$$RDA\% = \frac{avg\left(BIP_i(tol_j)\right) - avg\left(BIP_i(tol_{ref})\right)}{avg\left(BIP_i(tol_{ref})\right)} \quad \text{(Eq. 86.)}$$

and the average is calculated for all the five temperatures *i* calculated using each tolerance *j*.

Those values can be summarized in the following plot, where it becomes clear that decreasing the tolerance – from the default 10^{-6} as a reference - does not bring significant improvement in the prediction of the optimum BIP using the non-linear curve fitting algorithm:

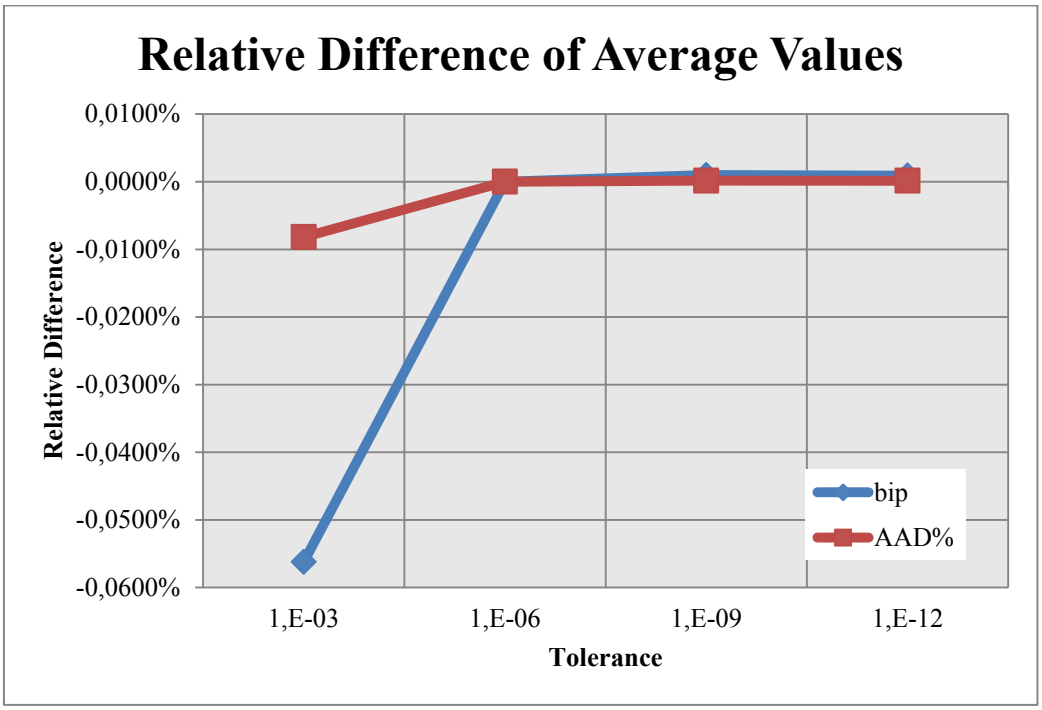

Figure 73: Sensitivity Analysis – Tolerance

4.3.2. Algorithm

The two algorithms compared are the trust-region and the Levemberg-Marquandt, because both are built-in components of the non-linear curve fitting in Matlab. For that simulation, the tolerance is be set to the default (10^{-6}), and no difference was observed for the N1 or N2 mixtures, as it can be seen in the following table:

Table 21: Mixture N1&N2 for different optimization algorithms

N1 Mixture					
T	303,22	323,18	343,15	363,15	383,14
Levemberg-Marquandt					
bip	-0,032873	-0,409818	-0,275097	-0,145953	0,301229
AAD%	2,131443	2,469618	2,428011	1,837671	1,916450
Trust-Region					
bip	-0,032873	-0,409818	-0,275097	-0,145953	0,301229
AAD%	2,131443	2,469618	2,428011	1,837671	1,916450
N2 Mixture					
T	303,22	323,18	343,15	363,15	383,14
Levemberg-Marquandt					
bip	-0,082881	-0,137911	-0,131629	-0,086654	-0,036833
AAD%	1,810053	2,164249	2,527314	1,948463	2,033574
Trust-Region					
bip	-0,082881	-0,137911	-0,131629	-0,086654	-0,036833
AAD%	1,810053	2,164249	2,527314	1,948463	2,033574

4.3.3. Initial value of BIP

The initial value of the BIP used for the optimization has not affected the results as well. The initial values of -15, -5, 0, 5, and 15 have been tested for all mixtures, with no change in the results.

4.4. Sensitivity Analysis – Variation of the BIP

Now, the variation of the isotherms and deviation (AAD%) will be tested against the variation of the BIP. The BIP values were changed in the range -1 to 1 (with more values in between for the AAD% plots than for the Isotherms to make the visualization easier), because that is the range of values usually found for that parameter. The following curves were obtained, where every pair shows the calculated pressure for each isotherm in the first plot and the deviation for each isotherm in the second one - where the red circle shows the minimum deviation – for every mixture, N1, N2, O1, O2 , A1 and A2:

4.4.1. Plots Mixture N1

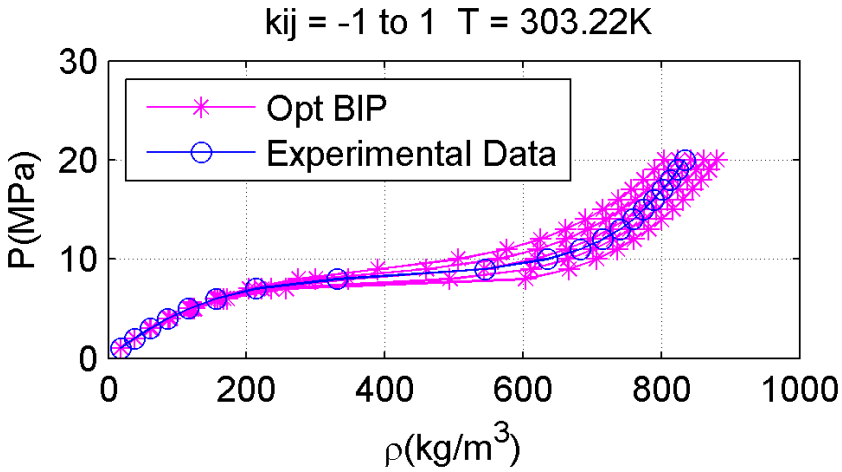

Figure 74: Variation of BIP – mixture N1 - 303K

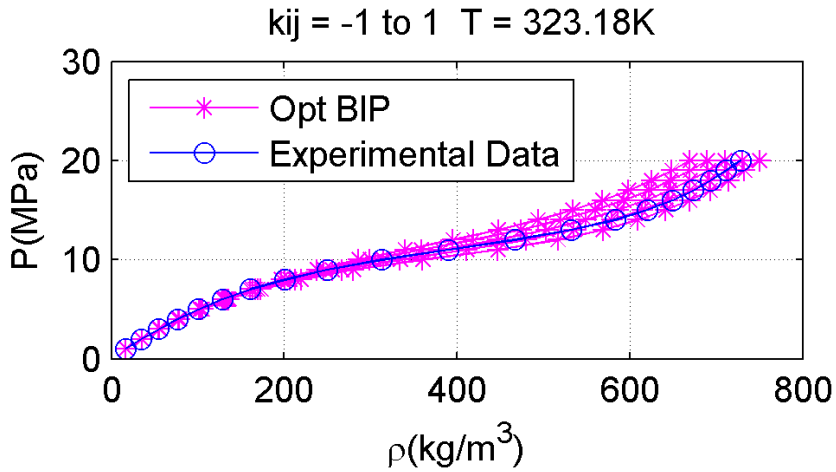

Figure 75: Variation of BIP – mixture N1 - 323K

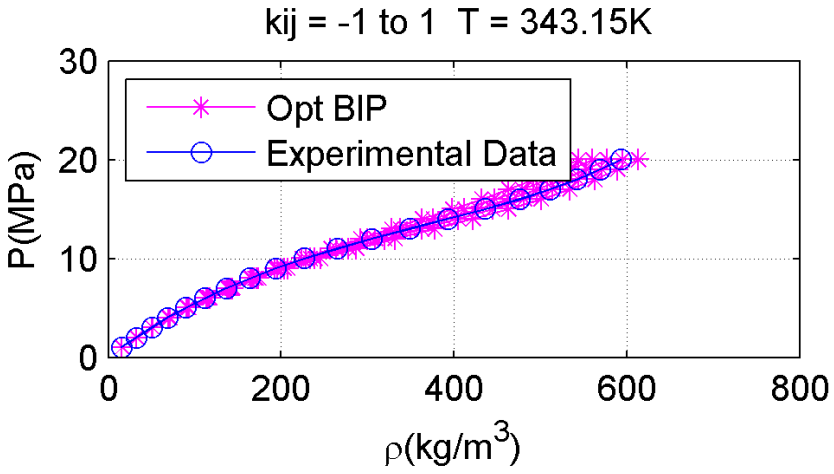

Figure 76: Variation of BIP – mixture N1 - 343K

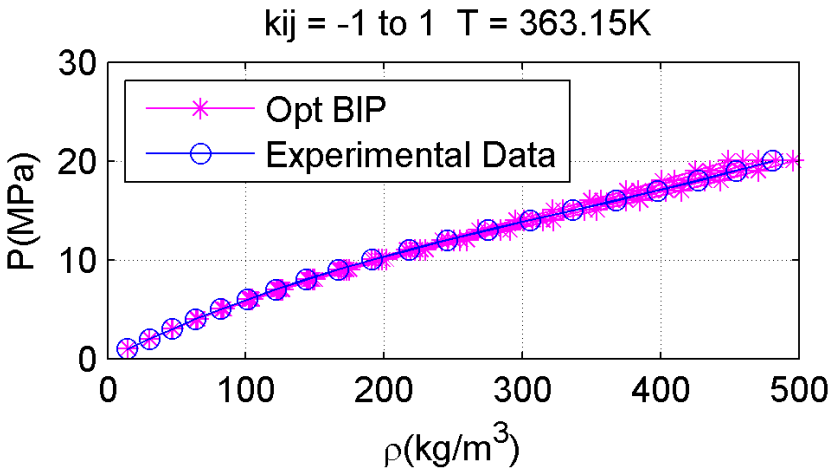

Figure 77: Variation of BIP – mixture N1 - 363K

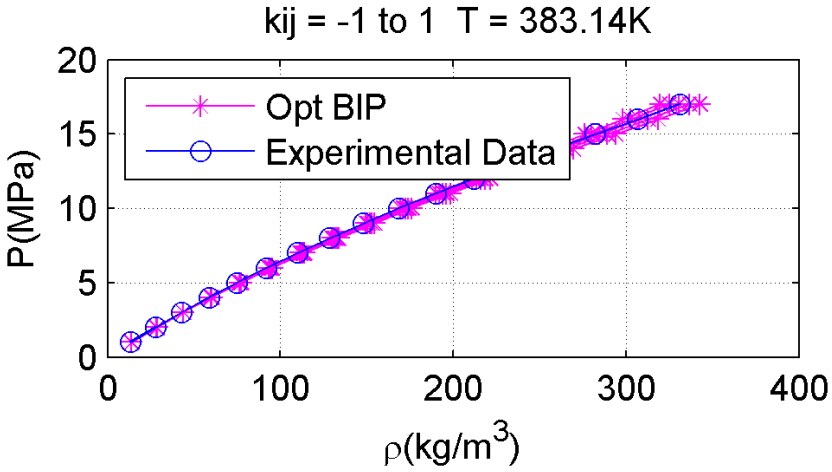

Figure 78: Variation of BIP – mixture N1 - 383K

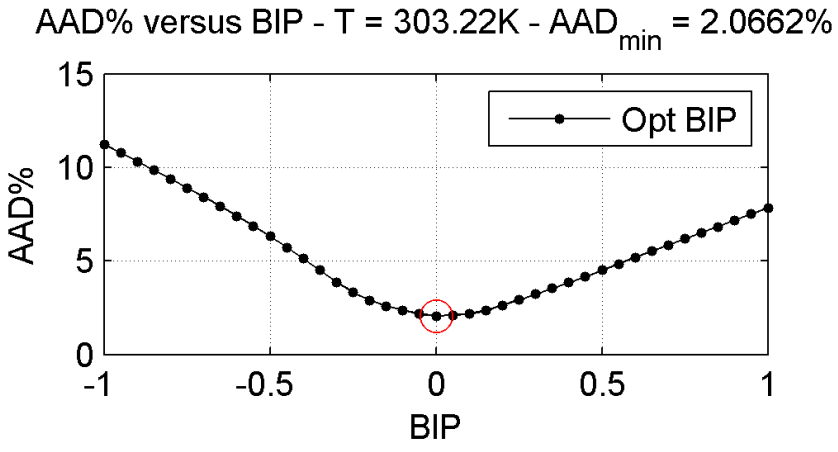

Figure 79: AAD% Variation with BIP – mixture N1 - 303K

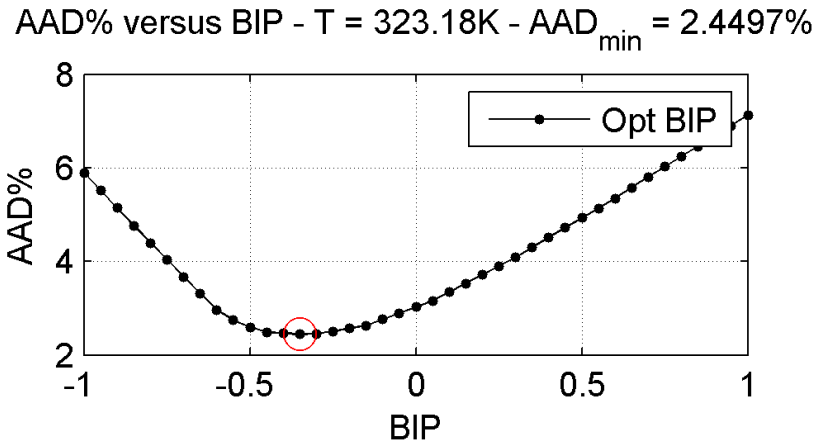

Figure 80: AAD% Variation with BIP – mixture N1 - 323K

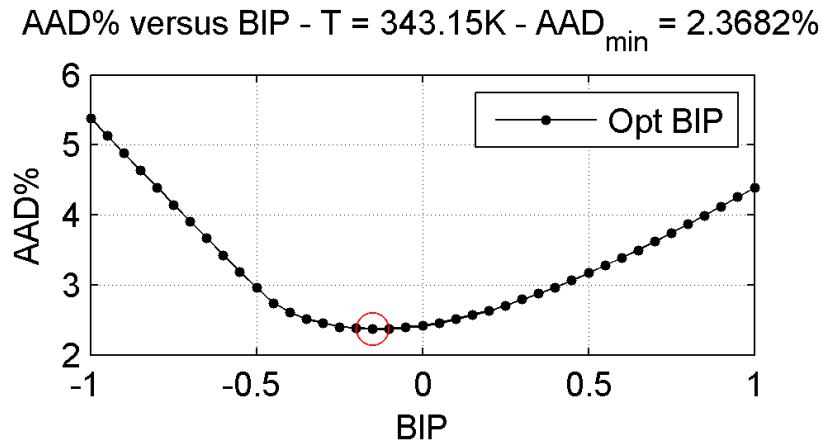

Figure 81: AAD% Variation with BIP – mixture N1 - 343K

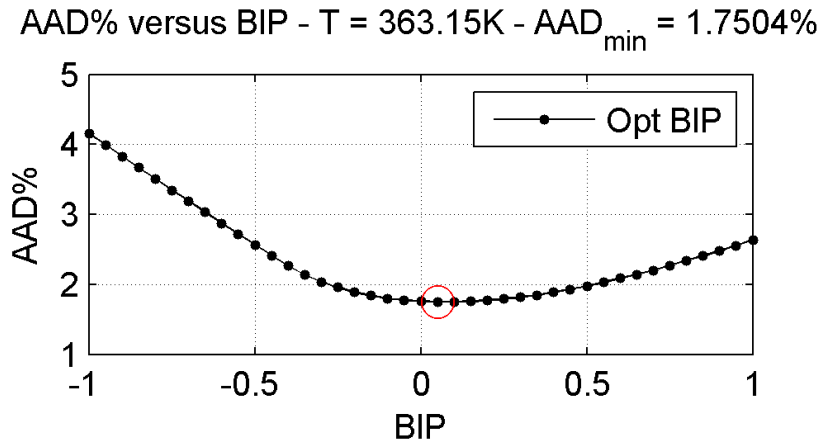

Figure 82: AAD% Variation with BIP – mixture N1 - 363K

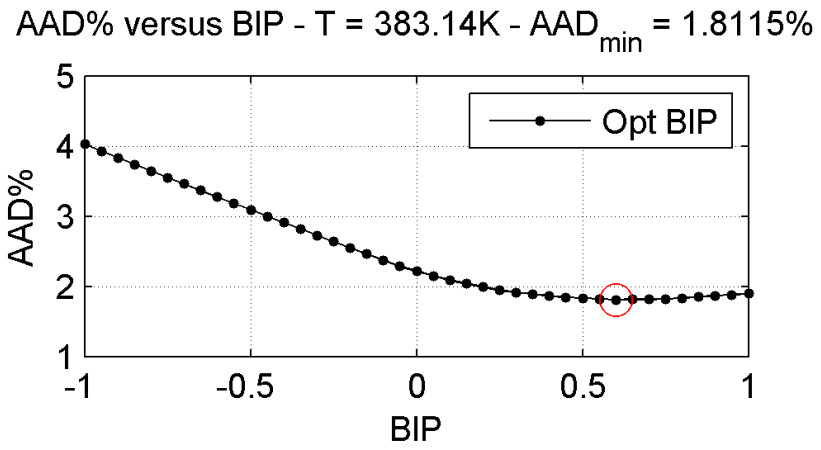

Figure 83: AAD% Variation with BIP – mixture N1 - 383K

4.4.2. Plots Mixture N2

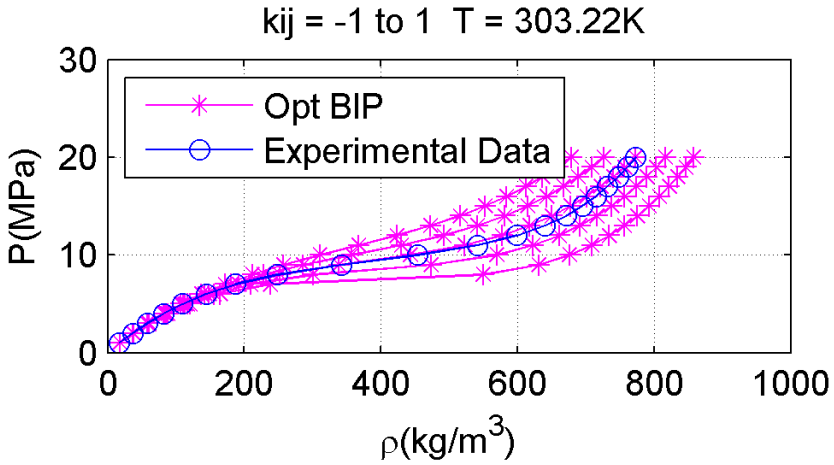

Figure 84: Variation of BIP – mixture N2 - 303K

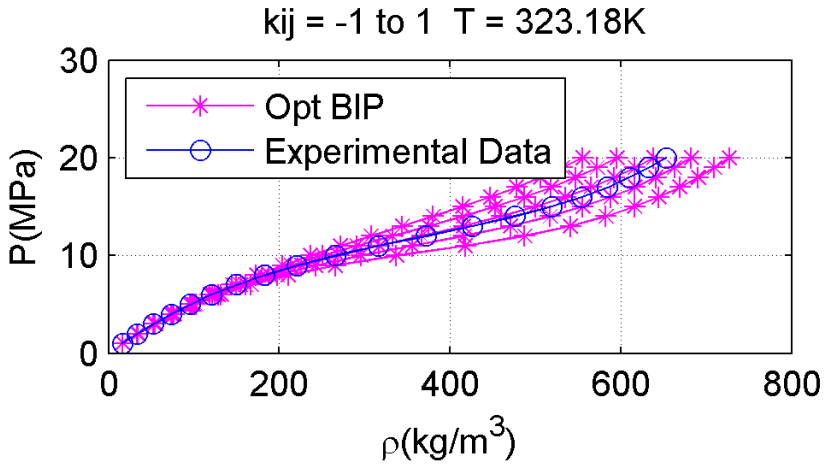

Figure 85: Variation of BIP – mixture N2 - 323K

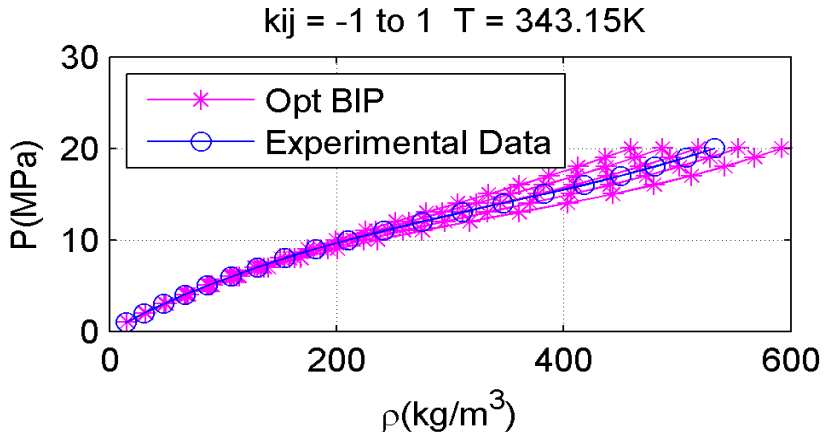

Figure 86: Variation of BIP – mixture N2 - 343K

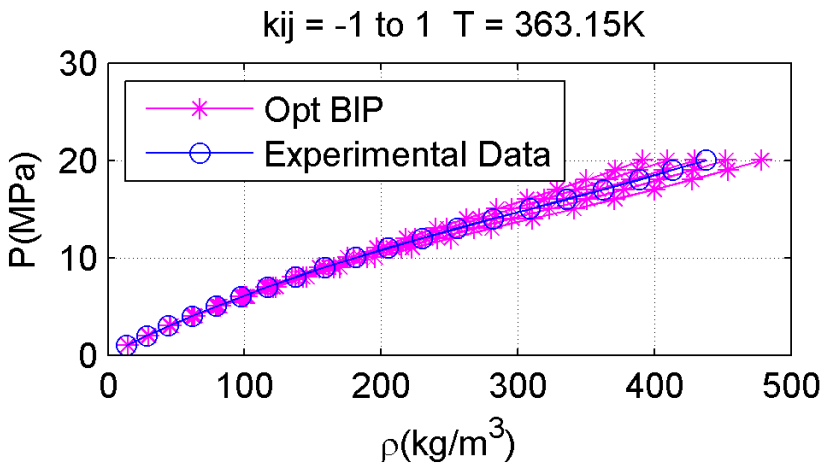

Figure 87: Variation of BIP – mixture N2 - 363K

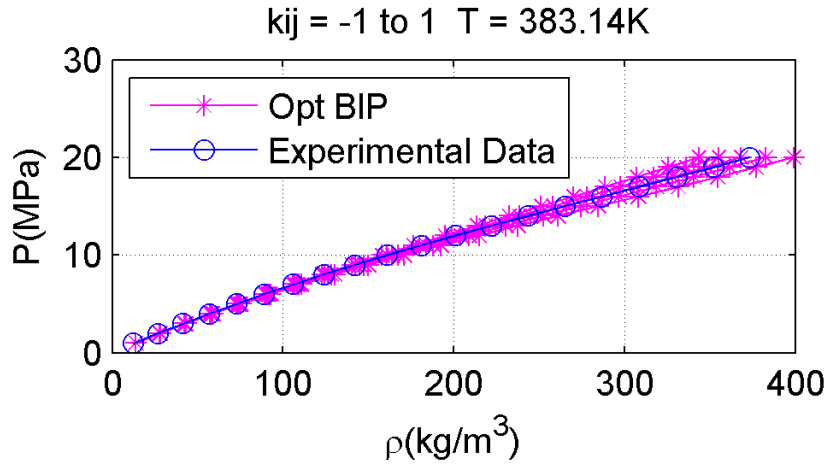

Figure 88: Variation of BIP – mixture N2 - 383K

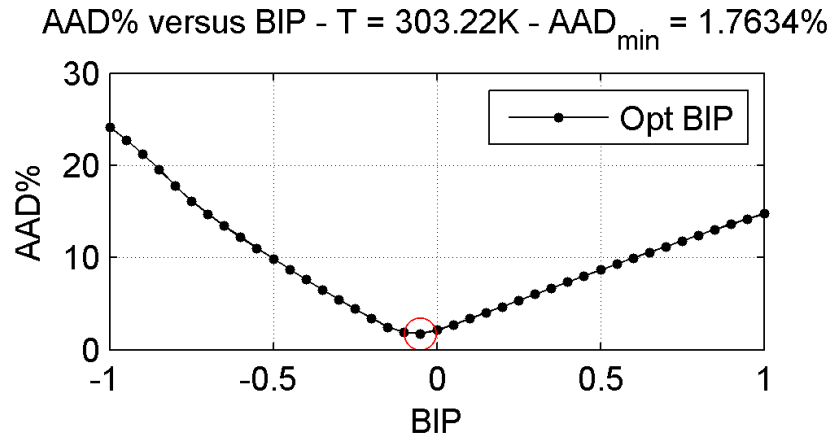

Figure 89: AAD% Variation with BIP – mixture N2 - 303K

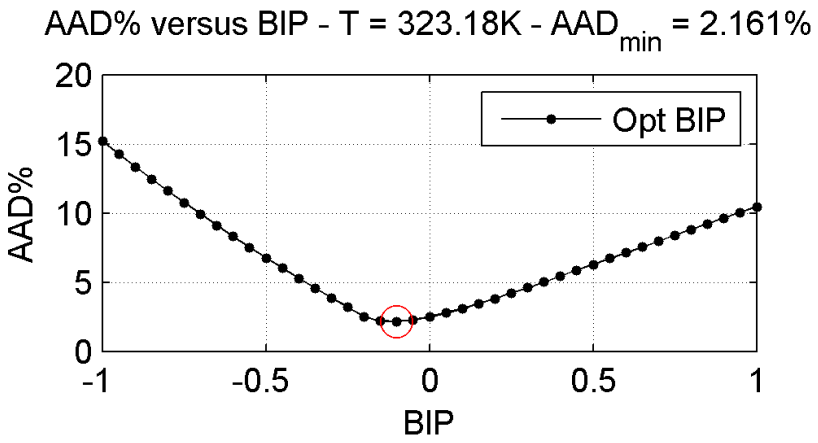

Figure 90: AAD% Variation with BIP – mixture N2 - 323K

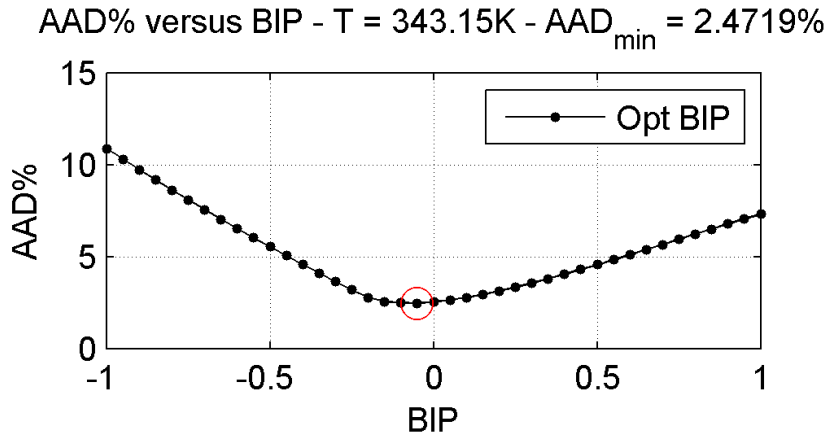

Figure 91: AAD% Variation with BIP – mixture N2 - 343K

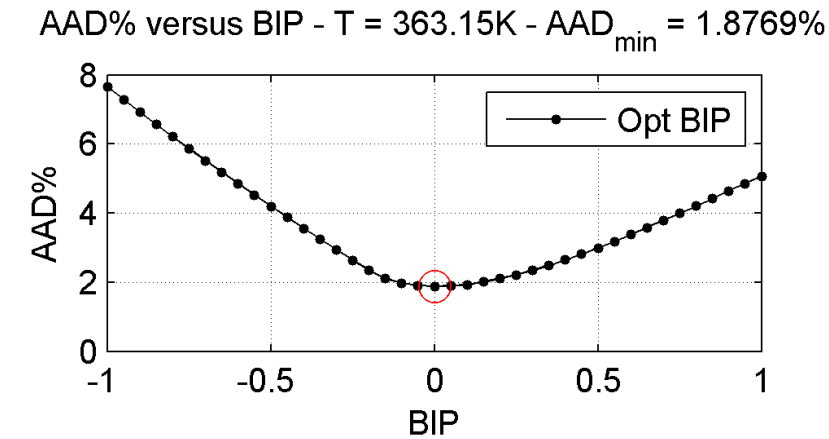

Figure 92: AAD% Variation with BIP – mixture N2 - 363K

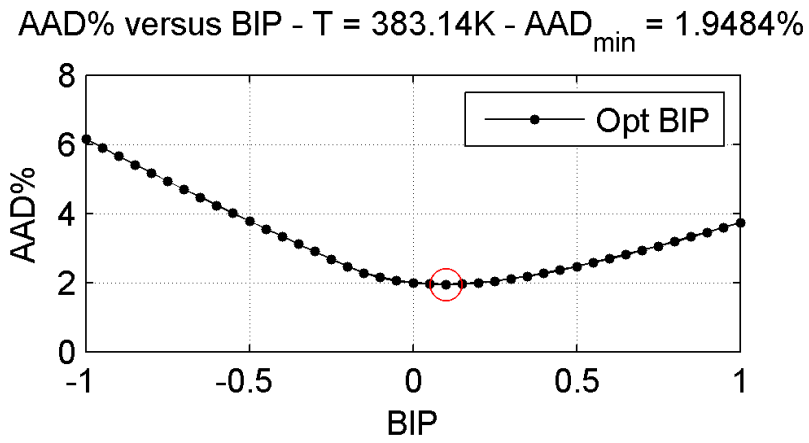

Figure 93: AAD% Variation with BIP – mixture N2 - 383K

4.4.3. Plots Mixture O1

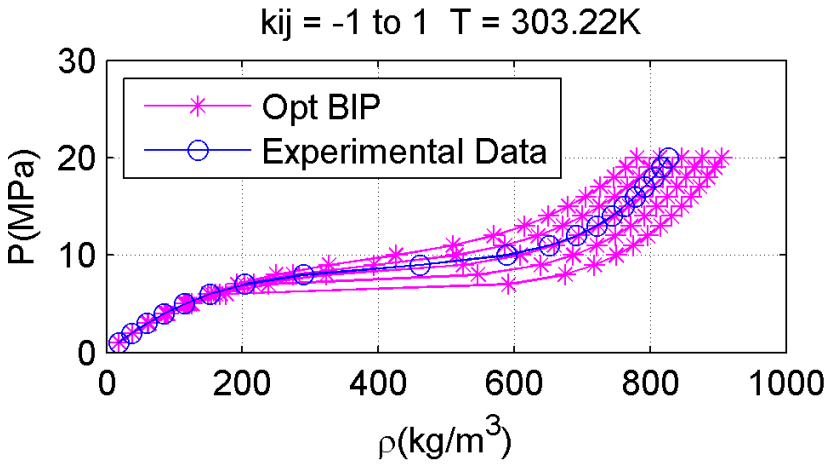

Figure 94: Variation of BIP – mixture O1 - 303K

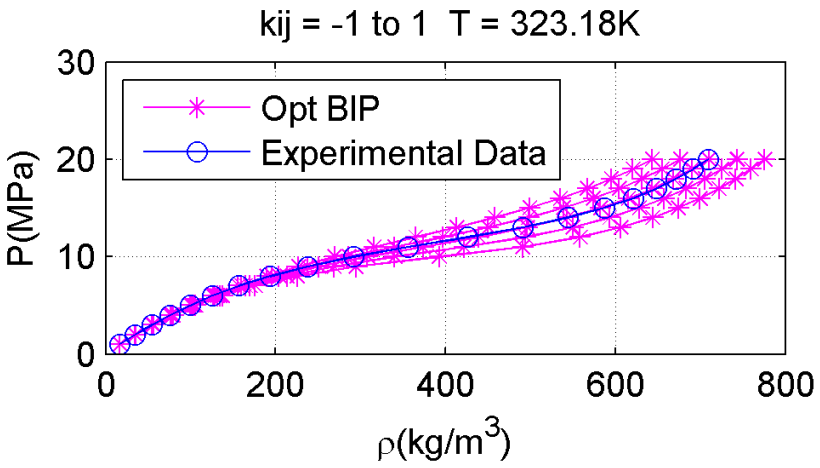

Figure 95: Variation of BIP – mixture O1 - 323K

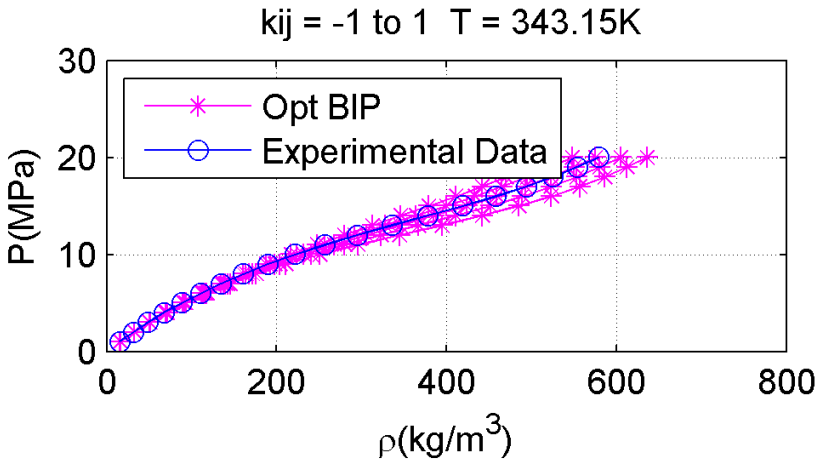

Figure 96: Variation of BIP – mixture O1 - 343K

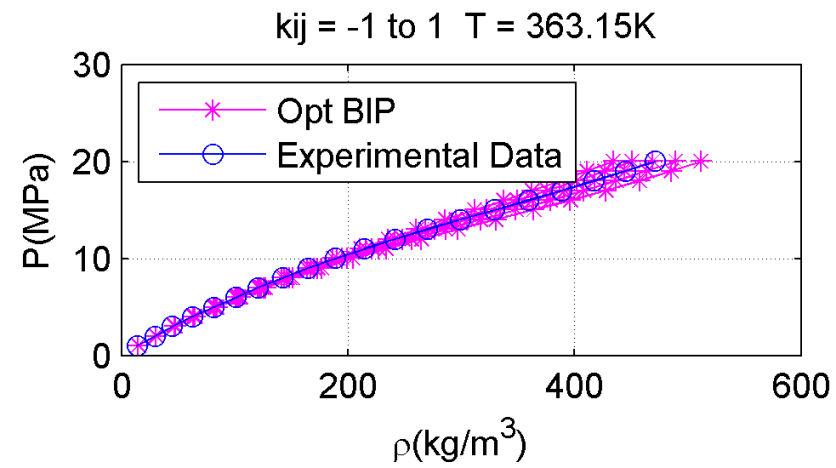

Figure 97: Variation of BIP – mixture O1 - 363K

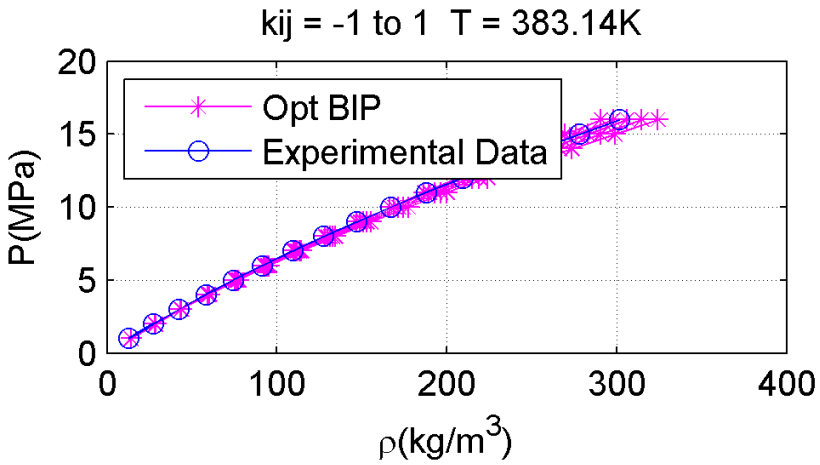

Figure 98: Variation of BIP – mixture O1 - 383K

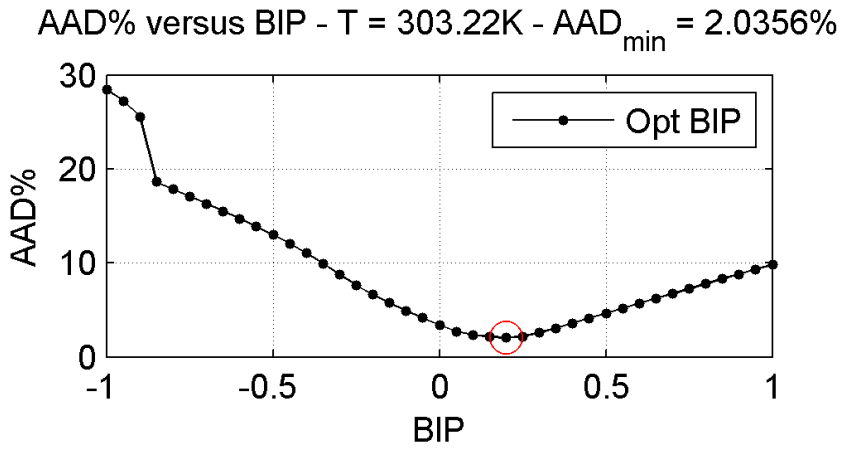

Figure 99: AAD% Variation with BIP – mixture O1 - 303K

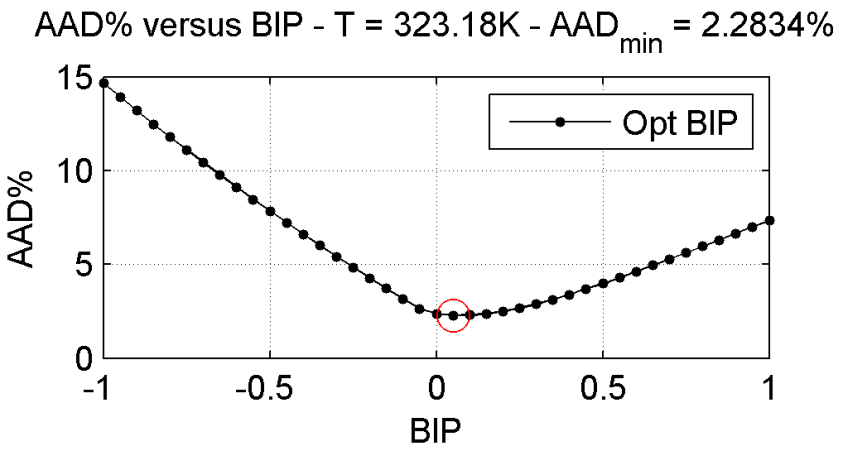

Figure 100: AAD% Variation with BIP – mixture O1 - 323K

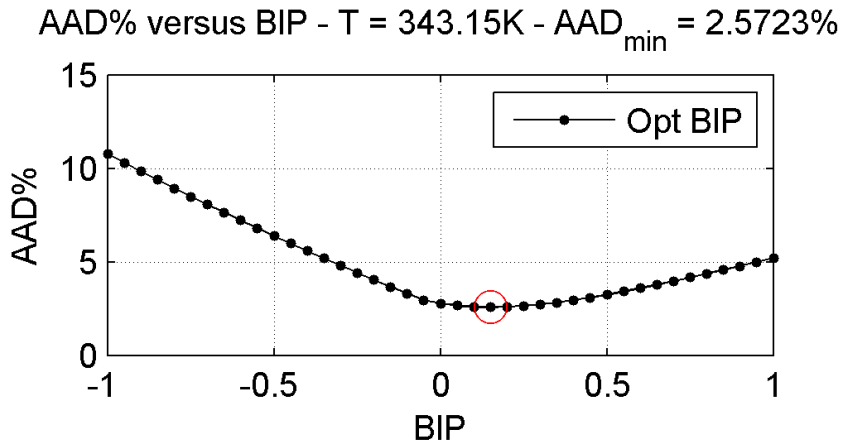

Figure 101: AAD% Variation with BIP – mixture O1 - 343K

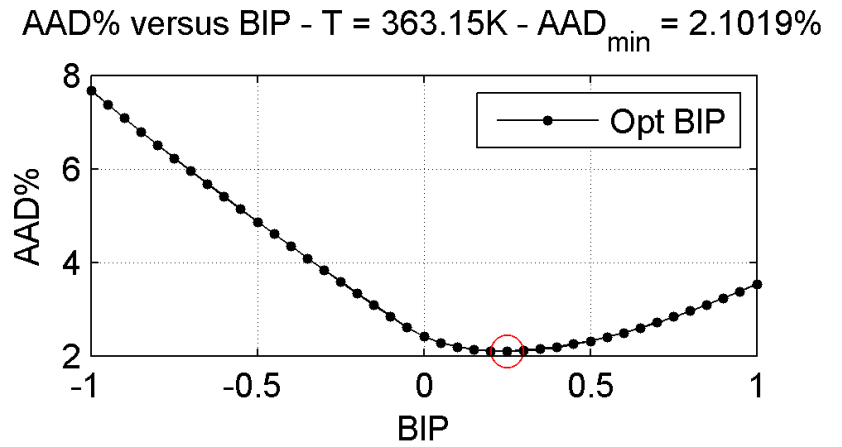

Figure 102: AAD% Variation with BIP – mixture O1 - 363K

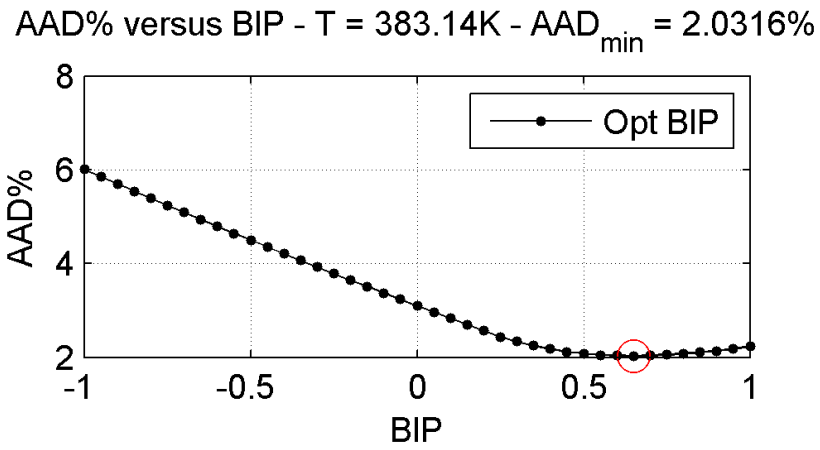

Figure 103: AAD% Variation with BIP – mixture O1 - 383K

4.4.4. Plots Mixture O2

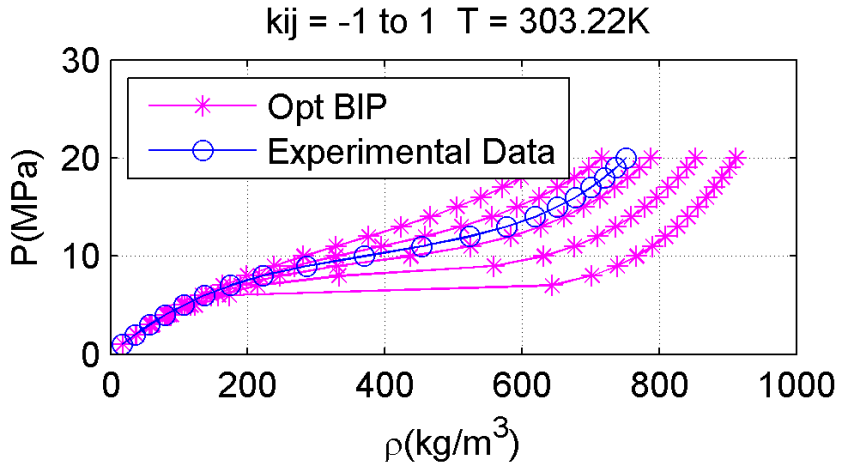

Figure 104: Variation of BIP – mixture O2 - 303K

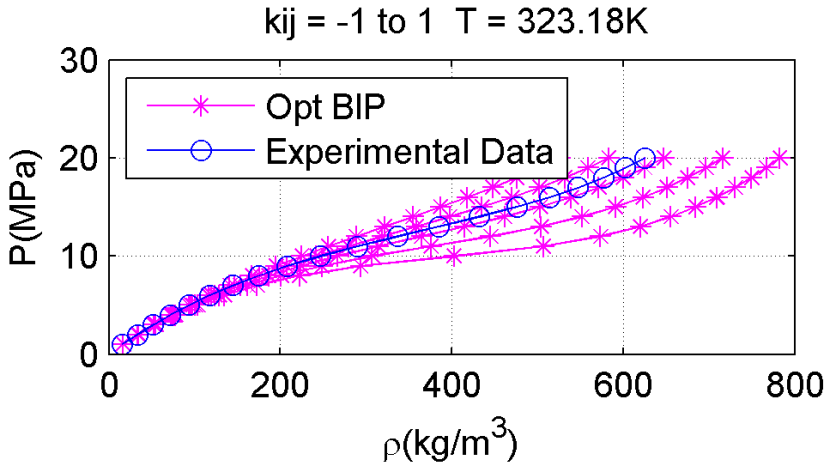

Figure 105: Variation of BIP – mixture O2 - 323K

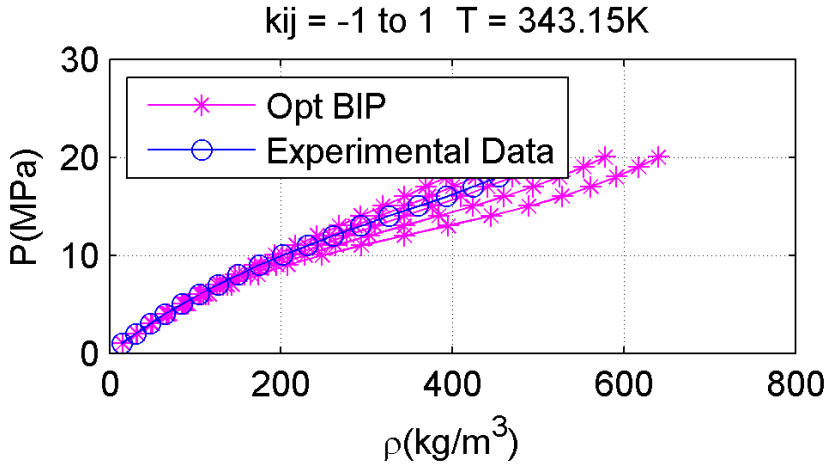

Figure 106: Variation of BIP – mixture O2 - 343K

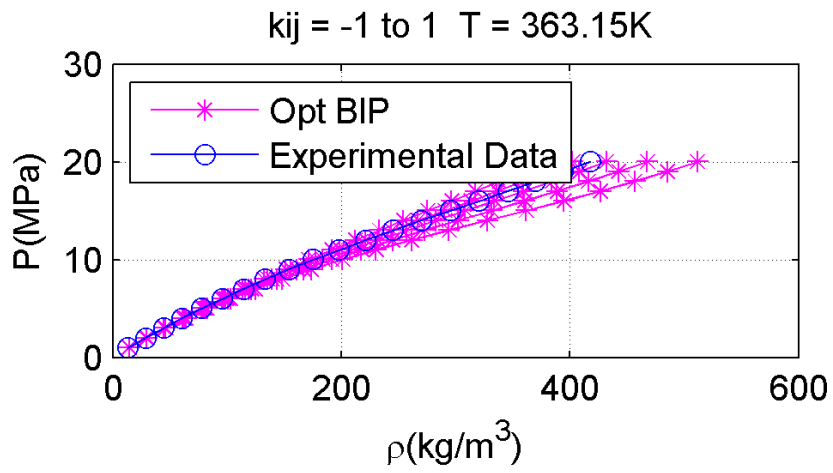

Figure 107: Variation of BIP – mixture O2 - 363K

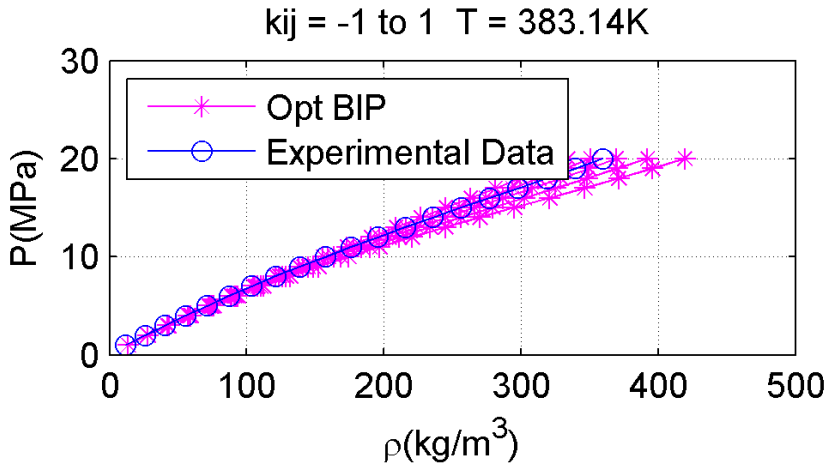

Figure 108: Variation of BIP – mixture O2 - 383K

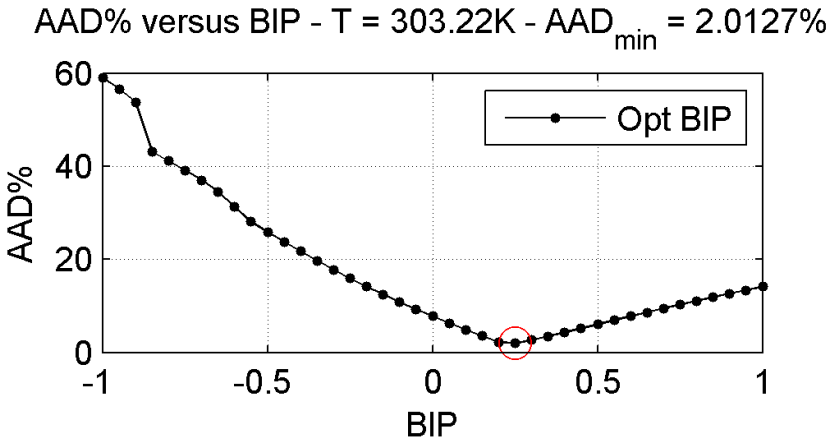

Figure 109: AAD% Variation with BIP – mixture O2 - 303K

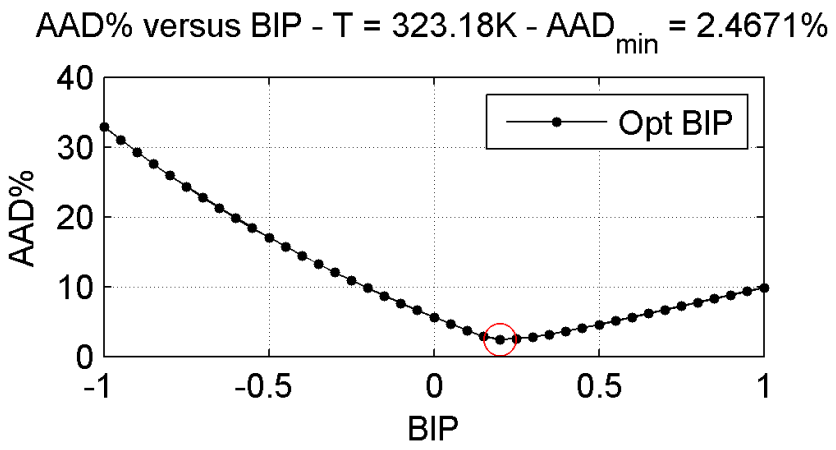

Figure 110: AAD% Variation with BIP – mixture O2 - 323K

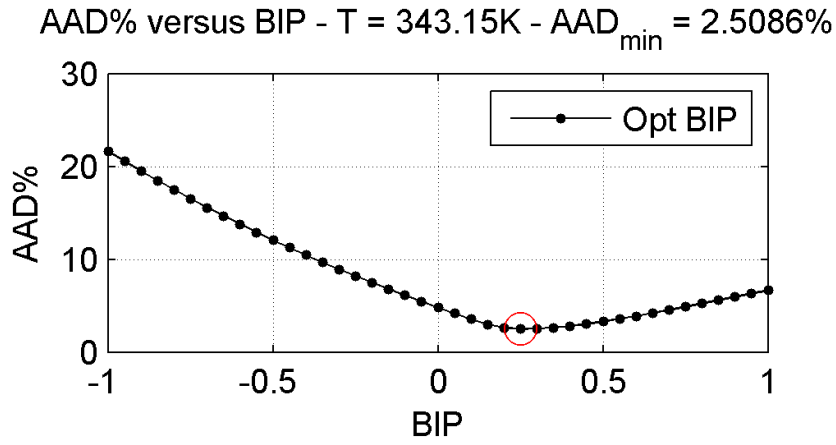

Figure 111: AAD% Variation with BIP – mixture O2 - 343K

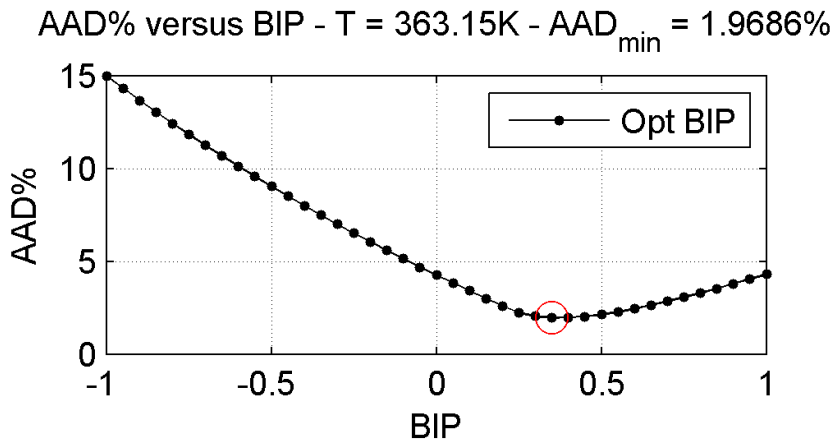

Figure 112: AAD% Variation with BIP – mixture O2 - 363K

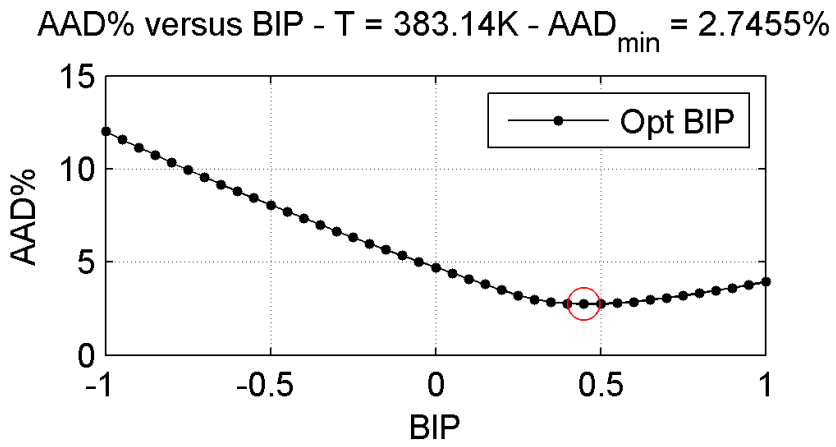

Figure 113: AAD% Variation with BIP – mixture O2 - 383K

4.4.5. Plots Mixture A1

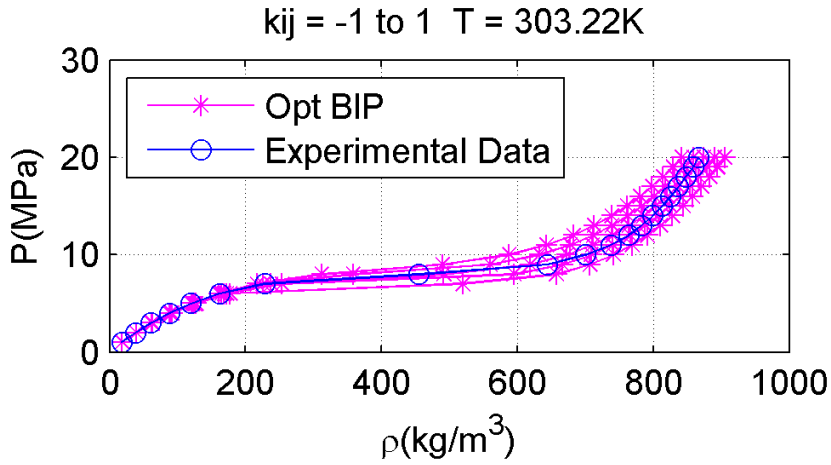

Figure 114: Variation of BIP – mixture A1 - 303K

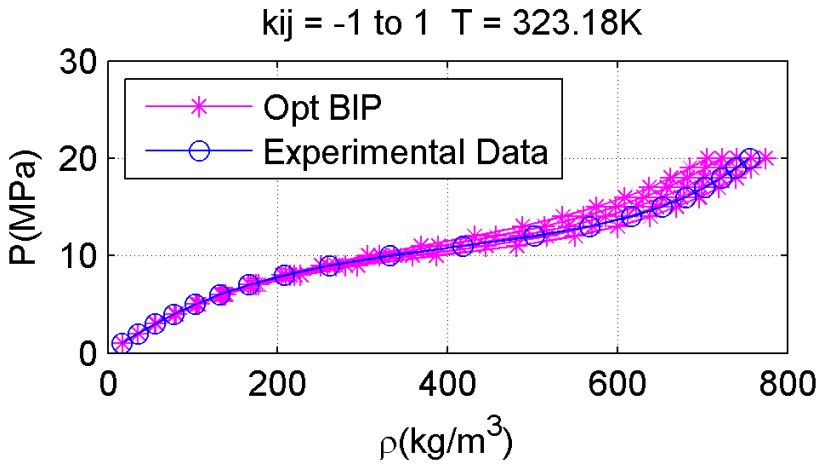

Figure 115: Variation of BIP – mixture A1 - 323K

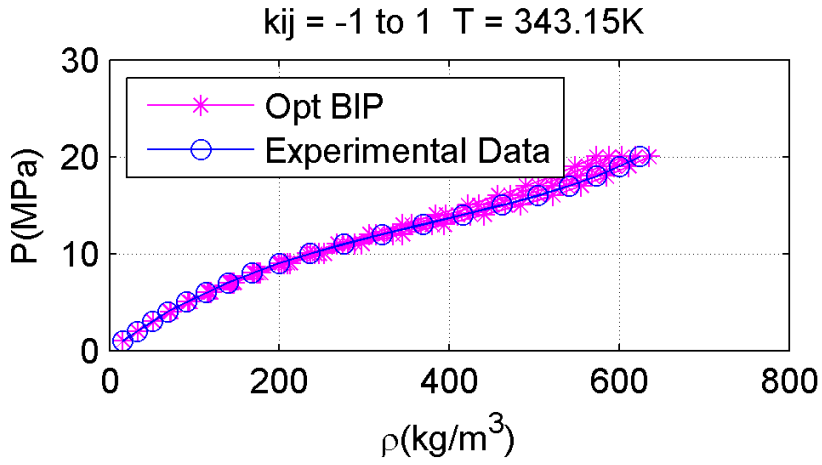

Figure 116: Variation of BIP – mixture A1 - 343K

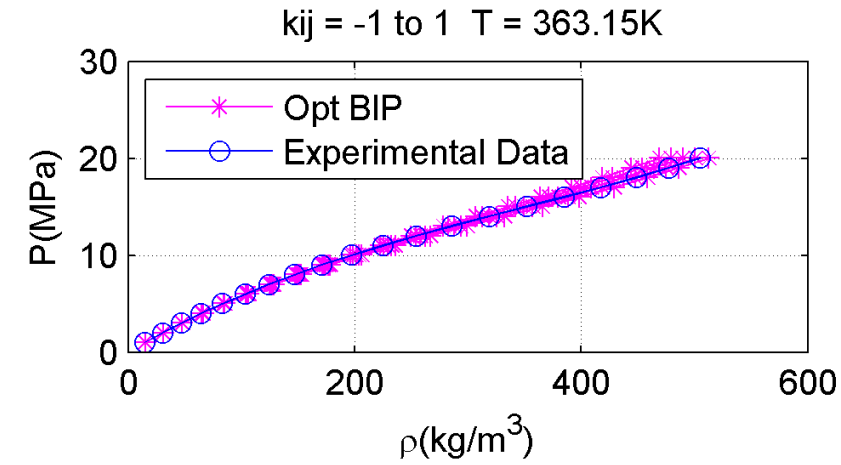

Figure 117: Variation of BIP – mixture A1 - 363K

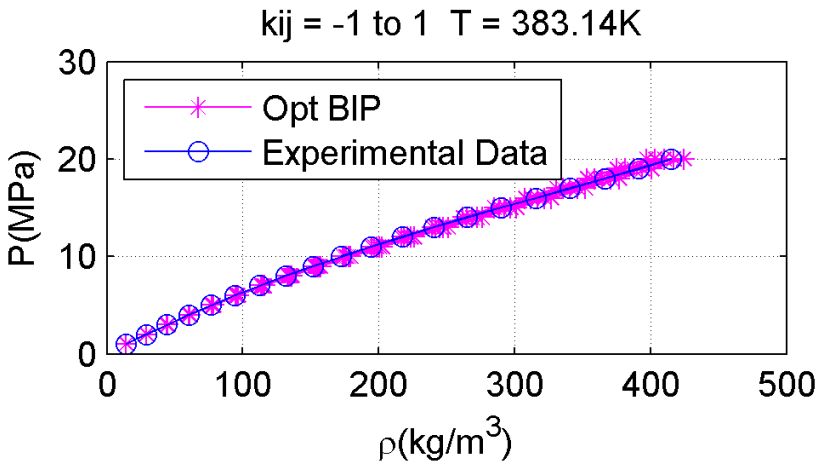

Figure 118: Variation of BIP – mixture A1 - 383K

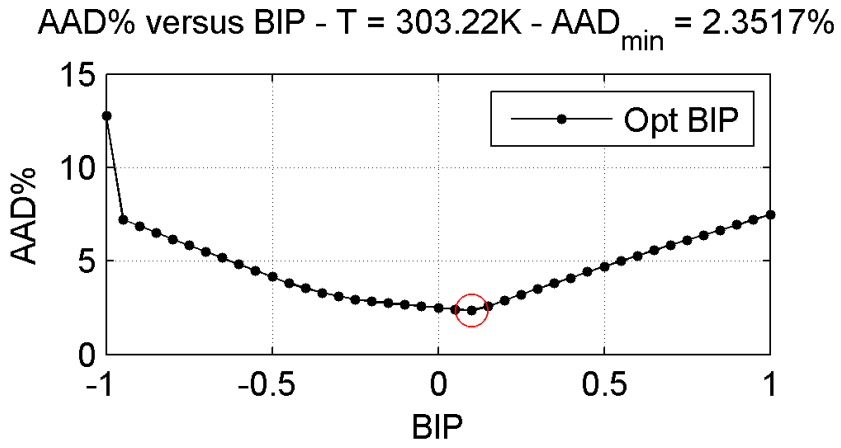

Figure 119: AAD% Variation with BIP – mixture A1 – 303K

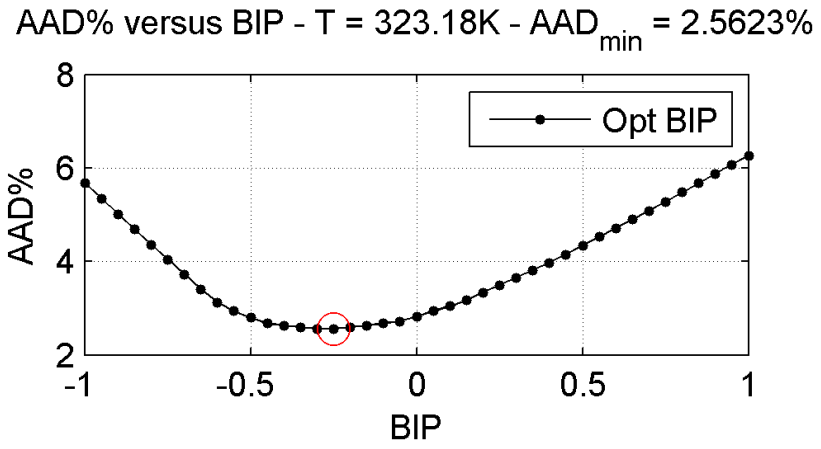

Figure 120: AAD% Variation with BIP – mixture A1 – 323K

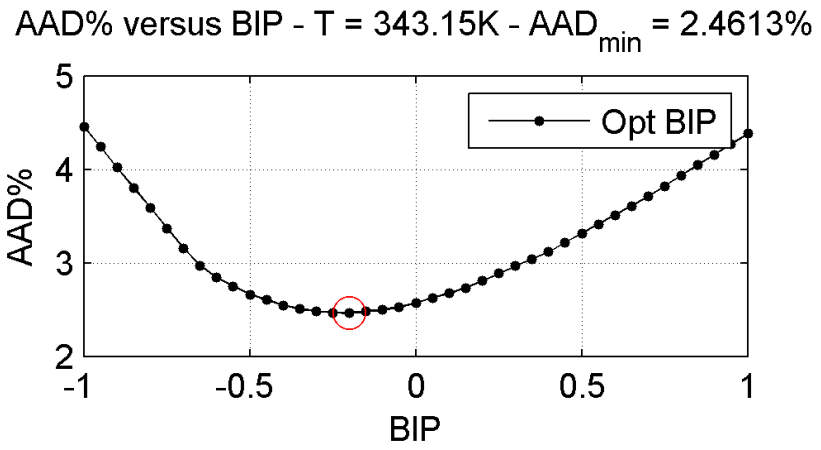

Figure 121: AAD% Variation with BIP – mixture A1 – 343K

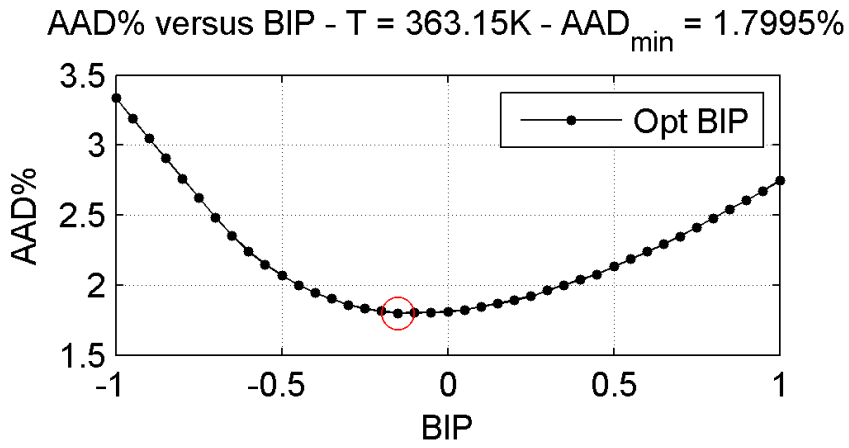

Figure 122: AAD% Variation with BIP – mixture A1 – 363K

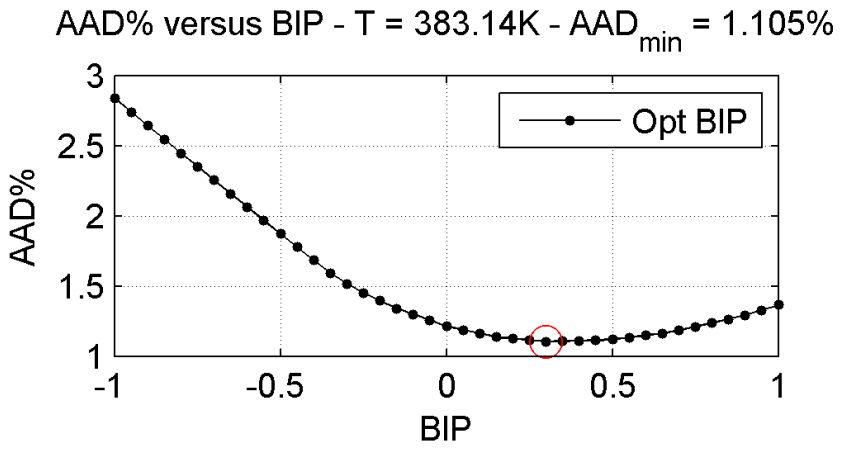

Figure 123: AAD% Variation with BIP – mixture A1 – 383K

4.4.6. Plots Mixture A2

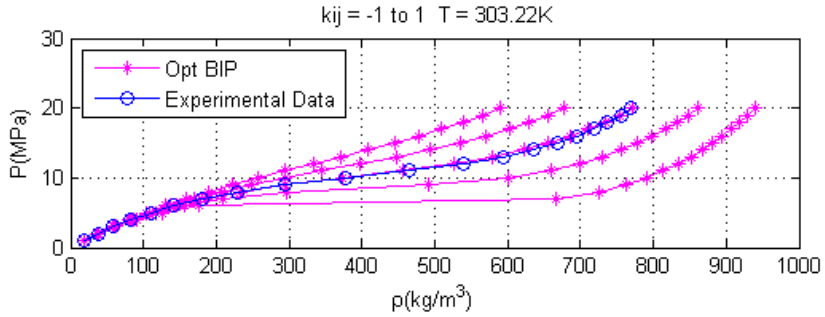

Figure 124: Variation of BIP – mixture A2 - 303K

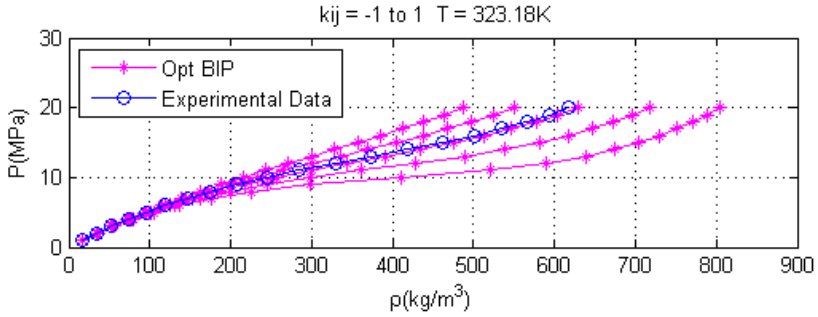

Figure 125: Variation of BIP – mixture A2 - 323K

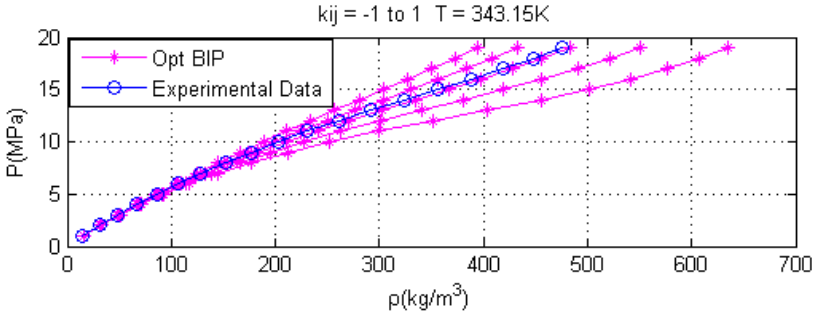

Figure 126: Variation of BIP – mixture A2 - 343K

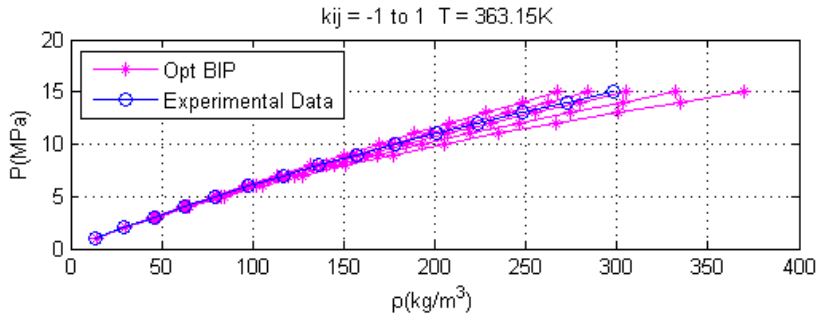

Figure 127: Variation of BIP – mixture A2 - 363K

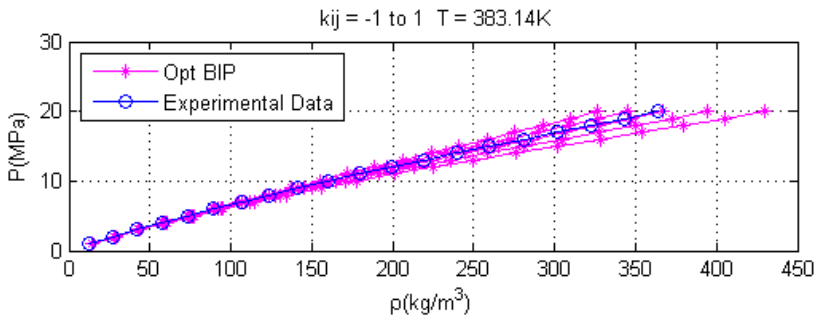

Figure 128: Variation of BIP – mixture A2 - 383K

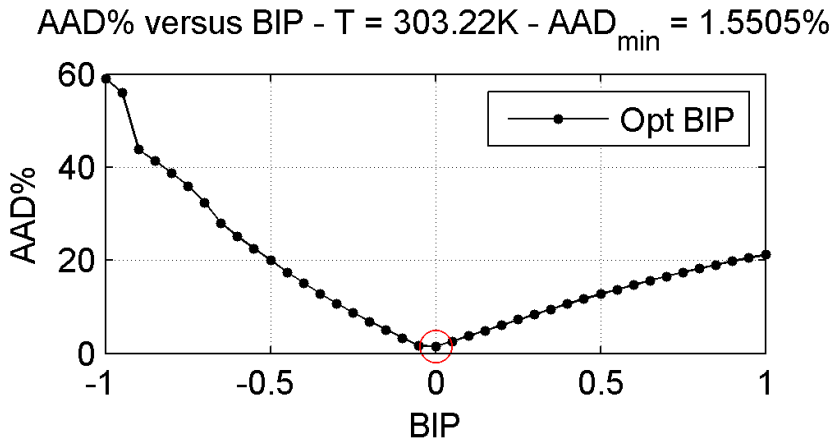

Figure 129: AAD% Variation with BIP – mixture A2 - 303K

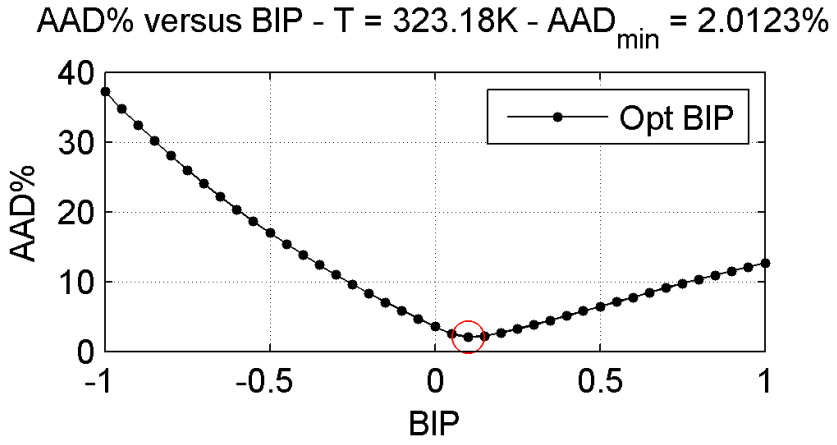

Figure 130: AAD% Variation with BIP – mixture A2 - 323K

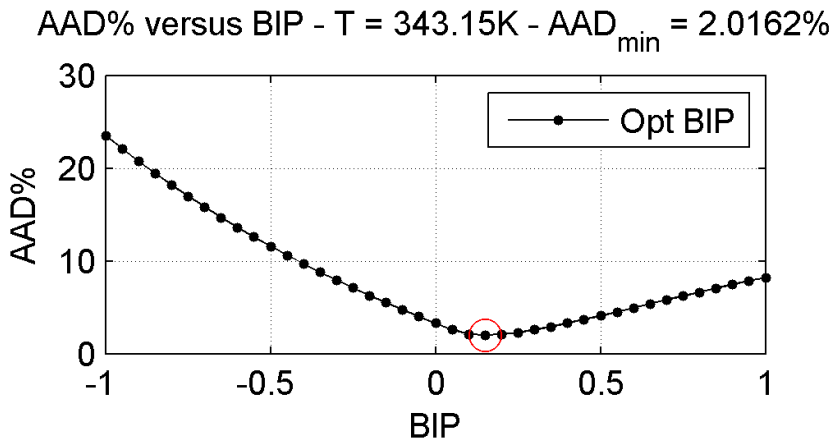

Figure 131: AAD% Variation with BIP – mixture A2 - 343K

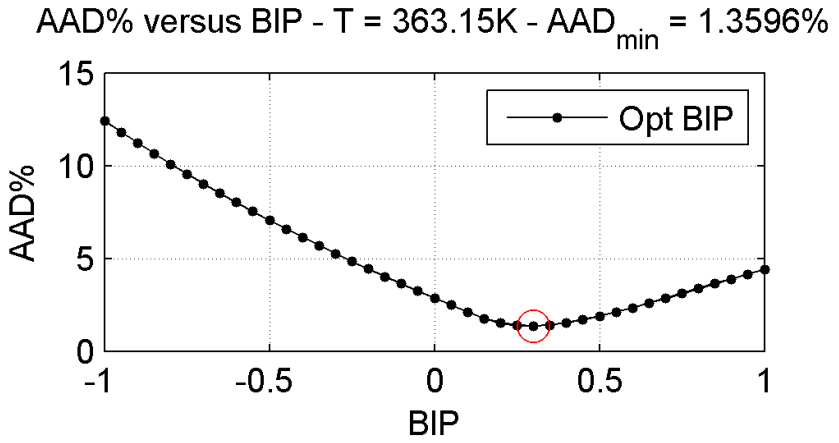

Figure 132: AAD% Variation with BIP – mixture A2 - 363K

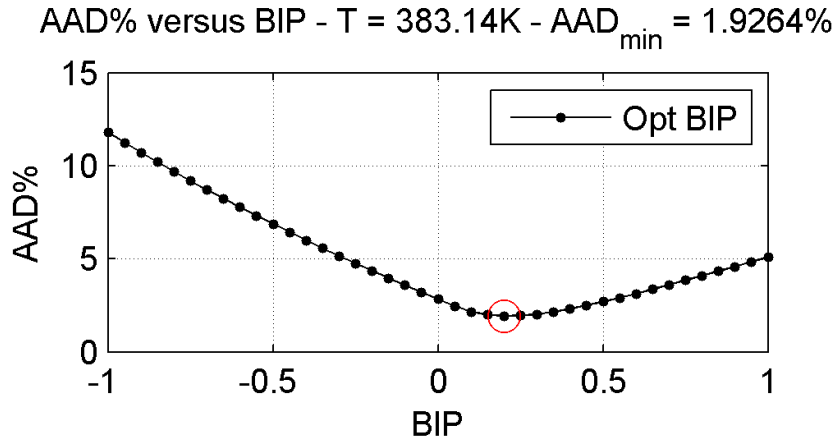

Figure 133: AAD% Variation with BIP – mixture A2 - 383K

4.4.7. Explanation of the Plots

In the isotherms (Fig 74 to 78, 84 to 88, 94 to 98, 104 to 108, 114 to 118 and 124 to128), the curves start from the bottom-right (for BIP=-1) and the BIP increases moving to the top-left.

The first tendency that can be noted from the plots (figures 79 to 83, 89 to 93, 99 to 103, 109 to 113, 119 to 123 and 129 to 133) is that the deviation curve (AAD%) gets flatter as the temperature increases. That means that the deviation is not as strongly dependent on the BIP as the fluids temperature increase.

Regarding the isotherms, it is clear that the mixtures with higher quantities of Ar, O_2 or N_2 are more sensitive to the variation of the BIP (see figures 84 to 88, 104 to 108 and 124 to 128) in comparison with the ones where those quantities are lower (see figures 74 to 78, 94 to 98 and 114 to 118) – since the range of values for the BIP is the same, the wider are the magenta curves, the more sensitive is the EoS to the BIP. Also, for all mixtures, the sensitivity appears to increase as the temperature decreases.

Furthermore, a comparison between the minimum achievable deviations (the ones circled in the figures 79 to 83, 89 to 93, 99 to 103, 109 to 113, 119 to 123 and 129 to 133) and the ones obtained in the minimization of the BIP for each isotherm (figures 6 to 17) is made. The aim is to analyze how close to the minimum are the deviations when the optimum BIP is used, because the optimization is done by means of the least square of the residuals, not the lowest deviation. In the following tables (22, 23 and 24) it can be seen that the deviations obtained with the optimum BIP were close to the minimum one.

Table 22: Comparison between minimum AAD% and AAD% obtained with optimum BIP – Mixture N

N1 Mixture					
T	303,22	323,18	343,15	363,15	383,14
AAD%	2,131	2,470	2,428	1,838	1,916
AAD%_min	2,066	2,439	2,360	1,749	1,812
Difference	0,065	0,031	0,068	0,088	0,105

N2 Mixture					
T	303,22	323,18	343,15	363,15	383,14
AAD%	1,810	2,164	2,527	1,948	2,034
AAD%_min	1,763	2,161	2,472	1,877	1,948
Difference	0,047	0,003	0,055	0,072	0,085

Table 23: Comparison between minimum AAD% and AAD% obtained with optimum BIP – Mixture O

O1 Mixture					
T	303,22	323,18	343,15	363,15	383,14
AAD%	2,107	2,295	2,651	2,187	2,119
AAD%_min	2,023	2,283	2,570	2,097	2,031
Difference	0,085	0,005	0,032	0,043	0,043

O2 Mixture					
T	303,22	323,18	343,15	363,15	383,14
AAD%	1,970	2,478	2,559	2,029	2,826
AAD%_min	1,955	2,460	2,509	1,966	2,745
Difference	0,015	0,017	0,051	0,064	0,081

Table 24: Comparison between minimum AAD% and AAD% obtained with optimum BIP – Mixture A

A1 Mixture					
T	303,22	323,18	343,15	363,15	383,14
AAD%	2,483	2,600	2,561	1,906	1,211
AAD%_min	2,336	2,549	2,457	1,799	1,105
Difference	0,147	0,052	0,104	0,107	0,106

A2 Mixture					
T	303,22	323,18	343,15	363,15	383,14
AAD%	1,324	2,033	2,077	1,439	1,997
AAD%_min	1,311	2,012	2,016	1,360	1,926
Difference	0,014	0,020	0,061	0,080	0,071

4.5. Sensitivity Analysis – Variation of Mixture Component

The optimum BIPs were plotted against the temperature, for the mixtures N1, A1 and O1 in the same plot. This is important to understand the relationship between the type of mixture – if it has strongly polar bonds, if it is a mixture with a noble gas – and how it affects the binary interaction parameter for the different temperatures.

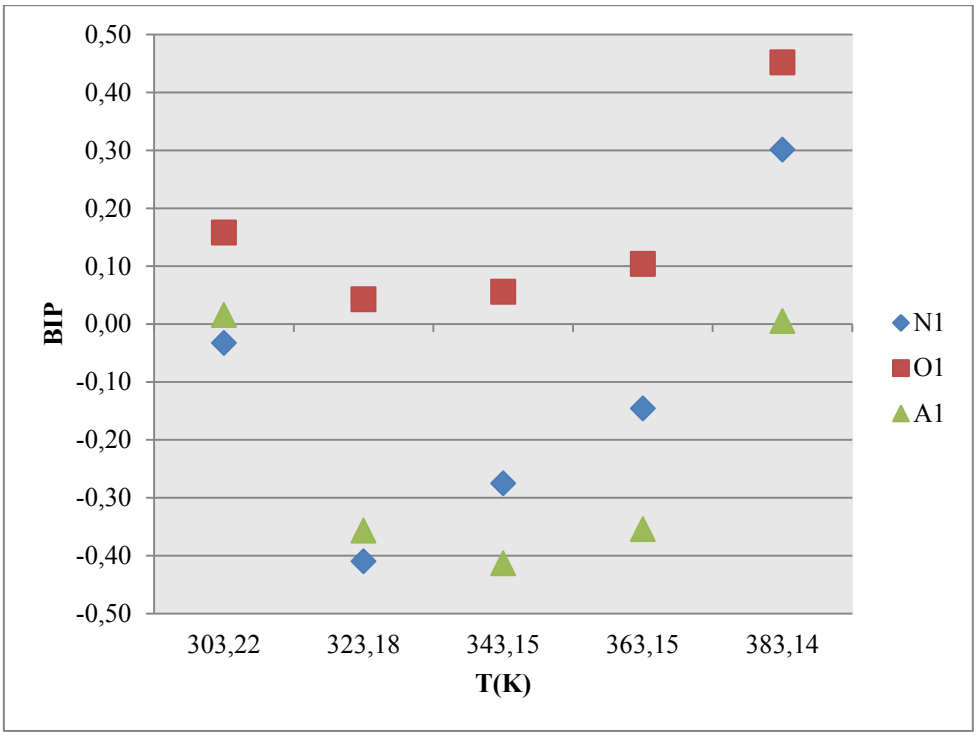

Figure 134: BIPxT for Mixtures N1, O1 and A1

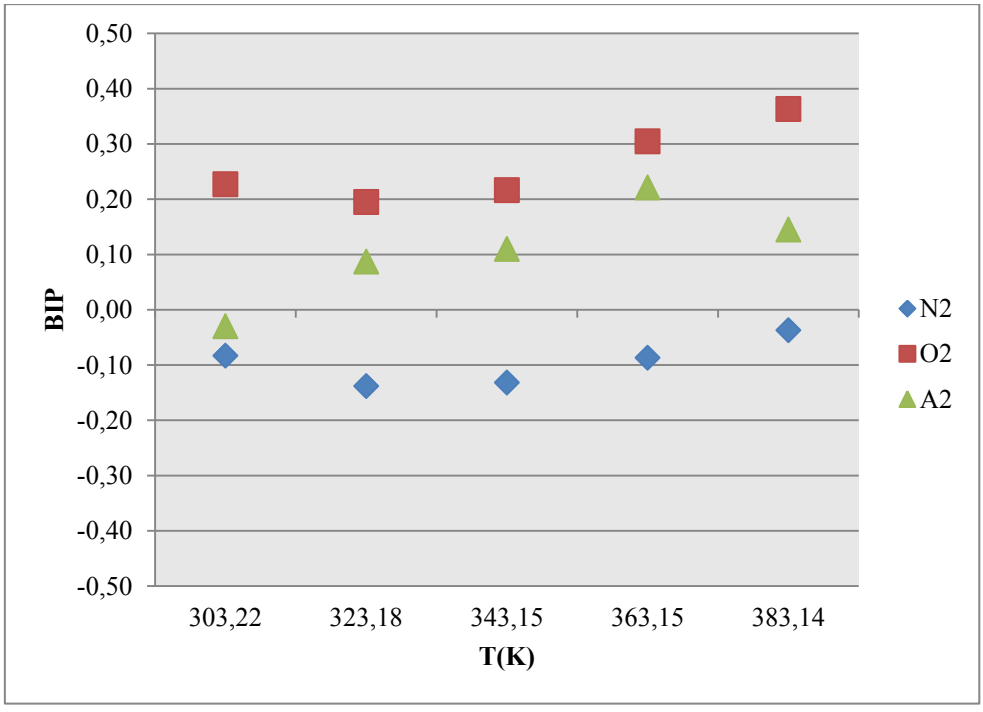

Figure 135: BIPxT for Mixtures N2, O2 and A2

The first point that should be reminded is that the mixtures with index 2 present a higher concentration of the respective gases (N_2, O_2 and Ar). That being said, the mixtures with higher concentrations of those gases presented a lower variation of the BIP with temperature. Also, the BIPs were closer to zero. Furthermore, the increased presence of Argon in the mixture (green triangles) shifted the BIP upwards into the positive values. That has strong implications in the parameters of the (Eq. 86.) and it shows the high sensitivity of the BIP estimation with the mixture composition in that case. For the other two components (O_2 and N_2), although the BIP variation diminishes with the increased concentration, that change is not as noticeable as the one with the Argon mixture.

Chapter 5: Conclusion

The presented study confirms that the Peng-Robinson EoS can be applied to model the volumetric behavior of the CO_2 mixtures studied (CO_2-N_2, CO_2-Ar, CO_2-O_2) in the case where accuracies in the range 1.2% to 2.8% are acceptable. The robustness analysis showed that there is little to no influence both of the optimization method utilized (Levenberg-Marquardt or Trust-Region) and of the initial BIP value used in the optimization process. However, the tolerance of the algorithm implemented may influence the results substantially and the default value used by Matlab (equal to 10^{-6}) shows a good compromise between calculation time and precision (see table 20).

The use of a temperature-dependent relationship for the regression of the BIP improved the quality of the results by providing a continuous equation for calculating the BIP, for temperatures inside the range studied, without increasing the deviation substantially (maximum increase of AAD = 0.064%). However, by analyzing the plots obtained for the regression (figures 43 to 72) it can be noticed that the curve for the BIP regression presents a change of concavity for the mixture A when the composition is changed from A1 to A2 (figures 41 and 42). This indicates that the overall shape of the function BIP(T) can be strongly dependent on the mixture composition, and the use of the calculated coefficients (page 76) for general calculations of the optimum BIP should be made with caution.

In the interest of further developments, other EoS and mixing rules may be analyzed. For the cubic EoS, the study of different mixing rules and EoS models would contribute to a better understanding of what is the most accurate analytical model available for the CO_2 mixtures studied and how the optimization methods influence the calculations with these other methods. Non-analytical EoS are certainly more accurate, but they could be studied with the intention of optimizing their calculation to minimize the computational effort needed to calculate the solutions, since they are iterative. It may also prove useful to compare these models with respect to the sensitivity of their BIP(T) function to the change in composition.

References

1. Mantovani, M. *Supercritical Pressure–Density–Demperature Measurements on CO2–N2, CO2–O2*: Elsevier 34-43, 2012, The Journal of Supercritical Fluids, Vol. 61.

2. Mazzoccoli, M. *Carbon Capture, Storage and Transportation (CCS&T) Process: General Aspects and Focus on CO2 Pipeline Modelling.* PhD Thesis, Università Degli Studi di Genova, 2011.

3. Poling, B. E., Prausnitz J. M. and O'Connell, J. P. *The properties of gases and liquids, 5th edition.* McGrall-Hill, 2001.

4. van der Waals, J. D. *The law of corresponding states for different substances.* KNAW, Proceedings, 1913, Vol. XV.

5. Bejan, A. *Advanced Engineering Thermodynamics.* Wiley, 2006.

6. Pitzer, K. S. *The volumetric and thermodynamic properties of fluids, I: Theoretical basis and viral coefficients.* pp. 3427-3433: J. Am. Chem. Society, 1955, Vol. 77.

7. Soave, G. *Equilibrium constants from a modified Redlich-Kwong equation of state.* 1197-1203,Chem. Eng. Sci., 1972, Vol. 27.

8. Aspen physical property system, Aspen Tech, 2012.

9. Sandler, S. I. *Chemical, Biochemical, and Engineering Thermodynamics 4th edition*, John Wiley & Sons, Inc 2006.

10. Joback Method. *Wikipedia.* http://en.wikipedia.org/wiki/Joback_method.

11. Span, R. *Multiparameter Equations of State.* Springer, 2000.

12. Mantovani, M. *Oxy-combustion flue gases purification systems: numerical and experimental analysis*. PhD Thesis, Politecnico di Milano 2010.

13. Nocedal, J. and Wright, S. J. *Numerical Optimization* : Springer, Second Edition, 2006.

14. *Sklogwiki.* http://www.sklogwiki.org/SklogWiki/index.php/Law_of_corresponding_states.

15. Mansoori, G. A., Patel, V. K. and Edalat, M. *The Three-Parameter Corresponding States Principle.* International Journal of Thermophysics. 1980, Vol. 1, 3 pp 285-298.

16. Perrot, P. *A to Z of Thermodynamics.* Oxford University Press, 1998.

17. Riedlich, O. and Kwong, J. N. S. *On the thermodynamic of solution, V: An equation of state. Fugacities of Gaseous Solutions.* 233-244, 1944, Vol. Chem. Rev. 44.

18. Lydersen, A. L. *Estimation of Critical Properties of Organic Compounds.* Madison, WI : Engineering Experimental Station Report, 1955, Vol. 3.

19. Wang, J L. *Global Phase Diagrams and Critical Phenomena of Binary Mixtures*. Swinburne University of Technology, 2003.

Appendix 1 - Matlab Code

In the following pages, the Matlab code that was used for the simulations is presented. For the sake of simplicity, the code showed here is the one used for the CO_2 - N_2 mixtures. To use it for the other two mixtures, the lines up to "Optimization N1", where the data is read, need to be changed. The lines where the data is plotted or printed to a file should also be changed so the name is coherent with the data used.

```
%%%%%%%%%%%%%%%%%%%%%%%%%%%%%%%%%%%%%%%%%%%%%%%%%%%%%%%%%%%%%%%%%%%%%%%
%%%%
%%%%%% Optimization of the Data Fitting for the Density Estimate
%%%
%%%%%% Peng Robinson EoS
%%%%%%%%%%%%%%%%%%%%%%%%%%%%%%%%%%%%%%%%%%%%%%%%%%%%%%%%%%%%%%%%%%%%%%%
%%%%%% Working - 27/11
%%%%%%%%%%%%%%%%%%%%%%%%%%%%%%%%%%%%%%%%%%%%%%%%%%%%%%%%%%%%%%%%%%%%%%%
%%%%%%%%%%%%%%%%%%%%%%%%%%%%%%%%%%%%%%%%%%%%%%%%%%%%%%%%%%%%%%%%%%%%%%%
%%%%


clc
close all
clear all


%%% Load Data from files
%%%%%%%%%%%%%%%%%%%%%%%%%%%%%%%%%%%%%%%%%%%%%%%%%%%%%%%%%%%%%%%%%%%%%%%


load mixture_N1.txt


for j=1:5


    P1(:,j) = mixture_N1(2:end,2*j-1)*1e6; %Pa
    T_lin1(j) = mixture_N1(1,2*j-1); %K
    rho1(:,j) = mixture_N1(2:end,2*j);


end


load mixture_N2.txt
```

```
for j=1:5

    P2(:,j) = mixture_N2(2:end,2*j-1)*1e6; %Pa
    T_lin2(j) = mixture_N2(1,2*j-1); %K
    rho2(:,j) = mixture_N2(2:end,2*j);

end

load mol_fraction_N1.txt
x1(1) = mol_fraction_N1(1,1); %x_CO2
x1(2) = mol_fraction_N1(2,1); %x_N2

load mol_fraction_N2.txt
x2(1) = mol_fraction_N2(1,1); %x_CO2
x2(2) = mol_fraction_N2(2,1); %x_N2

load critical_data_CO2N2_PR.txt

crit_data = critical_data_CO2N2_PR;

%CO2
M(1) = crit_data(1,1); %kg/kmol
Tc(1) = crit_data(2,1) + 273.15; %K
Pc(1) = crit_data(3,1) * 1e6; %Pa
omega(1) = crit_data(4,1);

%N2
M(2) = crit_data(1,2);
Tc(2) = crit_data(2,2) + 273.15;
Pc(2) = crit_data(3,2) * 1e6;
omega(2) = crit_data(4,2);

%% Optimization N1

% Caltulate the specific gas constant for each mixture
```

```
R = 8314.462; %J/kmol*K
M_mix1 = (x1(1)*M(1)+x1(2)*M(2)); %kg/kmol
M_mix2 = (x2(1)*M(1)+x2(2)*M(2)); %kg/kmol

bip = -0.5;

% To change the opt algorithm
mode = 1;

for j=1:5

% Assemble Co-volume Vector and Energy Parameter Matrix for each
mixture

    T_num1 = T_lin1(j);

    for i=1:2

        b1(i) = 0.07780*R*Tc(i)/Pc(i);%b mixture N1 1=CO2, 2=N2
        m(i) = 0.37464 + 1.54226*omega(i) - 0.26992*omega(i)^2;
        alpha_spec1(i,j) = (1+m(i)*(1-
(T_num1/Tc(i))^0.5))^2;%alphaCO2, alphaN2
        a1(i,j) =
0.45724*R^2*Tc(i)^2/Pc(i)*alpha_spec1(i,j);%aCO2, aN2

    end

    b_mix1 = x1(1)*b1(1) + x1(2)*b1(2);

    nonzero_p = max(find(P1(:,j),20,'first'));

    P_col1 = P1(1:nonzero_p,j);
    rho_col1 = rho1(1:nonzero_p,j);

    rho_PR1 = @(bip,P_col1) paramPR(P_col1, T_num1, a1(:,j), R,
```

```
b_mix1, bip, x1);




    switch mode
        case 1
        options = optimset('Algorithm','levenberg-marquardt');
        case 2
        options = optimset('Algorithm','trust-region-
reflective');
    end


    options = optimset('TolFun',1e-12);


    bip1(j) = lsqcurvefit(rho_PR1,bip,P_col1,rho_col1./M_mix1);


    rho_calcN1(1:nonzero_p,j) = rho_PR1(bip1(j),P_col1)*M_mix1;


    AAD1(j) =
(100/nonzero_p).*sum(abs((rho_calcN1(1:nonzero_p,j)-
rho_col1)./rho_col1),1);


%     figure(j)
    figure(1)
    subplot(3,2,j)
    plot(rho_calcN1(1:nonzero_p,j),P_col1.*1e-6,'m*-',
rho1(1:nonzero_p,j),P_col1.*1e-6,'bo-');
    legend('Opt BIP','Experimental
Data','Location','NorthWest');
    xlabel('\rho(kg/m^3)');
    ylabel('P(MPa)');
    title(['AAD% N1 = ',num2str(AAD1(j)),'%',' kij =
',num2str(bip1(j)), ' T = ', num2str(T_num1),'K']);
%     title('Mixture N1');
    grid on
    hold on
```

```
    figure(6)
    plot(T_num1,bip1(j),'m*-');
    legend('Opt BIP');
    xlabel('T(K)');
    ylabel('BIP');
    title('BIP versus Temperature - mixture N1');
    grid on
    hold on



end
% print('-dpng','-r300',sprintf('N1_indiv.png'));

% Interpolation for T dependence

s = fitoptions('Method','NonlinearLeastSquares','Maxiter',1e3);
ffun = fittype('aa + bb.*T +
cc./T','independent','T','options',s);
[reg gg hh] = fit(T_lin1(1,:)',bip1',ffun);
TT = [T_lin1(1,1):1:T_lin1(1,5)];

for i=1:length(TT)
    y(i)=reg(TT(i));
end

figure(100)
scatter(T_lin1(1,:),bip1,'b*');
hold on
plot(TT,y,'r-')
title('BIP_o_p_t CO_2-N_1 = f(T) = a + b*T +c/T');
xlabel('T(K)');
ylabel('BIP');
grid on



for j=1:5
```

```
% Assemble Co-volume Vector and Energy Parameter Matrix for each
mixture


    T_num1 = T_lin1(j);


    for i=1:2


        b1(i) = 0.07780*R*Tc(i)/Pc(i);%b mixture N1 1=CO2, 2=N2
        m(i) = 0.37464 + 1.54226*omega(i) - 0.26992*omega(i)^2;
        alpha_spec1(i,j) = (1+m(i)*(1-
(T_num1/Tc(i))^0.5))^2;%alphaCO2, alphaN2
        a1(i,j) =
0.45724*R^2*Tc(i)^2/Pc(i)*alpha_spec1(i,j);%aCO2, aN2


    end


    b_mix1 = x1(1)*b1(1) + x1(2)*b1(2);


    nonzero_p = max(find(P1(:,j),20,'first'));


    P_col1 = P1(1:nonzero_p,j);
    rho_col1 = rho1(1:nonzero_p,j);


    bip1_reg(j) = reg(T_num1);


    rho_PR1 = @(bip,P_col1) paramPR(P_col1, T_num1, a1(:,j), R,
b_mix1, bip1_reg(j), x1);


    rho_calcN1_reg(1:nonzero_p,j) =
rho_PR1(bip1_reg(j),P_col1).*M_mix1;


    AAD_reg1(j) =
(100/nonzero_p).*sum(abs((rho_calcN1_reg(1:nonzero_p,j)-
rho_col1)./rho_col1),1);


%     figure(6+j)
```

```
    figure(2)
    subplot(3,2,j)
    plot(rho_calcN1_reg(1:nonzero_p,j),P_col1.*1e-6,'m*-',
rho1(1:nonzero_p,j),P_col1.*1e-6,'bo-');
    legend('Opt BIP','Experimental
Data','Location','NorthWest');
    xlabel('\rho(kg/m^3)');
    ylabel('P(MPa)');
    title(['AAD% N1 = ',num2str(AAD_reg1(j)),'%',' kij =
',num2str(bip1_reg(j)), ' T = ', num2str(T_num1),'K']);
%     title('Mixture N1 - Regressed BIP');
    grid on
    hold on
%     print('-dpng','-
r300',sprintf(['N1_T',num2str(T_num1),'K.png']));


    figure(12)
    scatter(T_lin1(1,:),bip1,'b*');
    hold on
    plot(T_num1,bip1_reg(j),'m*-',TT,y,'r-');
    legend('Opt BIP');
    xlabel('T(K)');
    ylabel('BIP');
    title('BIP versus Temperature - mixture N1');
    grid on
    hold on



end
% print('-dpng','-r300',sprintf('N1_indiv_BIP(T).png'));
%% Optimization N2


bip = -0.5;


for j=1:5


% Assemble Co-volume Vector and Energy Parameter Matrix for each
```

```
mixture


    T_num2 = T_lin2(j);


    for i=1:2


        b2(i) = 0.07780*R*Tc(i)/Pc(i);%b mixture N1 1=CO2, 2=N2
        m(i) = 0.37464 + 1.54226*omega(i) - 0.26992*omega(i)^2;
        alpha_spec2(i,j) = (1+m(i)*(1-
(T_num2/Tc(i))^0.5))^2;%alphaCO2, alphaN2
        a2(i,j) =
0.45724*R^2*Tc(i)^2/Pc(i)*alpha_spec2(i,j);%aCO2, aN2


    end
        b_mix2 = x2(1)*b2(1) + x2(2)*b2(2);


    nonzero_p = max(find(P2(:,j),20,'first'));


    P_col2 = P2(1:nonzero_p,j);
    rho_col2 = rho2(1:nonzero_p,j);


    rho_PR2 = @(bip,P_col2) paramPR(P_col2, T_num2, a2(:,j), R,
b_mix2, bip, x2);


    switch mode
        case 1
        options = optimset('Algorithm','levenberg-marquardt');
        case 2
        options = optimset('Algorithm','trust-region-
reflective');
    end


    options = optimset('TolFun',1e-12);


    bip2(j) = lsqcurvefit(rho_PR2,bip,P_col2,rho_col2./M_mix2);


    rho_calcN2(1:nonzero_p,j) = rho_PR2(bip2(j),P_col2).*M_mix2;
```

```
    AAD2(j) =
(100/nonzero_p).*sum(abs((rho_calcN2(1:nonzero_p,j)-
rho_col2)./rho_col2),1);


%     figure(12+j)
    figure(3)
    subplot(3,2,j);
    plot(rho_calcN2(1:nonzero_p,j),P_col2.*1e-6,'m*-',
rho2(1:nonzero_p,j),P_col2.*1e-6,'bo-');
    legend('Opt BIP','Experimental
Data','Location','NorthWest');
    xlabel('\rho(kg/m^3)');
    ylabel('P(MPa)');
    title(['AAD% N2 = ',num2str(AAD2(j)),'%',' kij =
',num2str(bip2(j)), ' T = ', num2str(T_num2),'K']);
%     title('Mixture N2');
    grid on
    hold on


%     figure(18)
%     plot(T_num2,bip2(j),'m*-');
%     legend('Opt BIP');
%     xlabel('T(K)');
%     ylabel('BIP');
%     title('BIP versus Temperature - mixture N2');
%     grid on
%     hold on



end
% print('-dpng','-r300',sprintf('N2_indiv.png'));


% Interpolation for T dependence


s = fitoptions('Method','NonlinearLeastSquares','Maxiter',1e3);
ffun = fittype('aa + bb.*T +
cc./T','independent','T','options',s);
```

```
[reg2 gg hh] = fit(T_lin2(1,:)',bip2',ffun);
TT2 = [T_lin2(1,1):1:T_lin2(1,5)];

for i=1:length(TT2)
    y2(i)=reg2(TT2(i));
end

figure(101)
scatter(T_lin2(1,:),bip2,'b*');
hold on
plot(TT2,y2,'r-')
title('BIP_o_p_t CO_2-N_2 = f(T) = a + b*T +c/T');
xlabel('T(K)');
ylabel('BIP');
grid on



for j=1:5

% Assemble Co-volume Vector and Energy Parameter Matrix for each
mixture

    T_num2 = T_lin2(j);

    for i=1:2

        b2(i) = 0.07780*R*Tc(i)/Pc(i);%b mixture N1 1=CO2, 2=N2
        m(i) = 0.37464 + 1.54226*omega(i) - 0.26992*omega(i)^2;
        alpha_spec2(i,j) = (1+m(i)*(1-
(T_num2/Tc(i))^0.5))^2;%alphaCO2, alphaN2
        a2(i,j) =
0.45724*R^2*Tc(i)^2/Pc(i)*alpha_spec2(i,j);%aCO2, aN2

    end

    b_mix2 = x2(1)*b2(1) + x2(2)*b2(2);
```

```
    nonzero_p = max(find(P2(:,j),20,'first'));


    P_col2 = P2(1:nonzero_p,j);
    rho_col2 = rho2(1:nonzero_p,j);


    bip2_reg(j) = reg2(T_num2);


    rho_PR2 = @(bip,P_col2) paramPR(P_col2, T_num2, a2(:,j), R,
b_mix2, bip2_reg(j), x2);


    rho_calcN2_reg(1:nonzero_p,j) =
rho_PR2(bip2_reg(j),P_col2).*M_mix2;


    AAD_reg2(j) =
(100/nonzero_p).*sum(abs((rho_calcN2_reg(1:nonzero_p,j)-
rho_col2)./rho_col2),1);


%     figure(18+j)
    figure(4)
    subplot(3,2,j);
    plot(rho_calcN2_reg(1:nonzero_p,j),P_col2.*1e-6,'m*-',
rho2(1:nonzero_p,j),P_col2.*1e-6,'bo-');
    legend('Opt BIP','Experimental
Data','Location','NorthWest');
    xlabel('\rho(kg/m^3)');
    ylabel('P(MPa)');
    title(['AAD% N2 = ',num2str(AAD_reg2(j)),'%',' kij =
',num2str(bip2_reg(j)), ' T = ', num2str(T_num2),'K']);
%     title('Mixture N2 - Regressed BIP');
    grid on
    hold on


%     figure(25)
%     scatter(T_lin2(1,:),bip2,'b*');
%     hold on
%     plot(T_num2,bip2_reg(j),'m*-',TT2,y2,'r-');
%     legend('Opt BIP');
```

```
%     xlabel('T(K)');
%     ylabel('BIP');
%     title('BIP versus Temperature - mixture N2');
%     grid on
%     hold on



end
% print('-dpng','-r300',sprintf('N2_indiv_BIP(T).png'));
```

And the function used to calculate the pressure using the Peng-Robinson EoS:

```
function rho_PR = paramPR(P_col, T_num, a, R_spec, b_mix, bip,
x)


    a_CO2 = a(1);
    a_N2 = a(2);


    x_CO2 = x(1);
    x_N2 = x(2);


    a_mix = x_CO2^2*a_CO2 + x_N2^2*a_N2 + (1-
bip)*2*x_CO2*x_N2*(a_CO2*a_N2)^0.5;


    for j=1:length(P_col)


    a(j) = P_col(j);
    b(j) = P_col(j)*b_mix - R_spec*T_num;
    c(j) = a_mix - 2*b_mix*R_spec*T_num - 3.*b_mix^2.*P_col(j);
    d(j) = -a_mix*b_mix + b_mix^2*R_spec*T_num +
P_col(j)*b_mix^3;


    r = [a(j) b(j) c(j) d(j)];


    v(j,:) = roots(r);
             for i=1:3
```

```
                if  imag(v(j,i))==0
                    rho_PR(j,1)= v(j,i)^-1;
                end
            end
    end
end
```

For last, the code used to vary the BIP, for each mixture:

```
%%%%%%%%%%%%%%%%%%%%%%%%%%%%%%%%%%%%%%%%%%%%%%%%%%%%%%%%%%%%%%%%%%%%%%%%%%%%%%%
%%%%
%%%%%% Optimization of the Data Fitting for the Density Estimate
%%%
%%%%%% Peng Robinson EoS
%%%%%%%%%%%%%%%%%%%%%%%%%%%%%%%%%%%%%%%%%%%%%%%%%%%%%%%%%%%%%%%%%%%%%%%%%%%%%%%
%%%%%% Working - 27/11
%%%%%%%%%%%%%%%%%%%%%%%%%%%%%%%%%%%%%%%%%%%%%%%%%%%%%%%%%%%%%%%%%%%%%%%%%%%%%%%
%%%%%%%%%%%%%%%%%%%%%%%%%%%%%%%%%%%%%%%%%%%%%%%%%%%%%%%%%%%%%%%%%%%%%%%%%%%%%%%
%%%%


clc
close all
clear all


%%% Load Data from files
%%%%%%%%%%%%%%%%%%%%%%%%%%%%%%%%%%%%%%%%%%%%%%%%%%%%%%%%%%%%%%%%%%%%%%%%%%%%%%%


load mixture_N2.txt


for j=1:5


    P1(:,j) = mixture_N2(2:end,2*j-1)*1e6; %Pa
    T_lin1(j) = mixture_N2(1,2*j-1); %K
    rho1(:,j) = mixture_N2(2:end,2*j);


end
```

```
load mol_fraction_N2.txt
x1(1) = mol_fraction_N2(1,1); %x_CO2
x1(2) = mol_fraction_N2(2,1); %x_N2

load critical_data_CO2N2_PR.txt

crit_data = critical_data_CO2N2_PR;

%CO2
M(1) = crit_data(1,1); %kg/kmol
Tc(1) = crit_data(2,1) + 273.15; %K
Pc(1) = crit_data(3,1) * 1e6; %Pa
omega(1) = crit_data(4,1);

%N2
M(2) = crit_data(1,2);
Tc(2) = crit_data(2,2) + 273.15;
Pc(2) = crit_data(3,2) * 1e6;
omega(2) = crit_data(4,2);

%% Optimization N1

% Caltulate the specific gas constant for each mixture

R = 8314.462; %J/kmol*K
M_mix1 = (x1(1)*M(1)+x1(2)*M(2)); %kg/kmol

bip = -0.5;

% To change the opt algorithm
mode = 1;

for j=1:5

% Assemble Co-volume Vector and Energy Parameter Matrix for each
```

```
mixture


    T_num1 = T_lin1(j);


    for i=1:2


        b1(i) = 0.07780*R*Tc(i)/Pc(i);%b mixture N1 1=CO2, 2=N2
        m(i) = 0.37464 + 1.54226*omega(i) - 0.26992*omega(i)^2;
        alpha_spec1(i,j) = (1+m(i)*(1-
(T_num1/Tc(i))^0.5))^2;%alphaCO2, alphaN2
        a1(i,j) =
0.45724*R^2*Tc(i)^2/Pc(i)*alpha_spec1(i,j);%aCO2, aN2


    end


    b_mix1 = x1(1)*b1(1) + x1(2)*b1(2);


    nonzero_p = max(find(P1(:,j),20,'first'));


    P_col1 = P1(1:nonzero_p,j);
    rho_col1 = rho1(1:nonzero_p,j);


    rho_PR1 = @(bip,P_col1) paramPR(P_col1, T_num1, a1(:,j), R,
b_mix1, bip, x1);


    bip1 = [-1:0.5:1];


    for jj=1:length(bip1)


    rho_calcN1(1:nonzero_p,j) = rho_PR1(bip1(jj),P_col1)*M_mix1;


    AAD1(jj,j) =
(100/nonzero_p).*sum(abs((rho_calcN1(1:nonzero_p,j)-
rho_col1)./rho_col1),1);


    figure(1)
    subplot(3,2,j)
```

```
    plot(rho_calcN1(1:nonzero_p,j),P_col1.*1e-6,'m*-',
rho1(1:nonzero_p,j),P_col1.*1e-6,'bo-');
    legend('Opt BIP','Experimental
Data','Location','NorthWest');
    xlabel('\rho(kg/m^3)');
    ylabel('P(MPa)');
    title([' kij = ',num2str(bip1(1)),' to ',num2str(bip1(end)),
'  T = ', num2str(T_num1),'K']);
%     title('Mixture N1');
    grid on
    hold on


    end




%     figure(2)
%     subplot(3,2,j)
%     plot(bip1,AAD1(:,j),'k.-
',bip1(find(AAD1(:,j)==min(AAD1(:,j)))),min(AAD1(:,j)),'ro','Mar
kerSize',10);
%     legend('Opt BIP');
%     xlabel('BIP');
%     ylabel('AAD%');
%     title(['AAD% versus BIP - T = ',num2str(T_num1),'K -
AAD_m_i_n = ',num2str(min(AAD1(:,j))),'%']);
%     grid on
%     hold on



end
print('-dpng','-r300',sprintf('N2_var_BIP.png'));
% print('-dpng','-r300',sprintf('AADxBIP_N2.png'));
```